

The surface circulation in the eastern basin of the Mediterranean Sea

NAJWA HAMAD, CLAUDE MILLOT and ISABELLE TAUPIER-LETAGE

Laboratoire d'Océanographie et de Biogéochimie Centre National de la Recherche Scientifique (UMR 6535) and
Université de la Méditerranée (Centre d'Océanologie de Marseille) Antenne de Toulon, BP 330,
F-83507 La Seyne-sur-Mer. E-mail: itaupier@ifremer.fr

SUMMARY: The schema of the Atlantic Water (AW, 100-200 m thick) circulation in the eastern basin of the Mediterranean Sea elaborated in the 1990s (and widely referred to nowadays) mainly shows jets meandering offshore across the whole basin. However, all previous schemata (since the 1910s) and an analysis of infrared (IR) satellite images in the 1990s show counterclockwise circulation at basin scale. A former controversy about the circulation was elucidated in the western basin where IR images helped describe the mesoscale features and demonstrate their role in the circulation. This motivated the detailed analysis of IR daily and weekly composites (~1000) from 1996 to 2000, and of monthly composites since 1985. We show that AW circulates along the upper part of the continental slope in a counterclockwise direction around the whole basin. In the south and all year long, this circulation is unstable and generates mesoscale anticyclonic eddies that spread AW offshore; in the north dense water formation induces larger seasonal variability. These mesoscale eddies, as well as the Etesian-induced eddies Ierapetra and Pelops, can be followed for years, sometimes several hundreds of km away from where they are formed, and they can merge and/or interact with the alongslope circulation.

Keywords: Mediterranean Sea, eastern basin, surface circulation, mesoscale eddies, infrared satellite imagery, 30-46°N and 10-36°E.

RESUMEN: LA CIRCULACIÓN SUPERFICIAL EN LA CUENCA ORIENTAL DEL MAR MEDITERRÁNEO. – Los esquemas de circulación del Agua Atlántica (AW, 100-200 m de grosor) en el Mediterráneo oriental elaborados en los años 1990 (y abundantemente citados en la actualidad) presentan principalmente una corriente en chorro ondulante atravesando el centro de la cuenca. Por el contrario, todos los esquemas anteriores (desde los años 1910) y un análisis de imágenes infrarrojas (IR) de satélite en los noventa presentan una circulación antihoraria a escala de la cuenca. Una controversia anterior sobre la circulación en la cuenca occidental fue resuelta gracias a que las imágenes IR ayudaron a describir los fenómenos de mesoescala y demostrar su papel en la circulación. Esto motivó un análisis detallado de imágenes IR compuestas diarias y semanales (~1000) durante 1996-2000 y mensuales desde 1985. Aquí demostramos que el AW en general circula sobre la parte superior del talud continental, de forma antihoraria por toda la cuenca. En el sur, y a lo largo de todo el año, esta circulación es inestable y genera remolinos anticiclónicos de mesoescala que esparcen el AW hacia alta mar; en el norte la formación de agua densa induce una gran variabilidad estacional. Estos remolinos de mesoescala, así como los inducidos por los vientos Etesios (Ierapetra y Pelops), pueden ser seguidos durante años, a veces por varios centenares de kilómetros a partir de su lugar de formación, y pueden unirse y/o interactuar con la circulación a lo largo del talud.

Palabras clave: Mar Mediterráneo, cuenca oriental, circulación superficial, remolinos de mesoescala, imágenes infrarrojas de satélite, 30-46°N y 10-36°E.

INTRODUCTION

The circulation of Atlantic Water (AW, <http://www.ciesm.org/catalog/WaterMassAcronyms.pdf>, 100-200 m thick) in the eastern basin of the

Mediterranean Sea is still debated. Four major schemata have been proposed up to now: Nielsen (1912; Fig. 1a), Ovchinnikov (1966; Fig. 1b), Lacombe and Tchernia (1972; Fig. 1c), and Robinson *et al.* (1991; Fig. 1d), completed by

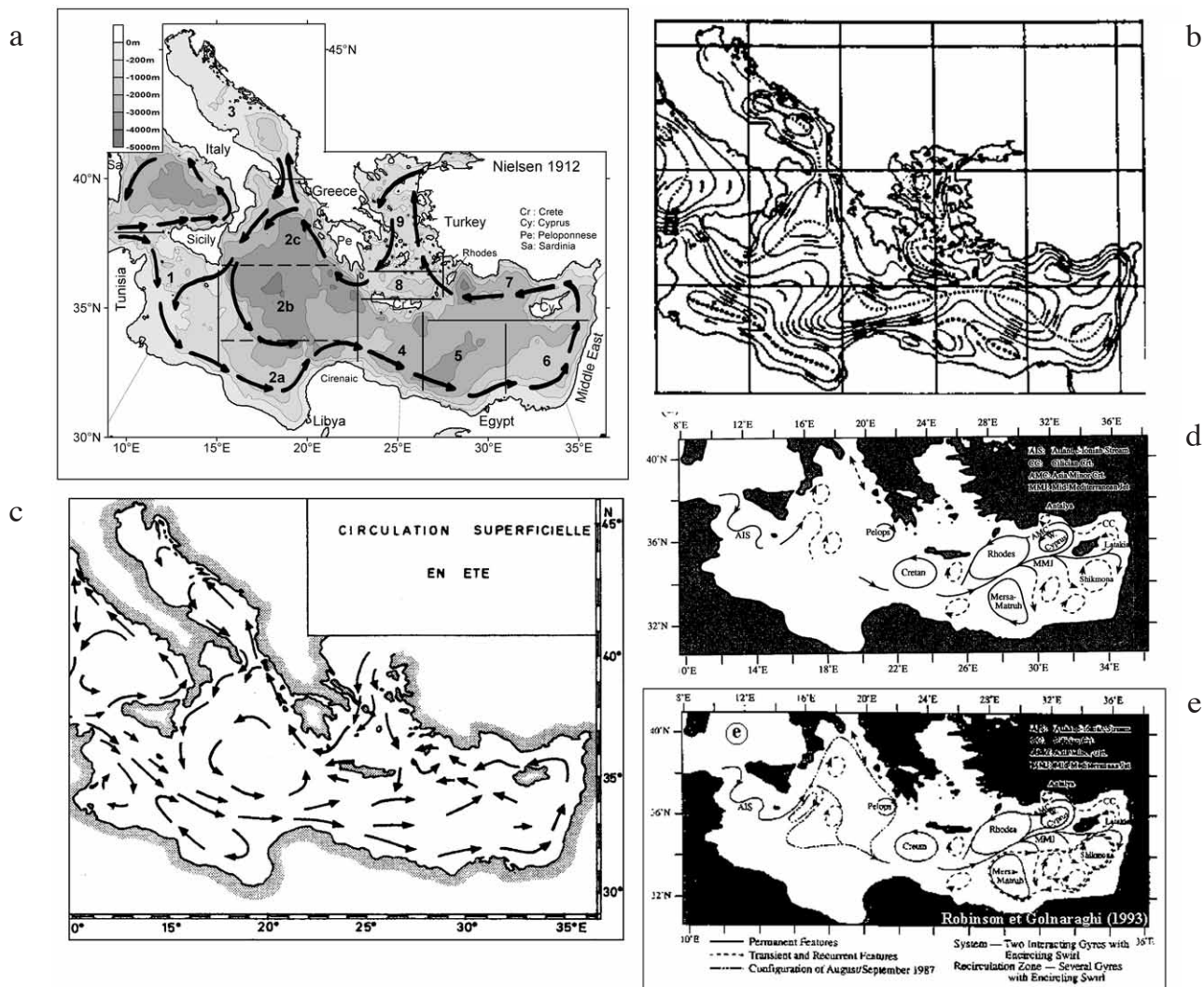


FIG. 1. – The different schemata of the surface circulation in the eastern basin of the Mediterranean Sea. a) Nielsen (1912); bathymetry in m. Index of subbasins: 1: Channel of Sicily, 2a: southern Ionian, 2b: central Ionian, 2c: northern Ionian; 3: Adriatic; 4: southern Cretan; 5: western Levantine (deeper than 3000m: the Herodotus trough); 6: southeastern Levantine; 7: northern Levantine; 8: northern Cretan; 9: Aegean. b) Ovchinnikov (1966). c) Lacombe and Tchernia (1972). d) Robinson *et al.* (1991); e) Robinson and Golnaraghi (1993).

Robinson and Golnaraghi (1993; Fig. 1e) and by Malanotte-Rizzoli *et al.* (1997). The three older schemata could not be very accurate or detailed because of the limited amount of in situ data and because the mesoscale dynamics were unknown. Nevertheless, the Coriolis effect is considered dominant in these schemata that describe an overall circulation that is essentially counterclockwise around the basin. Hereafter they will be referred to as the “historical schemata”. Our geographical terminology and the bathymetry are superimposed on Nielsen’s schema (Fig. 1) because it is relatively simple, and it is fully consistent with our own analysis.

The fourth schema is based on data and model results from the programme Physical Oceanography of the Eastern Mediterranean (POEM group, 1992).

It has benefited from a wealth of in situ and satellite data, and differs markedly from the historical ones. It describes central meandering jets crossing: i) the central part of the Ionian subbasin or spreading clockwise in its northern part (the “Atlantic Ionian Stream, AIS” and the “Mid-Ionian Jet, MIJ”), ii) the southern Cretan subbasin (i.e. the Cretan passage; the “North African Current, NAC”) and iii) the Levantine subbasin (the “Mid-Mediterranean Jet, MMJ”) before iv) flowing off the Middle East and Turkey (the “Cilician Current, CC” and the “Asia Minor Current, AMC”). In the rest of the paper, schemata based on central meandering jets will be referred to as “POEM-type” schemata.

The POEM-type schemata also disagree with a contemporaneous analysis of infrared (IR) satellite

images spanning the eighties (Le Vourch *et al.*, 1992). The thorough analysis presented hereafter was undertaken considering firstly a preliminary comparison between the western and eastern basins that evidenced marked similarities (Millot, 1992), and secondly that the numerous studies we have conducted during ~20 years in the western basin (e.g. Millot *et al.*, 1997; Taupier-Letage *et al.*, 2003) have established the good correlation between satellite and in situ observations. Hence, using satellite data (not only IR but also visible and altimetric) for circulation studies has been validated, and has played a pivotal role in solving the controversy about the circulation of the Levantine Intermediate Water off the Algerian slope (Millot and Taupier-Letage, 2005a) as well as several aspects of the circulation in the whole Mediterranean Sea (Millot, 2005). Given the scarcity of in situ observations in the eastern basin and the discrepancies between their various interpretations, we decided to perform an intensive analysis of IR images prior to any new observational effort. The first results of this analysis were presented in 2002 by Hamad *et al.* (2004) and the definitive results at basin scale were published by Hamad *et al.* (2005). Here we present the detailed results down to subbasin scale.

In the rest of the paper, when reporting previous findings, we identify the original terms with inverted commas, and use (and suggest using) terms that we think are more adequate in our own analysis. As an example, we use the term *subbasin* (or omit it) for all parts of the eastern basin of the Mediterranean Sea that have been defined up to now indifferently as *seas*, *basins* or *passages* (see Fig. 1a). For the sake of clarity in our papers, we have adopted the terminology defined hereafter. We consider that the terms *gyres* and *eddies* imply different generation processes and dynamical features, and therefore we differentiate them. We define *gyres* as circuits induced by wind and/or thermohaline forcings, which are clearly constrained by the bathymetry along most of their periphery, i.e. at basin or subbasin scale; gyres are thus stationary for the most part. We characterise them as clockwise / counterclockwise. We define *eddies* as mesoscale phenomena generated either by processes that destabilise the circulation or by the wind stress curl locally induced by orographic effects. We characterise them as cyclonic / anticyclonic. Eddies are not constrained by the bathymetry (but can be guided by it), and thus can grow and move. We consider that they *propagate* when

embedded in their parent current (a propagation speed can be theoretically defined) and that they *drift* when separated / isolated. Eddies are mesoscale phenomena that can reach diameters up to 250 km, even in the Mediterranean Sea, last for years and extend down to the bottom.

In the next section we present our use of the IR images. First we briefly describe the AW circulation in the western basin to show the relevance of the information provided by these images and to allow further comparisons with the eastern basin (see Millot and Taupier-Letage, 2005b for more details); then we present our data set, describe the visual analysis technique and stress its validity by comparing it with other observations. In the following section we present the surface circulation schemata available at basin scale, as well as those at subbasin and meso-scales. Another section contains our interpretation of the images in terms of surface circulation. We discuss the previous analyses and schemata, and finally propose our own schema for the AW circulation.

VISUAL ANALYSIS OF SATELLITE IR IMAGES

The findings inferred in the western basin

From the experience gained in analysing IR images to deduce dynamical patterns (Le Vourch *et al.*, 1992), Millot (1992) suggested that the overall circulation in the western basin was similar to that in the eastern basin, and that mesoscale dynamics played a major role in both basins. In the western basin, a few images prompted new hypotheses about the processes (Millot, 1985) and led to original circulation schemata being elaborated (Millot, 1987). Complementary sets of images (e.g. Taupier-Letage and Millot, 1988) and in situ experiments guided by satellite information (e.g. Millot *et al.*, 1990, 1997) have allowed the schemata to be refined (Millot, 1999). The sampling strategy of operations such as ELISA (Eddies and Leddies Interdisciplinary Study off Algeria, 1997-1998, www.ifremer.fr/lobtln/ELISA) is now adjusted according to the imagery received aboard in near real time, and mesoscale features are sampled in the most efficient way (Taupier-Letage *et al.*, 2003; Millot and Taupier-Letage, 2005a). The circulation in the western basin is first described to emphasise similarities / differences with its eastern counterpart.

Upon entering the Alboran, the AW generally describes one or two clockwise gyres before flowing along the Algerian slope. Then, specific instability processes generate mesoscale meanders and eddies off Algeria, so that this flow of AW (100-200 m thick) was named the Algerian Current (Millot, 1985). Most of the time the current meanders and generates a series of coastal (paired) eddies ~50 km in diameter but once or twice a year a meander increases in size (~100 km). Such a meander generates an embedded anticyclonic eddy, and both generate an anticyclonic eddy in the lower layer that can extend down to the bottom (~3000 m; Obaton *et al.*, 2000; Millot and Taupier-Letage, 2005a). The ensemble (named event) can remain stationary or propagate downstream (up to 3-5 km/day), follow the deep isobaths and finally detach from its parent current at the entrance of the channel of Sardinia. After pinching off, an event looks like an open-sea anticyclonic eddy, intense in the surface layer and still able to extend down to the bottom (Ruiz *et al.*, 2002). Then, probably because of the trough formed by the deepest isobaths in the eastern Algerian, most eddies drift along a counterclockwise circuit in this area. Since the Algerian eddies (AEs) have lifetimes of up to ~3 years (Puillat *et al.*, 2002), the subbasin can be almost filled with these eddies, which frequently interact with each other and with their parent current.

The AW that has been entrained seawards by the AEs accumulates northwards (thus forming the North-Balearic front) before concentrating and flowing along western Corsica. Then it merges with the part of the AW that has not been entrained seawards off Algeria but has progressed along the southern and eastern slopes of the Tyrrhenian (without entering the eastern basin): the western Corsican and Tyrrhenian flows join and form the Northern Current. The Northern Current displays a marked seasonal variability, since it is linked to the formation of the Western Mediterranean Dense Water (WMDW) that occurs in the Liguro-Provençal subbasin. However, this is not a rim current *stricto sensu*, since it does not surround the zone of dense water formation in the south. This current is mainly affected by meanders up to ~100 km in wavelength that never evolve into eddies, and that propagate downstream at 10 to 20 km/day in winter (Crépon *et al.*, 1982) and 5 to 10 km/day in spring to autumn (Sammari *et al.*, 1995). Note that the former “Liguro-Provenço-Catalan Current” was named Northern Current (Millot, 1991)

to emphasise the fact that it was expected to be a common characteristic of both the western and eastern basins of the Mediterranean Sea, as well as of the Asian Mediterranean Sea, that is, the East/Japan Sea (Millot, 1992).

Other eddies are induced by the wind. Major ones develop as a pair, east of the Strait of Bonifacio, due to the effect of the orography of Corsica and Sardinia on westerly winds. Artale *et al.* (1994) have shown that the cyclonic eddy in the north was surrounded by a rim current and Fuda *et al.* (2002) have hypothesised it might be a zone of dense water formation. Note that this eddy results from AW diverging (uplifting of the interface), hence forming a motionless cool central area, while the anticyclonic eddy in the south is composed of AW converging (depression of the interface) and rotating as a warm isolated lens. As emphasised by Millot and Taupier-Letage (2005b), these basic differences also occur between such mesoscale eddies in the eastern basin.

The IR data set

The NOAA (National Oceanic and Atmospheric Administration) operates a series of quasi-polar orbiting satellites carrying an Advanced Very High Resolution Radiometer (AVHRR) that has channels in both the visible and the IR. Since the atmosphere contaminates the marine emitted signals, a multi-IR-channel algorithm is used to compute a Sea Surface Temperature (SST). A major problem to face is that the IR signal is emitted by the very surface (skin temperature), which is not always representative of the bulk temperature, which is the one of interest. For instance, solar heating on calm days leads to warm superficial spots, and intense evaporation leads to colder skin temperature. However, as it will be seen hereafter, these situations can be easily detected and thus disregarded in the analysis. In this paper we consider only the SSTs that are representative of the bulk temperature, and from which we intend to infer information about the surface (at least) layer dynamics.

The AVHRR thermal resolution is 0.125°C and the SST is generally retrieved with a precision higher than 1°C. The spatial resolution is ~1 km at nadir in the Local Area Coverage mode (otherwise ~4 km in Global Area Coverage mode), the swath width is ~3000 km and several orbits are available per day over the Mediterranean. Generally, AVHRR data are

put through a series of procedures to remove data that is out of range, detect the presence of clouds, reduce the atmospheric contamination, compute SST and correct the geographical distortions. Daily, weekly, monthly, etc. composites are computed (in different ways), mainly to obtain cloud-free images. There is a general agreement that, given their spatio-temporal characteristics, time series of these images are an adequate tool for studying the Mediterranean. However, there are two major approaches that are based on different analysis strategies and can thus diverge: climatological studies vs. dynamical ones. To perform climatological studies at basin scale (e.g. Marullo *et al.*, 1999a,b), a pixel of ~4 km is often used and accurate SST values are needed everywhere, even where no data are available. The images are essentially composites to which spatial interpolation techniques are generally applied, which filter out tenuous gradients that we personally consider as significant. Even though averaging increases the information significance, the longer the time average the higher the damping of the real situation: for instance, in the case of warmer eddies propagating in line along the coast, a monthly/yearly average will only display a continuous warmer strip parallel to the coast. Therefore, even though this statistical approach is fully objective and does not require any personal input, it cannot be used for describing the circulation and performing dynamical studies.

To perform dynamical studies, one needs to describe phenomena that, considering their space and time scales, have permanent although variable SST signatures. Indeed, comparing the signature of an eddy during a calm and sunny day with its signature a few hours later after a wind speed increase, or this signature in summer vs. winter can hardly be done automatically with a computer. In addition, there is theoretically no direct relation between a streamline and an isotherm since both can be either parallel or perpendicular. Indeed, in the case of a jet, streamlines and isotherms are parallel at the base of the jet (giving the direction/sense of the jet), while they are perpendicular at its nose (the progression of the nose is computed from its successive positions). This is why all techniques proposed for inferring streamlines from SST gradients cannot be routinely applied and why only those following a given small-scale SST feature on a series of images allow the large-scale currents that have transported this feature to be inferred. Whatever the case, IR images are used worldwide to study the circulation, as it is easy

to intuitively infer features such as eddies and jets, and to recognise their signature from one image to the following one (up to several days apart), even if images were collected with different meteorological or stratification conditions. With some practice, this is as easy as inferring, just from the visual analysis of cloud images, the sense of rotation, and the size and location of either a tornado or a cyclone.

We have analysed ~1000 daily and weekly SST composites for the period 1996 to 2001, and all monthly composites from 1993 to 2001, from the German remote sensing centre DFD/DLR (<http://eoweb.dlr.de>, Figs. 4 to 21). To our knowledge, this is the only web site where images are available i) of the whole Mediterranean ii) geographically registered iii) at full resolution (~1 km) and iv) for free. Image processing and composing is described in http://eoweb.dlr.de:8080/short_guide/D-SST.html. The main DFD/DLR's composition characteristic is that there is no interpolation: the daily images are composed retaining the SST maximum value of every pixel to minimise cloud coverage and atmospheric contamination. The drawbacks are first that warm spots due to episodic solar heating are thus systematically selected (see Fig. 6d, off the Cyrenaïca), and second that artificial thermal fronts due to the thermal contrast between night and day may appear (see Fig. 8b, between H and P97). In the former case information on the SST (signing the surface circulation) is obliterated, while in the latter case it is preserved. However, these composition artefacts are easily detected, and disregarded in the qualitative dynamical analysis. Weekly and monthly products are derived from the daily composites using the average. We have also analysed images from the PODAAC Pathfinder Archive (~9 km, SST, night and day composites, 8-day and monthly composites, January 1985 to present, <http://podaac.jpl.nasa.gov/sst/>, Fig. 2 and 22), and from the SATMOS (agreement INSU/METEO-FRANCE, ~1 km, brightness temperature/ channel 4 (= relative temperature), individual paths, October 2001 to present).

The visual analysis

Contrary to the statistical/climatological approach, which focuses on absolute SST values which usually have a coarse spatial resolution, the visual analysis considers the shape, location and consistency of isotherms, even if they are only par-

tially visible due to cloud coverage, at high spatial resolution (1-2 km). The SST absolute value is not relevant for characterising a structure, since tenuous gradients can be as significant as stronger ones, due to meteorological conditions and/or stratification. In the same way, SST variations on day-night and seasonal scales must be disregarded, since the same eddy can be colder than its surroundings in summer, and warmer in winter. As a consequence, no threshold criteria can be determined to detect and track structures objectively (for more details see Taupier-Letage *et al.*, 1998). To identify oceanic phenomena in any season, stratification or meteorological conditions, it is thus necessary to stretch the colour scale according to the thermal dynamics, so that we only consider relative SST values. The colour scale (from blue (resp. light grey) for low temperatures to red (resp. dark grey) for higher temperatures) cannot be kept constant throughout time series, and there is no univocal correspondence colour-SST (examples are given by the ~ 3 year-time series of ~ 30 images used to track two Algerian eddies (Puillat *et al.*, 2002) and four generations of the Ierapetra eddy (see Fig. 13) during ~ 3 years).

The visual analysis of a given image consists in reporting the isotherms (even segments only, if cloudy) delineating a circulation feature and superimposing all corresponding isotherms detected in successive images (as illustrated by Figure 3 of Marullo *et al.*, 2003). The recurrence of some specific contouring ends up in delineating the whole feature, its centre in the case of an eddy, and if it is moving, its direction and speed. As no automated method can achieve such a visual/"subjective" analysis, which is also highly time-consuming, it is not used extensively. To validate our approach, we detail some arguments and compare our results with those inferred from other data sets.

The basic argument supporting the validity of visual analysis is that oceanic and atmospheric phenomena have dramatically different space and time scales. Essentially, clouds are changing and moving more rapidly than any oceanic phenomenon so that comparing two images, even if only a few hours apart, prevents the limits of a cloud being mistaken for those of an eddy. Even when looking at a single image, most oceanic phenomena are differentiated from atmospheric ones because their size is generally intermediate between that of mid-latitude low-pressure systems and the size of single clouds. Moreover, patterns are also characteristic: isotherms

associated with oceanic phenomena are smoother and less patchy than those associated with atmospheric ones.

Aside from the problems due to atmospheric contamination and warm spots, one can also question the relation between the skin and the bulk temperatures, i.e. the SST significance. The most common argument is to say that waves occur almost permanently, so that the skin temperature is generally representative of the mixed layer. However, depending on the wave height and wavelength (i.e. the wind characteristics), the season (i.e. the thermocline) and the overall situation (i.e. a zone of dense water formation vs. a permanently stratified coastal current), the mixed layer thickness can range from a few metres to 100s of metres. Therefore, whether a 100-km eddy is signed by SST differences of 1°C or 10°C is not important for the visual analysis, which is only concerned with the size and location of the eddy. The problem of skin vs. bulk temperature appears to be crucial for climatological studies only, not for process studies.

Another aspect worth noting is that mesoscale eddies with diameters of a few 100 km are known from theoretical and worldwide field experiments to have lifetimes of a few months / years and propagation speeds of a few km/day. Thus, even if an eddy cannot be seen from space for a while, it will most likely be recognised with a roughly similar shape and location a couple of days/weeks apart. This not only helps when the cloud coverage is intense but also when the seasonal thermocline is relatively sharp (a few degrees) and thin (a few metres), after several sunny days with light winds, so that the eddy signature can be more or less masked although no warm spots occur (as frequently observed in the eastern Levantine).

Finally, the benefits of visual analysis can be illustrated by three examples. One concerns identifying AW. After entering one or the other basin (in their southern parts), AW is first warmed up while it progresses eastwards and then cooled when it progresses northwards and reaches the dense water formation zones. Since AW also encounters seasonal variability everywhere, just considering a certain definite SST range does not allow it to be automatically identified all along its course. Since a visual analysis pays more attention to the continuity and shape of a set of isotherms than to the value of one given isotherm, AW can be visually identified (see Figures 22 and 23a, where the warmer AW can be

identified all around the basin, including in the north, thus proving that there is no bias due to latitude). The second example concerns the characterisation of mesoscale eddies. In case 3 anticyclonic eddies (identified by higher SST) are close to each other (positioned on the summits of a triangle), any automatic pattern recognition will define a cyclonic eddy in-between (possibly even the unique structure detected), centred on the lower SST values. However, visual analysis, which considers only the shape of the isotherms, will clearly identify the 3 anticyclonic eddies, and will interpret the continuity of the isotherms in-between only as a transient eddy-induced (cyclonic) circulation (that will disappear as soon as one eddy moves away; see Figure 3 of Taupier-Letage and Millot, 1988). The last example concerns the characterisation of the so-called “Mersa-Matruh eddy or gyre” southwestern Levantine: while several (anticyclonic) mesoscale eddies clearly appear permanently in this area on images processed by visual analysis (see Figs. 9 to 13), the climatological method used by Marullo *et al.* (1999a) does not allow any such eddies to be evidenced in this area most of the time. Therefore, using IR imagery to study circulation features is specific, in that tracking the propagation of eddies from a time series of images is more informative than considering the averaged image for the same period, especially since averaging introduces biases for propagating eddies and places emphasis on stationary ones (note, however, that the actual technique for analysing altimetric data smoothes the stationary eddies and emphasises the propagating ones).

Comparisons with other data sets

Many papers, based on comparisons with other data sets, account for the efficiency of IR images to depict oceanic phenomena not only worldwide, but also in the eastern basin (e.g. Özsoy *et al.*, 1993; Horton *et al.*, 1994; Zodiatis *et al.*, 1998; Marullo *et al.*, 2003). Therefore, we have restricted this section to a few additional comparisons, among which are the POEM data sets. Let us first emphasise the agreement between the thermal (IR) and biological (visible) signatures of mesoscale features (e.g. Arnone and La Violette, 1986 and Fig. 17 in Taupier-Letage *et al.*, 2003, in the western basin; Fig. 1 in Taupier-Letage and Millot, 2003, in the easternmost part of the eastern basin). Consistency between IR images of Algerian eddies and drifting

buoy trajectories was also established by Salas *et al.* (2002) and Font *et al.* (2004). We also compared all XBT transects collected in 1999-2000 during the Mediterranean Forecasting System Pilot Project (MFSP) to IR images, both in the western basin (Fuda *et al.*, 2000) and the eastern one: all mesoscale anticyclonic features that were crossed have a clear in situ signature, at least down to 400-500 m (Manzella *et al.*, 2001; Zervakis *et al.*, 2002; Fusco *et al.*, 2003; Hamad, 2003). Analysing anticyclonic eddies propagating north off Crete and tracked by their IR signatures has also been backed by moored ADCP time series (Cardin and Hamad, 2003). Let us also emphasise the agreement with the most recent numerical results (e.g. Pinardi and Masetti, 2000; Alhammad *et al.*, 2003, 2005). Finally, agreement with altimetric data is also good, provided that the minima of the sea level anomalies generally associated with mesoscale cyclonic eddies (hence with negative values) are just considered as a kind of reference level (hence associated with nearly zero values, not corresponding to any coherent structure). Indeed, images show that anticyclones heavily outnumber cyclones and are roughly twice as intense and large as defined from altimetry.

This agreement between remotely sensed and in situ observations is to be expected, since valid observations cannot be questioned and must obviously be consistent. But what can differ is their interpretation, as in the case of the POEM data sets. Figure 2 shows the dynamical patterns encountered during the four major POEM campaigns, which spanned several week / month periods each, and the corresponding SST relevant composites. All the major features evidenced from in situ data are detected on IR images. For POEM ON 85 (Fig. 2a, b): the cool “West Cretan gyre”, the warm “Mersa-Matruh” in the southwestern Levantine, the 3-pole signature of “Shikmona”, the “Rhodes gyre” and its southeastern extension, the “AMC” meandering and its associated eddy. For POEM MA 86 (Fig. 2c, d): the warm “Mersa-Matruh” in the southwestern Levantine, the 2-pole structure of “Shikmona”, the warm eddy off the gulf of Antalya, the progression of the “AMC” towards Crete. For POEM AS 87 (Fig. 2e, f): the inflow meandering in the channel of Sicily, the northward branch in the Ionian, the coastal eddy off Libya and Egypt and the cooler one north of it, Ierapetra, the multi-pole structure of “Shikmona”, the large “AMC” meander, the “Rhodes gyre” and its northeastward extension. For

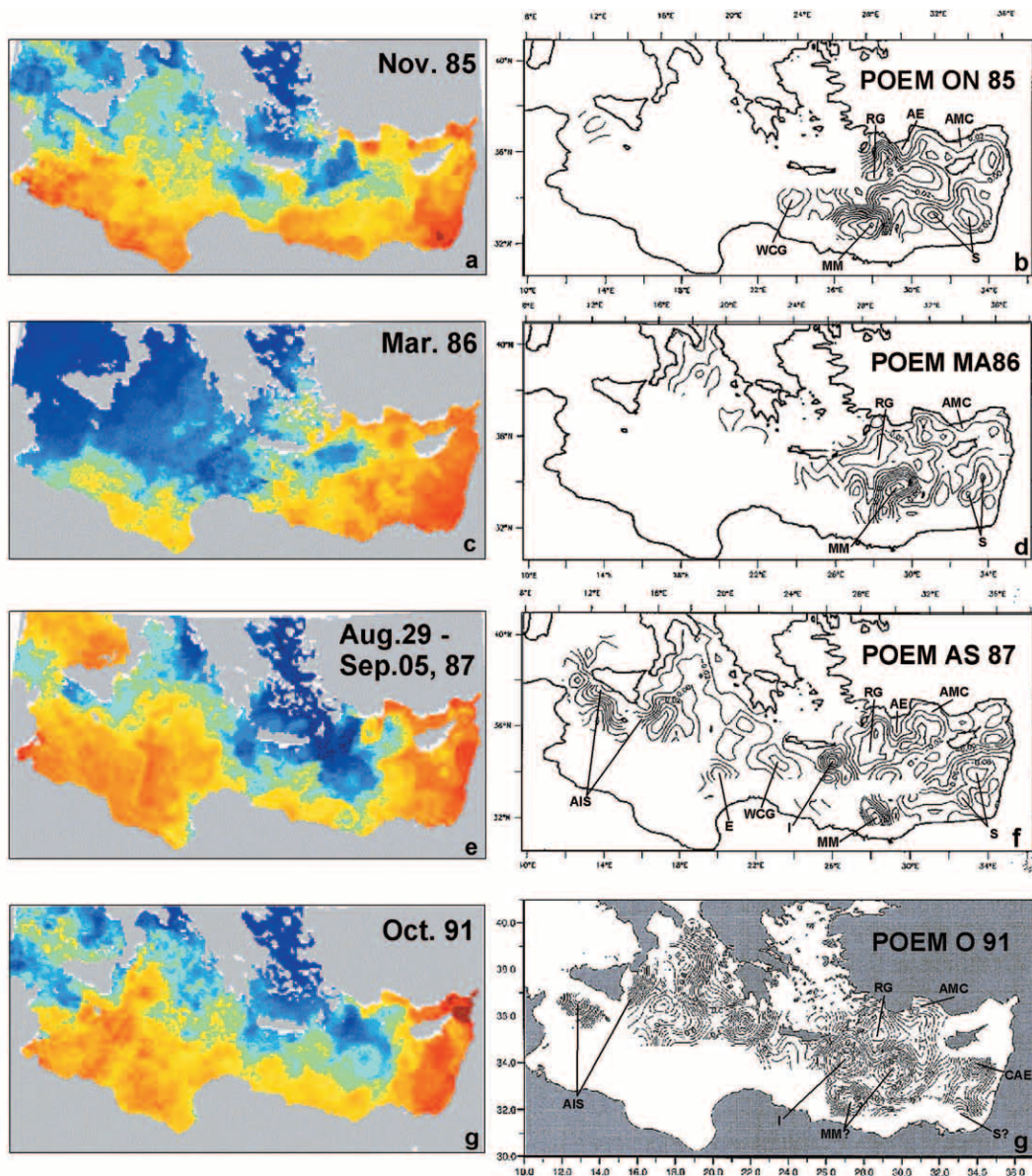


FIG. 2. – Comparison of satellite (IR composites) and *in situ* (dynamics heights anomaly of the surface during the POEM cruises, from Robinson *et al.* (1991) and from Malanotte-Rizzoli *et al.* (1999)) observations: a, b (November 1985, POEM ON 85), c, d (March 1986, POEM MA 86), e, f (August - early September 1987, POEM AS 87), g, h (October 1991, POEM O 91). The main features are identified, using the POEM nomenclature (AIS: Atlantic Ionian Stream, AMC: Asia Minor Current, AE: Antalya Eddy, CAE: Cyprus Anticyclonic Eddy, E: unnamed Eddy, I: Ierapetra, MM: Mersa Matruh, P: Pelops, RG: Rhodes Gyre, S: Shikmona, WCG: West Cretan Gyre).

POEM O 91 (Fig. 2g, h): the flow structure in the channel of Sicily (different from POEM AS 87), the northward branch in the Ionian, Pelops and Ierapetra, a coastal eddy in the southwestern Levantine and an offshore one in the southwestern Levantine, the more simple structure of “Shikmona”, the “Cyprus anticyclonic eddy”, the “Rhodes gyre” and its extensions towards both the northeast and southeast.

It is clear that our analysis of IR images agrees with our own analysis of all *in situ* data sets (in par-

ticular the POEM ones), basically evidencing an AW alongslope flow at basin scale and intense mesoscale eddies. In addition, many papers have shown that all these eddies generally extend down to the deepest levels that were sampled, sometimes down to ~2000 m at least (e.g. Feliks and Itzikowitz, 1987; Brenner, 1989, 1993; Özsoy *et al.*, 1991, 1993; Horton *et al.*, 1994; Zodiatis *et al.*, 1998). Therefore, as for the western basin, we think that the visual analysis of IR images can provide relevant information not only at the surface but also at depths (down to 100-200 m

for the AW flow, potentially down to the bottom for the mesoscale eddies).

THE AVAILABLE SURFACE CIRCULATION SCHEMA

Schema at basin scale

Nielsen's (1912) schema (Fig. 1a), although based on very few hydrological data, shows the AW circulating counterclockwise and alongslope in the Ionian and the Levantine before entering the Aegean entirely. Then, the Black Sea water joins the AW and both flow out of the Aegean around Greece before splitting into two branches. One branch enters the Adriatic and the other one continues flowing counterclockwise in the Ionian, thus joining the Adriatic outflow south of Italy. This overall counterclockwise and alongslope circulation is explained by Nielsen (p. 134) as "*due in the first place to the earth's rotation, which bends the current to the right and thus forces the inflowing AW up against the coast of Africa and constantly maintains the current system*" and is shown by any relevant numerical model (e.g. Spall, 2004).

Ovchinnikov's (1966) schema (Fig. 1b) is based on geostrophic computations from a larger set of hydrological data. The AW flow describes a meander in the central Ionian and generates two clockwise circuits off Tunisia and Libya. Two relatively large counterclockwise circuits are also indicated: one southwest of Crete and the other in the northern Ionian. Then, the AW flow meanders in the southwestern and central Levantine, generating small counterclockwise and clockwise circuits in the area of Mersa-Matruh before roughly splitting into two branches. One branch flows alongslope, thus enclosing an area that could be assimilated to "Shikmona", while the other one progresses directly towards Cyprus. Part of the former branch joins the latter east of Cyprus and both form the "AMC", which will join the other part west of Cyprus to form what could be assimilated to the counterclockwise "Rhodes gyre" and to a "West Cyprus gyre". The AW flow then penetrates the Aegean.

Lacombe and Tchernia's (1972) schema (Fig. 1c), based on complementary hydrological data, represents a kind of "AIS", a large counterclockwise circuit in the central and northern Ionian, and two clockwise circuits off Tunisia and Libya. Contrary

to Ovchinnikov's schema, it does not display a "Cretan gyre". In the Levantine the AW flow diverges, similarly to what was represented in the western basin (see Millot, 1985, for the related discussion). Part of the flow continues its progression alongslope and counterclockwise at basin scale, while the other part spreads seaward towards Cyprus. Within the "Rhodes gyre" area the schematised circulation is rather complex. No AW is shown entering the Aegean, where the major schematised feature is the outflow from the Black Sea.

The asset of Robinson *et al.*'s (1991) schema (Fig. 1d) is the introduction of a kind of mesoscale variability (even though they mainly describe gyres while we describe eddies). Little information is provided in the Ionian, where the AW flow meanders and forms the "AIS". Two permanent features are indicated, the Pelops eddy and the "Cretan gyre". In the northern Ionian the circulation is indicated to reverse seasonally. The AW flow continues in the central Levantine and forms the "MMJ" (called the "Central Levantine Basin Current" by Özsoy *et al.*, 1989). Then, the "MMJ" splits into a series of branches. Some branches turn counterclockwise west of Cyprus, forming the "Rhodes gyre" and the "West Cyprus gyre", before becoming the "AMC" that merges with the northern parts of both gyres. Other branches turn clockwise and feed a set of permanent or transient and recurrent clockwise gyres, the major two being known as "Mersa-Matruh" and "Shikmona" (as first named by Hecht *et al.*, 1988). There is no indication of a possible alongslope counterclockwise flow; furthermore, a clockwise alongslope flow is indicated off the Middle East coasts, south of Cyprus. AW outflows from the southeastern Levantine around Cyprus, forming the "recurrent CC" that will then join the "AMC". Other features are indicated either as recurrent or transient: the cyclonic "Latakia eddy", the anticyclonic "Antalya eddy" as well as other anticyclonic eddies in the Ionian, the southern Cretan and the southeastern Levantine. The transient anticyclonic eddy southeast of Crete (now named Ierapetra) is indicated with a relatively small size and there is no indication of a possible "AMC" penetration into the Aegean.

Robinson and Golnaraghi (1993) refined Robinson *et al.*'s schema (Fig. 1e), hence making it relatively complex. In the Ionian they represent the splitting that the "AIS" is said to have encountered in summer 1987, especially with a major branch that circulates clockwise alongslope off Italy and

Greece, enclosing the Pelops eddy and entering the southern Cretan. Another major branch of the “AIS” meanders and crosses the whole central Ionian before joining the former branch. In the Levantine, all mesoscale clockwise features previously indicated in the southeast can possibly merge into a unique clockwise circuit. Therefore, the resulting circulation in the southeastern Levantine is definitely clockwise off the Egyptian slope.

The schemata and analyses available at subbasin and meso- scales

The subbasin circulation schemata

With time and increasing data sets and modelling efforts, subbasin scale schemata sometimes differ markedly from the basin-scale ones, although mainly based on the same core of data. Within the channel of Sicily, the “AIS” undulates in very different paths according to Robinson and Golnaraghi (1993; Fig. 1e), Malanotte-Rizzoli *et al.* (1997, Fig. 3a) and Robinson *et al.* (1999, not shown). In the Ionian, the schema by Malanotte-Rizzoli *et al.* (1997) completed by Napolitano *et al.* (2000, not shown) is based on a revisit to the POEM 1986-1987 data set. The “AIS” flowing around southern Sicily bifurcates near 37°N into two main branches. The first branch reverses clockwise directly towards Africa and encloses two anticyclonic eddies. No possible development of this branch south of ~34°N is indicated, and this branch does not contribute any more to the general circulation, contrary to the schema of Robinson and Golnaraghi (1993) (Fig. 1e). The second branch extends further into the northeastern Ionian as far as ~39°N, and then turns clockwise to cross the entire Ionian southeastwards, forming the “Mid-Ionian Jet, MIJ”. Thus the circulation is no longer clockwise alongslope in the whole northern subbasin, as represented in the schema of Robinson and Golnaraghi (1993, Fig. 1e). The “MIJ” enters the southern Cretan from far offshore, and becomes the “MMJ”. South of Crete, some of the AW flow (transported eastwards by the “MMJ” and transformed into “Levantine Surface Water: LSW”) flows back northwestwards. When entering the Ionian, “LSW” forms two branches, one flowing into the southern Aegean, the other dividing into two smaller branches that surround the “Cretan cyclone” and the Pelops anticyclone. Surface water originat-

ing from the Adriatic (“Adriatic Sea Water: ASW”) is mainly entrained southeastwards by the “MIJ” across the Ionian and transformed into “Ionian Sea Water: ISW”. A cyclonic eddy south of Italy, a cyclonic eddy northwest of Greece and an anticyclonic eddy between Crete and the Peloponnese have been added.

In the central part of the basin (33-37°N, 20-30°E), it has been known for a long time (e.g. Lacombe *et al.*, 1958; Burman and Oren, 1970) that large exchanges of surface water between the Levantine and the Aegean / northern Cretan occur through the east-Cretan straits. The Zodiatis (1992, 1993) analysis is consistent with the Theocharis *et al.* (1993) schemata for late winter 1986 and late summer 1987 (Fig. 3b,c). The “AMC” always splits before Rhodes. One branch penetrates into the Aegean through the Rhodes strait while the other forms the northern part of the “Rhodes gyre” and penetrates through the other east-Cretan straits (Karpathos and Kasos) in winter only, when the “Rhodes gyre” has its maximum extension and strength. The circulation undergoes a large seasonal variability north and south of Crete. During winter 1986 (Fig. 3b), the “AMC” within the northern Cretan surrounds two cyclonic eddies while it merges with a meandering “MMJ” in the southern Cretan. During summer 1987 (Fig. 3c), the circulation meandered eastwards (in opposition to the winter one) within the northern Cretan and through the Karpathos and Kasos straits, while a huge Ierapetra and an intense southward flow due to the Etesians confined the “Rhodes gyre” to the east. Within the southern Cretan, the interpretation of the data is that the “MMJ” is located far to the south in summer. The “Pelops and Cretan gyres” are roughly similar in both schemata. The schema of Theocharis *et al.* (1999, Fig. 3d), based on CTD data from March 1994 to February 1995, shows an “AMC” partly entering the Aegean and partly veering south, where it appears likely to merge with the “MMJ”, which is indicated to form the northern border of the “Ierapetra gyre”. Refinement since the previous version includes the following permanent features in the northern Cretan: a gyre, an anticyclone and a cyclone.

The schema of Theodorou *et al.* (1997) (Fig. 3e), based on CTD data in winter 1994, confirms the northward spreading of the “AMC” through the east-Cretan straits shown by Theocharis *et al.* (Fig. 3b, d), but describes an eastward (i.e. opposed) circulation in the northern Cretan.

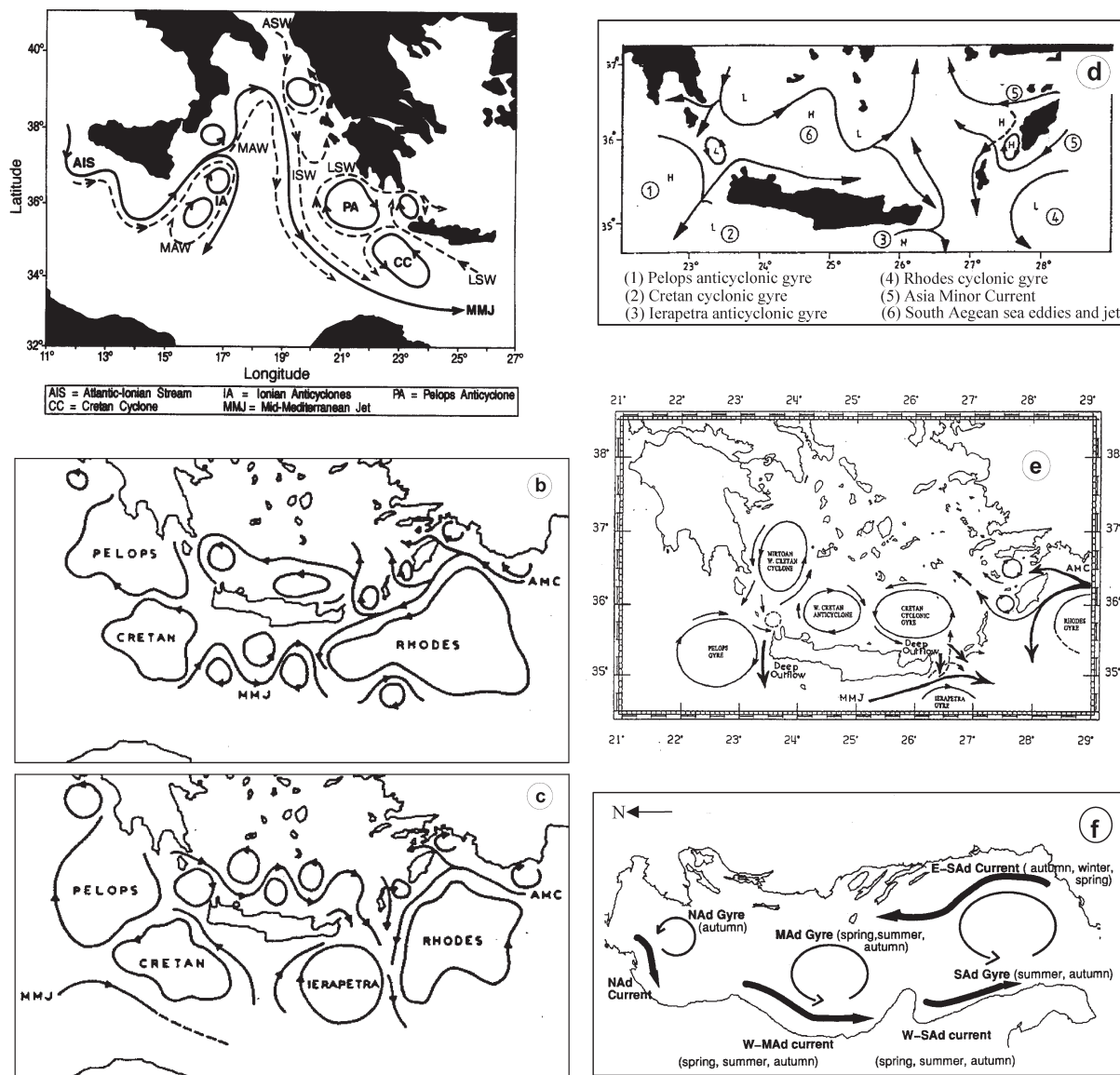


FIG. 3. – The different schemata of the surface circulation in: the Ionian (a) from Malanotte-Rizzoli *et al.* (1997); the Cretan in late winter 1986 (b) and late summer 1987 (c) from Theocharis *et al.* (1993), from Theocharis *et al.* (1999) (d), and from Theodorou *et al.* (1997) (e); the Adriatic from Artegiani *et al.* (1997) (f).

In the Adriatic, the schema of Artegiani *et al.* (1997) represents a counterclockwise circulation separated into segments, with a marked seasonal variability (Fig. 3f). In winter, the circulation is composed only of an inflow on the eastern side of the southern Adriatic and a southward current in the northwestern area. In summer, only southward segments appear along the remainder of the Italian coastline. Two major counterclockwise gyres are schematised in the central and southern Adriatic except during winter; they are therefore partially disconnected from the inflow which is mainly indicated for winter.

Studies of specific gyres and eddies

a) Pelops

According to Theocharis *et al.* (1999), Pelops is an anticyclonic deep (>2000 m) feature located southwest of Peloponnese. There is a general agreement that it is forced by the winds (Le Vourch *et al.*, 1992; Golnaraghi and Robinson, 1994; Ayoub *et al.*, 1998). However, it is also considered as an “AIS” meander by Marullo *et al.* (1999a), as a permanent eddy by Robinson *et al.* (1991) and gyre by Theocharis *et al.* (1993, 1999). Matteoda and Glenn (1996) suggest it is an almost persistent feature sub-

ject to interannual variability since, from weekly IR images, they infer its continuous presence from autumn 1990 to spring 1992, its absence during ~2 years, and then its temporary occurrence during the 1994 and 1995 winter-spring periods. According to Ayoub (1997) who analysed altimetric data (1992-1996), Pelops represents a complex series of eddies moving along the Greek coasts, which is generated in late autumn and persists until the end of the winter with a maximal intensity in November-December. Larnicol *et al.* (2002) analysed similar data (1993-1999) and indicate that Pelops is recurrent, displaying a seasonal variability with a strengthening in autumn-winter. Although they also indicate an interannual variability of its location, Pelops is generally located south of Peloponnese in autumn-winter and west-southwest of it in spring-summer, thus agreeing with Matteoda and Glenn (1996) on its tendency to propagate westward.

b) “Western Cretan gyre”

It has been described as a “permanent cyclonic gyre” located southwest of Crete, its size varying according to the authors (e.g. Ovchinnikov, 1966, Fig.1b, Robinson *et al.*, 1991-1993, Fig. 1d-e). However, according to satellite images and in situ data (e.g. Le Vourch *et al.*, 1992; Theocharis *et al.*, 1993; Matteoda and Glenn, 1996), the relatively cool SST values and the associated doming structure mainly occur from late summer to early winter as a consequence of the Etesians.

c) Ierapetra

This intense anticyclonic eddy located southeast of Crete was first studied by Burnett *et al.* (1991), who named it the “East Cretan eddy”, and by Theocharis *et al.* (1993) who first named it Ierapetra. It has a diameter of 100 to 150 km, it can occupy half of the southern Cretan (Hecht and Gertman, 2001) and its signature can extend down to at least 1500 m (Theocharis *et al.*, 1999). Although it is mentioned as a gyre (Larnicol *et al.*, 1995; Lascaratos and Tsantilas, 1997; Theocharis *et al.*, 1993, 1999), there seems to be a general agreement about the Horton *et al.* (1994) hypothesis that Ierapetra is due to the curl imposed on the Etesians by the Crete orography. Ierapetra could be intensified by the outflow from the Aegean through the Kasos strait (Kotsovinos, 1997).

However, there is a disagreement about its formation period and longevty. Larnicol *et al.* (1995)

indicate that Ierapetra intensified at the end of summer, was weak in spring and absent in June-July during the period October 1992 to September 1994. Ayoub (1997) and Ayoub *et al.* (1998) indicate a weakening of this eddy from winter to spring and an intensification from summer until late autumn during the period October 1992 to December 1993. According to Matteoda and Glenn (1996), Ierapetra persisted during the whole studied period (October 1990 to March 1995), except for the 1993 and 1994 summers. According to the Lascaratos and Tsantilas (1997) analysis of 155 weekly IR composites from the period July 1993 to June 1996, Ierapetra undergoes an annual cycle with some interannual variability. It is generated in spring-summer, becomes fully developed in late summer and disappears in the following spring. According to Larnicol *et al.* (2002), the Ierapetra formation in 1996 and 1997 was specific with an occurrence far to the south of its normal position. As already suggested by Theocharis *et al.* (1993), these authors closely link the Ierapetra variability with the variation in latitude of the position of the “MMJ”.

d) “Mersa-Matruh”

According to Brenner’s (1989) analysis of POEM data (October 1985, March 1986), this feature is an “Egypt eddy” that is generated in summer close to the Egyptian coasts by an unstable meandering of the “NAC” and then propagates ~160 km northeastwards at ~1 km/d. According to other studies, this feature is a permanent gyre called “Egypt gyre” (Said, 1984) or “Mersa-Matruh gyre” (Robinson *et al.*, 1991; Tziperman and Malanotte-Rizzoli, 1991; Malanotte-Rizzoli and Bergamasco, 1991). Golnaraghi (1993) claims it is the strongest gyre in the eastern basin (up to 350 km in diameter) frequently interacting with the “MMJ”. “Mersa-Matruh” is also described as a complex system composed of several mesoscale eddies (Özsoy *et al.*, 1989; Horton *et al.*, 1994; Ayoub, 1997) or as a meander of the “MMJ” (Larnicol *et al.*, 2002). Zervakis *et al.* (2002) consider that “Mersa-Matruh” is a stable anticyclone that progressively disappears along a specific transect, probably having disintegrated into smaller scales, and suggest that it is more a closed eddy (transport >4 Sv) than a meander of the “NAC”.

Horton *et al.* (1994) and Ayoub (1997) mention that the most convenient period to observe an

intense “Mersa-Matruh” would be during the weakening / absence of Ierapetra while the analysis of the POEM-1991 data (Malanotte-Rizzoli *et al.*, 1999) shows the simultaneous presence of a strong Ierapetra and a strong “Mersa-Matruh”. According to the numerical simulations of Roussenov *et al.* (1995), “Mersa-Matruh” is generated in summer and intensifies in November before splitting into two cells. Larnicol *et al.* (1995) mention that it does not have any clear recurrence period and is characterised by rather short time scales. According to other model results (Malanotte-Rizzoli, 1994; Zavatarelli and Mellor, 1995; Brankart and Brasseur, 1998) and the analysis of weekly and monthly IR satellite composites from the period 1983 to 1992 (Marullo *et al.*, 1999a,b), “Mersa-Matruh” can be absent.

e) “Shikmona”

Some authors indicate that “Shikmona” is composed of anticyclonic mesoscale eddies originating in the north (Feliks and Itzikowitz, 1987; Brenner, 1989). However, Özsoy *et al.* (1989, 1991), POEM Group (1992), Robinson *et al.* (1991) and Larnicol *et al.* (2002) indicate that a recurrent clockwise gyre is generated there by the “MMJ”. According to Ayoub *et al.* (1998) and Zodiatis *et al.* (1998), “Shikmona” represents a complex system composed of mesoscale eddies, the positions, sizes, and intensities of which vary markedly. An anticyclonic eddy lying south of Cyprus, which Brenner (1989) calls the Cyprus eddy, and estimated to have a ~3-year lifetime (Brenner, 1993) is expected to be the major element of this system by Özsoy *et al.* (1993) and Ayoub (1997).

“Shikmona” is given to be either permanent (Hecht, 1988; Özsoy *et al.*, 1989) or recurrent (Robinson *et al.*, 1991). According to models, “Shikmona” is either encountered in all seasons except in winter (Tziperman and Malanotte-Rizzoli, 1991), or generated in summer before propagating westwards and decaying in late autumn (Roussenov *et al.*, 1995), or absent (Malanotte-Rizzoli and Bergamasco, 1991; Malanotte-Rizzoli, 1994; Zavatarelli and Mellor, 1995). Larnicol *et al.*, (1995) indicate that it does not have any clear recurrence period and is characterised by rather short time scales. According to Brenner (1993) and Horton *et al.* (1994), its surface signature is weak in winter and not always detectable in summer due to the strong seasonal thermocline.

f) “Antalya gulf eddies”

Özsoy *et al.* (1993) indicate the occurrence (from 1986 to 1990) of eddies with a vertical extent of ~300 m at least at both the entrance (where the eddy is said to be recurrent) and the exit (where the eddy is said to be permanent) of the gulf.

g) “Rhodes gyre”

It is well known (at least from Nielsen, 1912, p. 140) that a process of dense water formation (mainly of LIW) occurs in the northern Levantine, more specifically south of Rhodes. Ovchinnikov (1966) as well as recent schemata (e.g. Fig. 21c,d, 22b,c) indicate that this occurs in an area permanently enclosed by a counterclockwise circulation commonly named the “Rhodes gyre”. Özsoy *et al.* (1989) correlate this gyre with the Etesians, so that it is expected to be more intense in summer. While the “Rhodes gyre” is said to be generated by the Cretan sea outflow (Kotsovinos, 1997) and/or to be delimited in the south by the “MMJ” (Robinson *et al.*, 1991), Theocharis *et al.* (1993, 1999) indicate that the “AMC” surrounds the gyre on its northern and western edges.

In summary, there is clearly no agreement at basin scale between the “historical” schemata and the recent (POEM) ones, the major question being the occurrence or not of an overall counterclockwise circulation. Additional debates concern the characteristics of nearly all mesoscale features of the circulation at subbasin scale, in particular their forcing mechanism (i.e. are they eddies or gyres?) and lifetime (i.e. are they permanent, recurrent or transient?).

RESULTS: THE SURFACE CIRCULATION INFERRED FROM THE IR IMAGES ANALYSIS

Given the amount of data and the time span, we have found it more efficient to identify regions where specific dynamics occur, and to present our analysis region by region. For each region, as roughly defined in Figure 1a, we detail one or a few situations that are representative of the overall dynamics there. Note that the AW upper part has been given specific names by previous authors depending on the subbasins. However, we consider that the AW transformation is a continuous process, and we identify surface water everywhere with AW only.

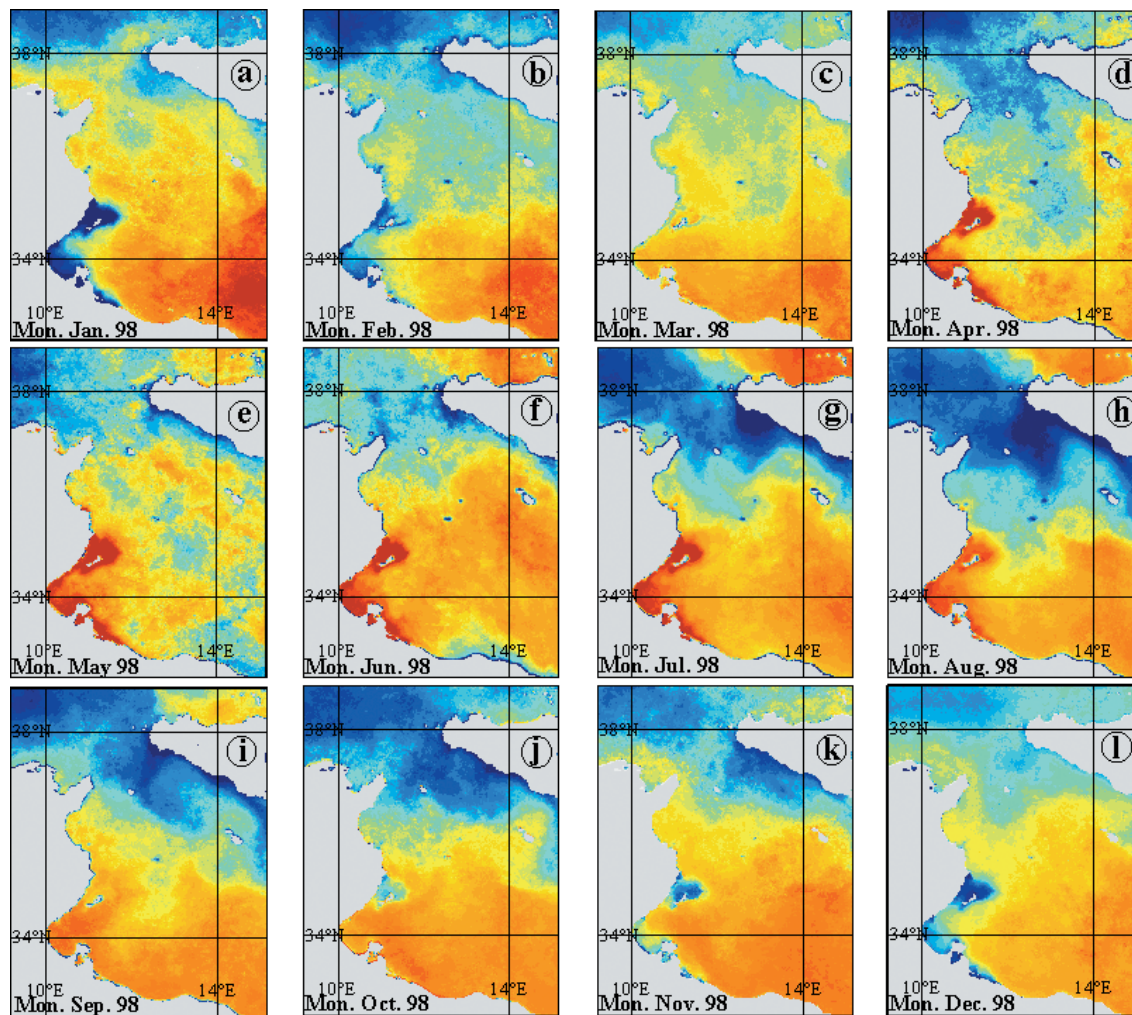


FIG. 4. – The channel of Sicily from January to December 1998. N.B.: In all images the temperature increases from blue (clouds in white) to red.

The channel of Sicily

The channel of Sicily is logically the first region to deal with for AW circulation in the eastern basin. However the visual analysis is most difficult there (see below), and therefore readers that are inexperienced in analysing thermal patterns might want to temporarily skip this sub-section. Indeed, complex and shallow bathymetry (continental shelves, banks, islands) within and southwards from the channel generates mesoscale turbulence that increases the AW “self-mixing” and tends to decrease the AW SST there. The frequent occurrence of several-day episodes of strong northwesterly winds, especially in winter, suddenly induces intense mixing within a strip through the channels of Sardinia and Sicily. Overall, SST values are lower near Sicily than near Tunisia due to the slope of the interface between the AW inflow and the

LIW (Levantine Intermediate Water) outflow, and to the upwelling induced by the dominant northwesterly winds. Out of the channel, the extremely shallow bathymetry around the Kerkennah and Djerba Islands ($\sim 34^{\circ}\text{N}$ - 11°E) leads to the largest (resp. lowest) SST values encountered in the whole sea in summer (resp. winter, except in the northern Adriatic and Aegean). Finally, the southward opening of the channel of Sicily allows AW to flow south and to rapidly warm up all year long. To overcome these specific difficulties, we focus on the annual cycle and analyse monthly composites (for 1998, Fig. 4). In January, there is a clear splitting of the AW flow exiting the channel of Sardinia into a branch that continues alongslope around the Tyrrhenian and a second main branch that penetrates through the channel of Sicily. This splitting can be seen during the other months as well, except during summertime, within the strip mentioned

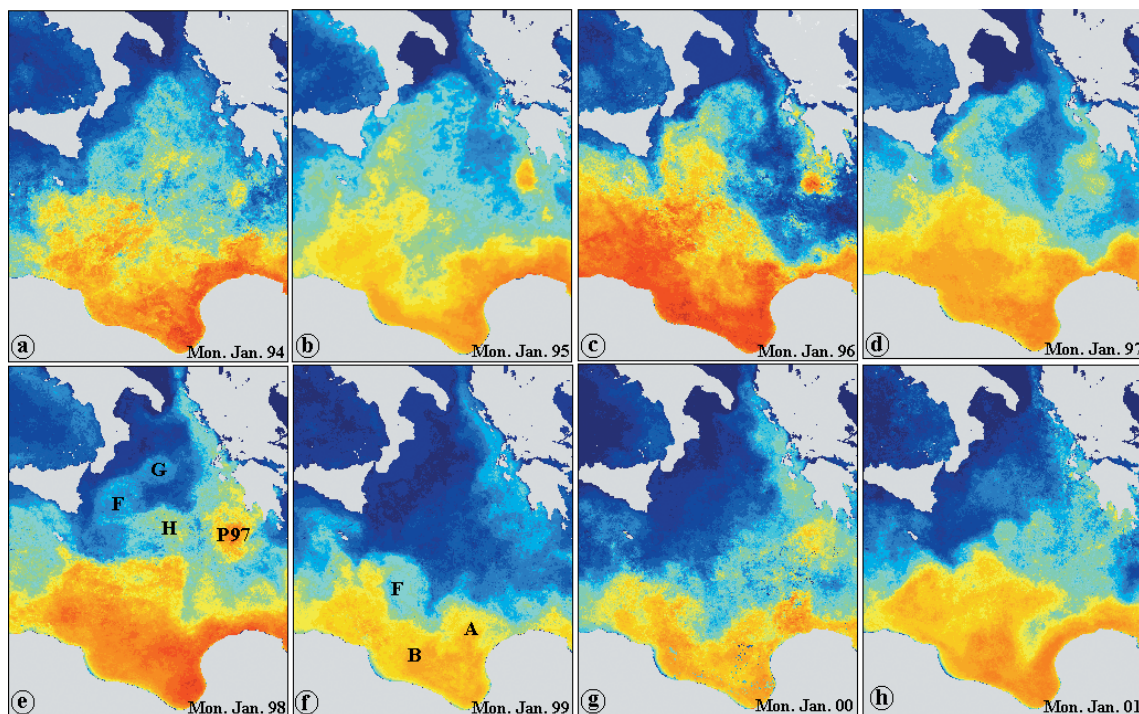


FIG. 5. – The Ionian in January from 1994 to 2001.

above, when the northwesterly winds mix AW. It is thus expected to occur all year long. Within the channel, AW first flows close to Tunisia. Then the continental shelf widens near 35–36°N (Fig. 1a), so that part of the flow tends to follow the coastline while another part tends to follow the shelf edge and spread in the middle of the channel. Although this is not very clear from Figure 4, a significant amount of AW continues following the (curved) shelf edge and thus hits the African coastline near 12–13°E. Images such as the one in Figure 4k suggest that some AW can then flow clockwise over the Tunisian (and partly Libyan) continental shelf.

The Ionian from 1994 to 2001 and from May 1997 to December 1999

Due to the complex bathymetry and processes occurring in the channel of Sicily, AW enters the Ionian over its whole southern part so that the surface circulation there is *a priori* relatively complex. In addition, the overall counterclockwise circulation expected from basic considerations should close there (see Fig. 1a). Moreover, as the Ionian has a large meridian extension and characteristic forcings and features, it varies markedly from north to south. Given the complexity of the phenomena, as well as the long lifetimes and the large drifts of mesoscale

eddies, we first describe the whole subbasin during a decadal period and then detail mesoscale features during a few consecutive years.

The whole subbasin from 1994 to 2001 (Fig. 5)

The January composites show a branch spreading in the northern half of the subbasin from 1994 to 1997 that is weaker in 1998 and absent from 1999 to 2001. Full-resolution monthly composites available from March 1993 and low-resolution composites from previous years (see Fig. 22) show that this branch has been present from the late eighties (at least) to January–February 1998. Although it could be partly associated with the alleged “AIS”, its signature does not resemble that of a meander involving most of the AW flow or at least re-joining another branch further east. Figure 5 suggests that this AW branch progressed north-northeastwards before spreading in a diffusive manner. This branch generated relatively large anticyclonic features in 1996 as well as mesoscale eddies such as F, G and H from May 1997 (see detailed tracking in Figs. 6 to 8). Southeast of Greece, the Pelops wind-induced eddy displays a marked interannual variability with, for instance, the occurrence of 2 eddies in January 1997, high intensity in January 1998 and a weak signature in January 1999 (but still detected in December 1998, see Fig. 8j).

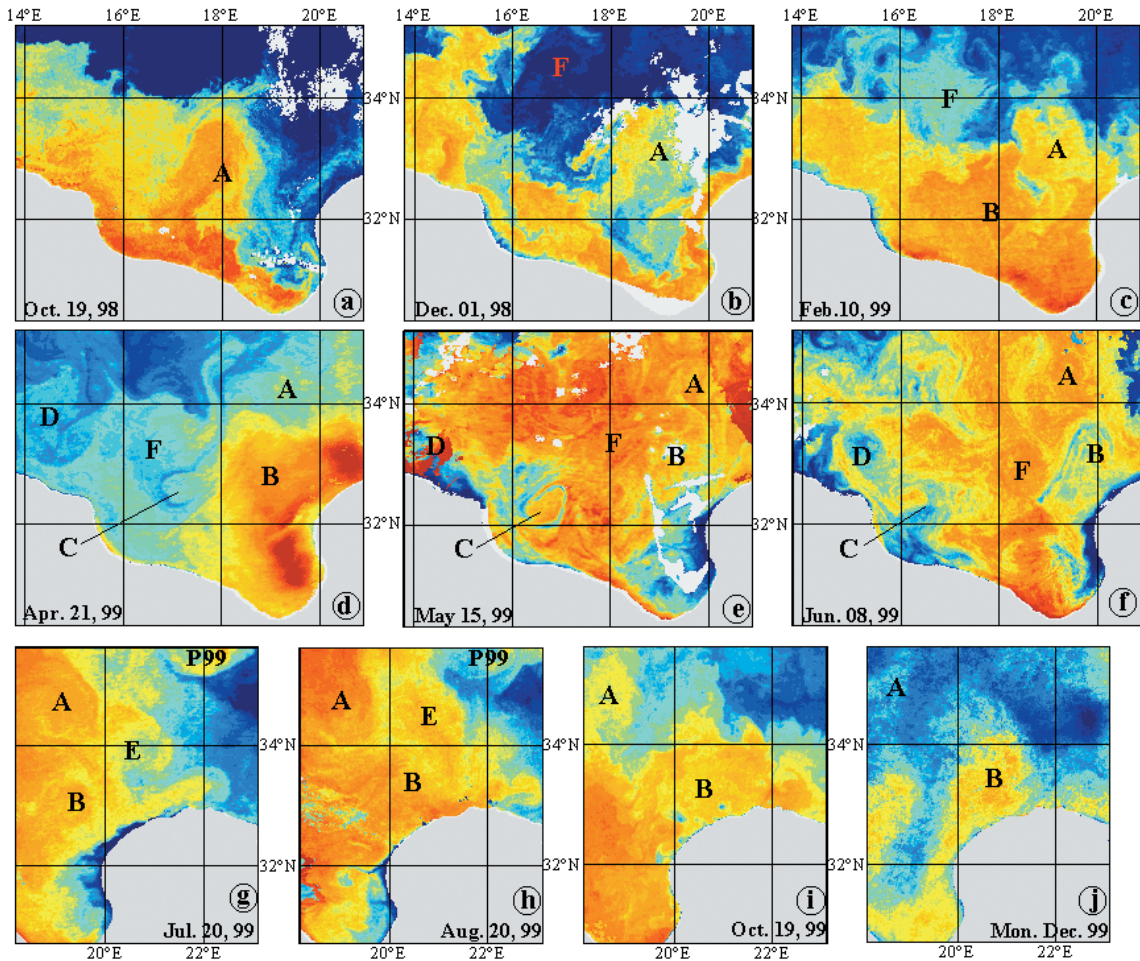


FIG. 6. – The southern Ionian from mid-October 1998 to December 1999.

The southern part from October 1998 to December 1999 (Fig. 6)

The October image shows that AW along Africa is more widespread in the west than in the east, which is the common overall distribution there. We hypothesise that this is due to the bathymetry, since the continental shelf which is more than 2° of latitude wide in the west rapidly disappears eastwards of $\sim 15^\circ\text{E}$ (see Fig. 1a), allowing AW to be deeper and thus narrower. As most of the eddies described hereafter (except F and C), A originates from the alongslope flow, it is anticyclonic, 100 to 200 km in diameter, and drifts at a few km/d maximum along the deeper isobaths. The AW flow continuity along the whole Libyan coast, its instability and variations in width, as well as the northeastward drift of A (that will pinch off near 18°E) are better evidenced in December. F (already located in Fig. 5) is cooler since it comes from the north. In February, A (temporarily) interacts with the flow from which it orig-

inated near $19\text{--}20^\circ\text{E}$, i.e. far downstream from where it pinched off three months earlier, while B develops just at that place. F continues drifting southwards (and now has a warmer signature).

In April (high SST values in the east are due to warm spots), B drifts northeastwards between the alongslope flow and A, which either is pushed seawards by B and / or drifts along the deeper isobaths. F, which is still relatively cool, has now reached the Libyan slope and starts interacting mainly with B. This interaction creates a cyclonic shear eddy C separated from B and F by a cool filament that is the continuation of the Maltese filament (defined in a following subsection). D, which is similar to A and B, developed upstream from where both A and B were formed. In May, A, B and D appear roughly similar but F and C have changed dramatically. F has decreased in size, it has drifted eastwards and it is now as warm as the surrounding waters. However, C has increased in size (such a large cyclonic eddy is rarely encountered), it has drifted

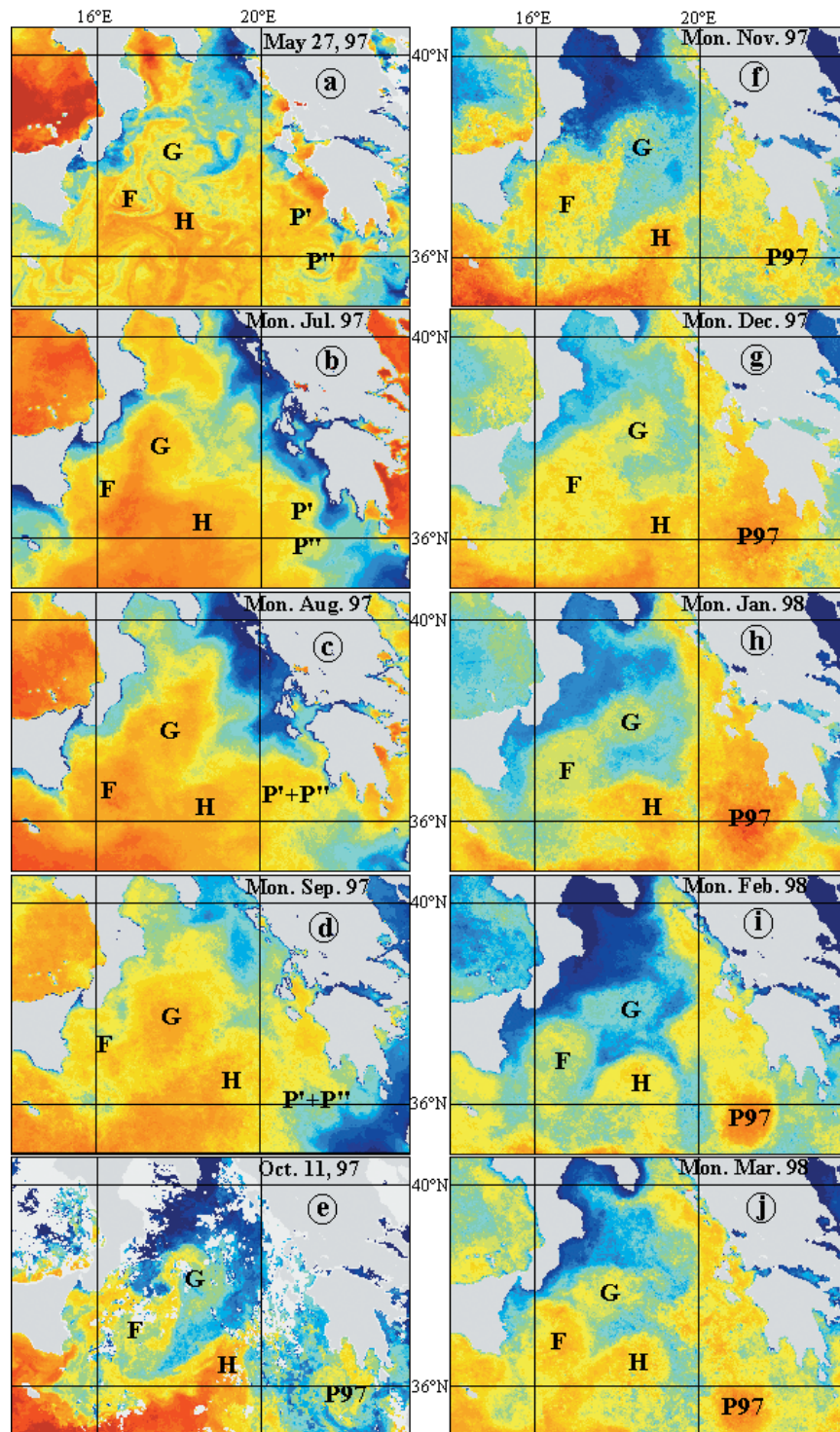


FIG. 7. – The northern Ionian from late May 1997 to March 1998.

southwestwards and thus strongly interacts with the alongslope flow in a large portion of the coastal zone. In early June, B which is now relatively cool is found between the alongslope flow and A. D has slightly propagated downstream, F has continued eastwards, and C is mainly unchanged. Although C

will disappear in late June, its 2.5-month lifetime represents a kind of a maximum for a cyclonic eddy. F will also be lost by late June but D will be recognised with the same location, shape and size during more than 6 months before being lost in winter (not shown).

The July-December images of the Cyrenaica zone (part of Libya centred near 32°N-22°E) show the general circulation of warm AW alongslope, the slow (a few km/d) downstream propagation of B as well as the westward drift and decay of A. It also shows E (created in April out of the Fig. 6a-f frame), its seaward drift and decay (mainly due to the fact that E fed P99, not shown). B will cross the zone (near 20°E) which is seemingly favourable for pinching-off (e.g. A and E), and will be lost downstream in the following months (not shown). The coastal upwellings often encountered west of Cyrenaica (Fig. 6e-j) display small-scale variability that allows their downstream propagation to be evaluated to a few km/d.

The northern part from May 1997 to March 1998 (Fig. 7)

The daily image in Figure 7a evidences in details all features tracked hereafter. In summer, the major feature at subbasin scale is the upwelling induced by the Etesians off the northeastern coasts. An alongslope counterclockwise circulation appears there as soon as the Etesians stop, i.e. in September, which lasts during the whole winter. Its penetration from the Ionian into the Adriatic and its splitting before the Otranto strait (south of the sub-basin) are evidenced during all of autumn and winter.

In late May, P' and P'' in the east as well as F (the late stages of which were analysed in the previous subsection) and G in the west are similar to the eddies shown by Le Vourch *et al.* (1992) in June and September 1985 resp. (numbered 3 and 7 resp.). P' and P'' are probably induced by the Etesians while F and G originate from the branch discussed in the subsection dealing with the whole Ionian. In-between, the origin of H and of the eddy south of F and H (not labelled since it will move southwards soon and be out of the image frames) cannot be specified. All eddies can still be recognised in July. In August, P' and P'' begin to merge while F and G interact but do not change significantly. In September P' and P'' have completely merged, H is drifting northeastwards and F and G are still interacting. In mid-October and in November, warm water accumulates roughly where P' and P'' were and in the Pelops area, so that we have named this feature P97. H is still individualised while F and G are still interacting. In December and January, P97 is warmer than the surroundings and definitely signs a coherent structure. H does not drift significantly,

while F and G begin separating. All these features are increasingly marked in February and March.

The central part from April 1998 to December 1998 (Fig. 8)

In mid-April and May, P97 drifts westwards, H drifts northwards and G decays. F, described in its earlier and later stages in the two previous subsections, is stationary. J and K develop along the western Libyan slope. In late June to early July, F starts drifting southwards, P97 and H continue drifting westwards and northwards resp., and J and K merge (noted K+J) while L is growing upstream. In late July, P97 is between F, which continues drifting southwards, and P98, which starts growing. Although the signature of F in early September is complex, that of P98 is clear. P97 is north of the segment joining F and P98 while K+J and L are still propagating downstream at a few km/d.

The cool filament that crosses most of the sub-basin in Figure 8f (see also Fig. 6d) and can be recognised on all preceding images originating from the southern tip of Sicily deserves a specific comment. The cool Sicilian coastal waters are entrained roughly southeastwards by the AW inflow, and possibly by the overall alongslope counterclockwise circulation in the Ionian (Fig. 1a). This filament, classically named the "Maltese Front", was studied in detail by Champagne-Philippe *et al.* (1982) and statistically analysed by Le Vourch *et al.* (1992). It separates recent AW in the south that continuously flows in (as described by Figs. 3, 4, 5) from resident / older AW in the north. Since SST values can be similar in both parts of it, it cannot be considered as a classical front and we propose naming it the Maltese filament. Whatever, this feature is associated with cool water entrained around the various anticyclonic eddies, through a paddle-wheel effect, and it has no relation with any kind of "AIS".

In early October, F and P97 are still well identified and P98 is as coherent as was P97 one year ago. A (see Fig. 6), which first appears in this series in Figures 8e-f, has now drifted northwards and entrains the Maltese filament. Figure 8h in late October does not allow F, P97 or P98 to be evidenced easily due to clouds, but shows that inflowing waters in the south can be separated by a well-marked front from cooler waters resident in the north. Hence, in situ data collected only in the northern part of the subbasin (thus sampling only the northern part of a

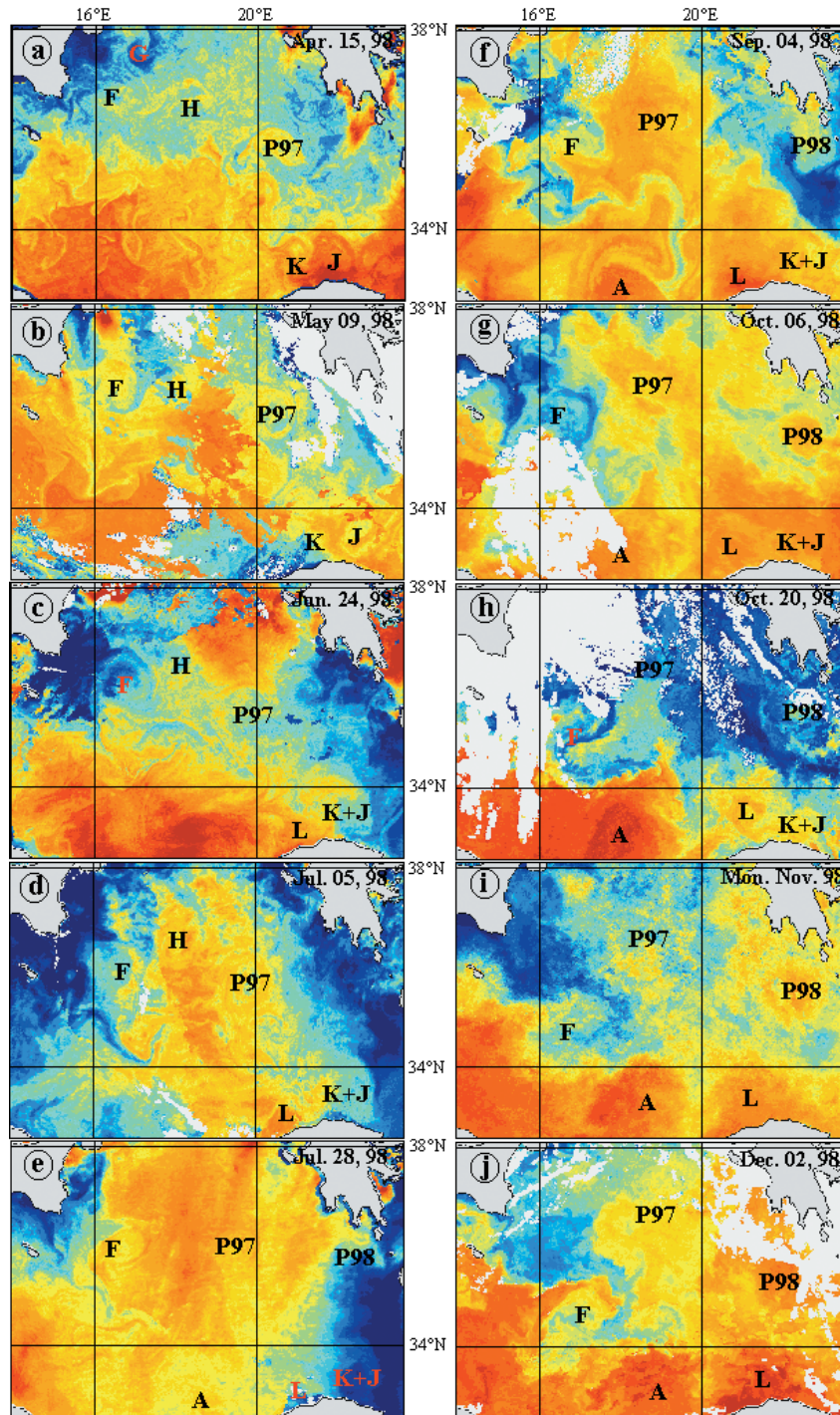


FIG. 8. – The central Ionian from mid-April to early December 1998.

turbulent inflow) and analysed without any help from space will erroneously suggest the occurrence of an “AIS” crossing the subbasin.

The November and December images first certify that F, P97 and P98 are still coherent structures. Incidentally, they show that two wind-induced eddies (P97 and P98), generated in the same place

according to the same seasonal process, can co-exist one year and a few 100 km apart. They also show that F, which was north of the Maltese filament before early September and south of it in early December, has “crossed” it. Therefore, this filament does not have any proper dynamics but just evidences waters entrained from a specific place across

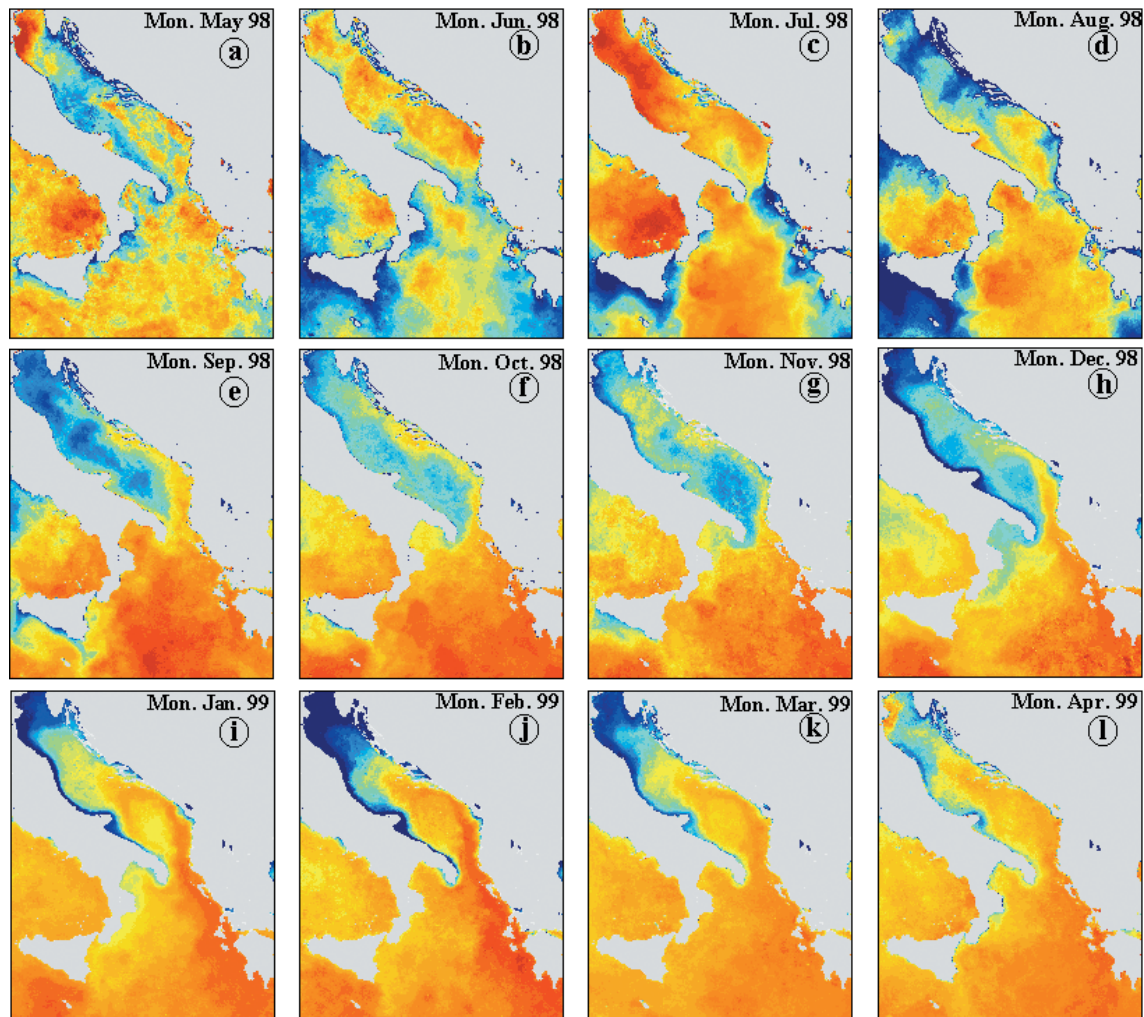


FIG. 9. – The Adriatic from May 1998 to April 1999.

the subbasin. Along the Libyan slope, K+J is out of the frame, while L has increased and is still propagating downstream.

Many eddies are found and seemingly grow where F was in October 1998, which is just east of the Sicilian-Maltese plateau and roughly where the overall counterclockwise alongslope circulation is expected to close (Fig. 1a). Whatever the reasons that make this area an essential place, eddies formed here or passing by can then drift in various directions. Indeed, while F propagated southward, three eddies were shown to drift in series southeastwards (i.e. towards Cyrenaica), one of which was tracked from May 1996 to at least December 1997 (not shown).

The Adriatic from May 1998 to April 1999

Since the dense water formation process dominates the regime here, we focus on the seasonal vari-

ability and show a yearly series of monthly composites (Fig. 9). There is no evidence of a clear circulation pattern in spring except the cool southward flow along the Italian coastline and the local warming of the Po outflow. In summer, the SST field is disturbed by upwellings induced by the Etesians in the northern Ionian and in the Adriatic itself. However, from September until spring, a marked inflow occurred during the 1998-1999 winter that is similar to the one mentioned for the 1997-1998 winter (Fig. 7). A counterclockwise gyre starts forming in the southern Adriatic in summer and develops in autumn. Its signature intensifies in winter and it is closely linked to the inflow. A second gyre occurs in the central Adriatic, from late summer to autumn and winter. No large mesoscale eddies develop there (although they cannot due to the narrowness of the subbasin, we suggest that this is more likely due to dynamical reasons).

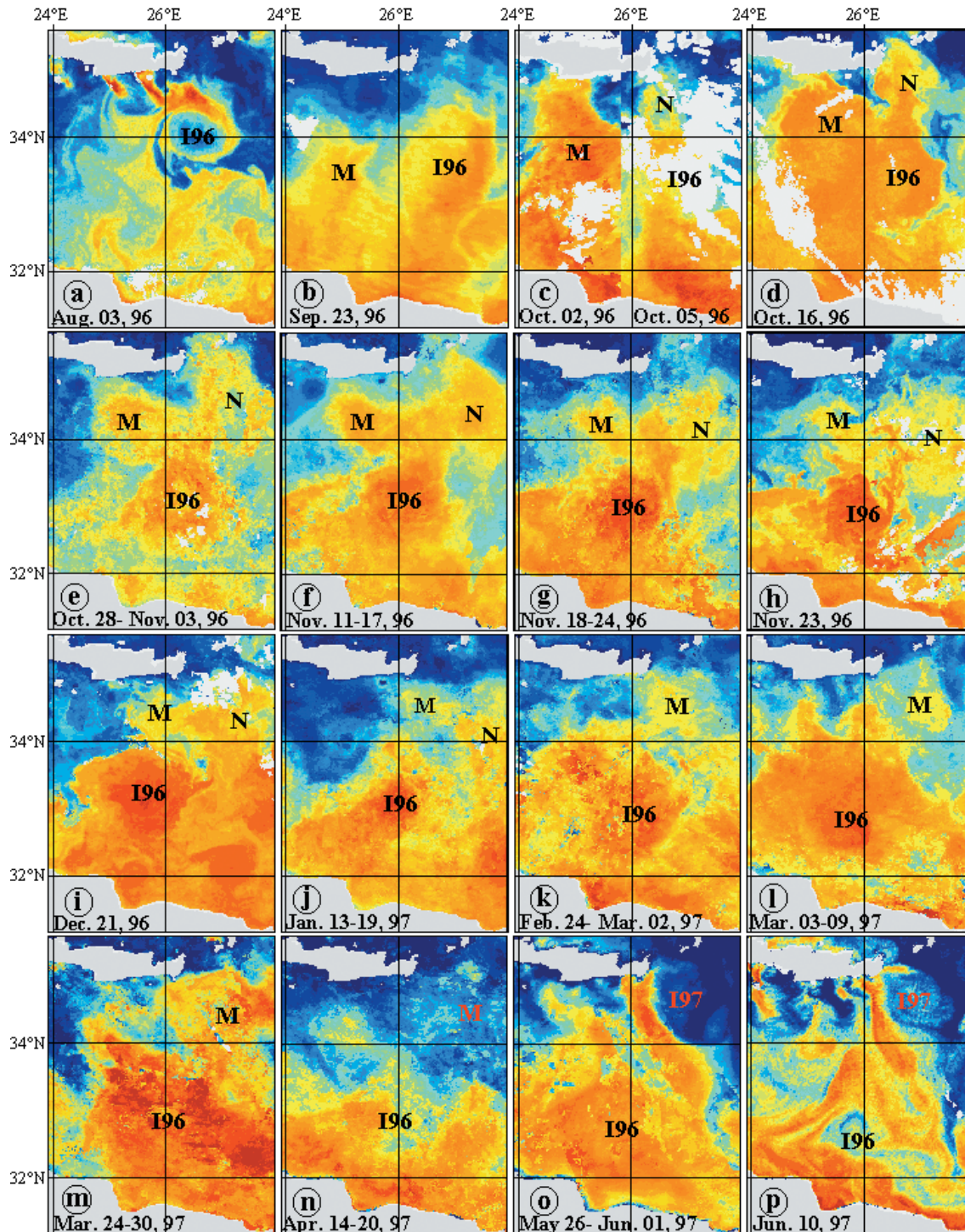


Fig. 10. – The southern Cretan and the western Levantine from early August 1996 to mid-June 1997.

The southern Cretan and the southwestern Levantine from 1996 to 1999

Next we describe features not reported up to now such as: the large southward drift of Ierapetra (I96); the merging of two generations of Ierapetra's

(I96+I97) and their drift; the persistence and stationarity of I98 and I00 as the reason for the strength of I99 and I01 resp.; the co-existence of I98/9 and I00/1; the downstream propagation of the Libyan eddies; the merging of two eddies generated by the AW flow.

The drift of I96 (Fig. 10)

In early August, I96 is fed from the south by a complex zone of relatively warm swirls. By late September, I96 has moved southeastwards while M is drifting northwards west of it. From early to mid-October, I96 continues drifting, M drifts around it towards Crete, and N grows in the north. From late October to January, I96 drifts further southwestwards while M and N still surround it before N disappears. From February to April, I96 stops drifting southwards. M represents water that mainly originated from the south and is present in spring where Ierapetra forms. In June, I97 begins forming, entraining not only old AW (associated with M) but also more recent AW, through a paddle-wheel interaction with I96 still evident alongslope, about 2° of latitude to the southwest.

The merging of I96 and I97 (Fig. 11)

One month later (Fig. 11a), I96 is still south of I97, ~100 km apart. O and Y were formed by instability of the flow along the eastern Libyan slope roughly where Y is, in October 1996 for O and in May 1997 for Y respectively. Note that O and I96 are similarly signed (by warm water from alongslope and cooler water from offshore), although different processes formed them. However, O and Y have a markedly different signature while they have the same origin. In August, I96 drifts northeastwards while I97 is stationary. Both I96 and I97 begin interacting in September and they have completely merged by October. They are recognised from now until February 1998 as a single structure named I96+97. O and Y, which remained stationary until October, start propagating slowly eastwards in November. Note that O and I96+97 are close together in February 1998 and are similarly signed. Meanwhile, Y has markedly decreased in size, it has pinched off from the alongslope flow and it begins drifting seawards around O.

The drift of the merged I96+97 towards the western Levantine (Fig. 12)

One month later (March 1998), Y continues drifting around O. In late April, Q has developed just downstream from O (still flanked by Y on its seaward side) that has drifted westwards. A complex zone R appears in the east. In June, I96+97

drifts southeastwards and is aligned with O (that has continued drifting westwards) and Q; warm water accumulates north of Q and I96+97, depicting an anticyclonic signature; downstream from I96+97, two eddies can be identified in zone R (the easternmost one named U' later in the text). In early July, the major evolutions are the diameter increase of Q, the quasi stationarity of O, the I96+97 location close to the coast, and the small eddies north of Q and I96+97. By mid-August, O is still driftless, Q is squeezed between I96+97 and O, and I98 appears close to Crete. In late August-early September, O and I98 display similar signatures while Q and I96+97 are elongated northeastwards. In early October, O becomes less organised, Q (that drifted westwards) feeds I98, I96+97 is now just upstream from R. In early November, O is no longer identified. It might have decayed, maybe due to its interaction with K+J approaching upstream (see Fig. 8), and be entrained seawards around Q (that has continued drifting westwards). Q is still well defined and continues feeding I98. In the southwestern Levantine, I96+97 has started interacting with R to form a huge (~200 km) anticyclonic feature. In late November, the remainder of O is in-between Q and I98, and the southwestern Levantine is still occupied by the feature that issued from I96+97 and R. Finally (in January), Q is flanked in the northwest by K+J that has propagated downstream and has been deflected around it (in the same way as O did with Y at the beginning of the Fig. 11 time series).

The formation and co-existence of I98/9 and I00/1 (Fig. 13)

Contrary to I96 and I97 that drifted southwards before merging, I98 (which displays a usual signature in autumn 1998) did not drift from winter to spring 1999. Moreover, it was still well developed in May-June 1999, i.e. before the Etesians onset. The August image shows that Ierapetra is fed with water that originated from both the south (the alongslope flow off eastern Libya and western Egypt and its associated mesoscale eddies) and the northeast (the so-called "AMC"). Thus the Etesians forced an already existing eddy, and I99 is logically named I98/9 (at least from October 1999), since its generation differs from that of I96+97. Its signature remained intense throughout the winter 1999-2000. In early spring, I98/9 starts drifting westwards, and

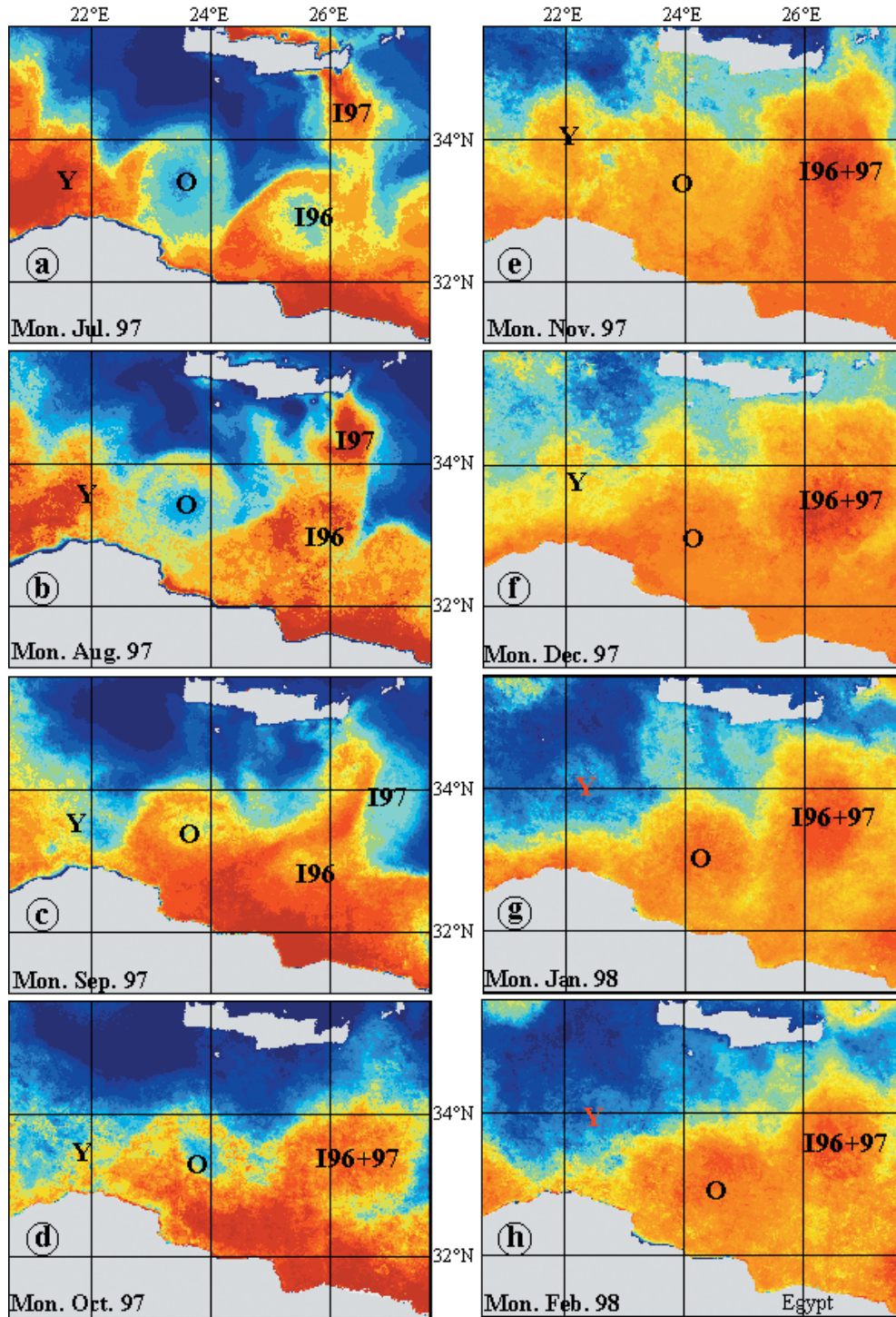


FIG. 11. – The southeastern Ionian and the southern Cretan from July 1997 to February 1998.

is located near mid-Crete when I00 starts growing in early summer 2000. Both are well identified close together and do not drift markedly until late spring 2001. Hence, I00 is located near the Ierapetra formation area in summer 2001 so that, like I98/9, it will evolve into I00/1. Both I98/9 and I00/1 are clearly identified until the end of autumn 2001.

Eddies merging in the southwestern Levantine (Fig. 14)

The warm feature associated with I96+97 and R in late February 1999 (Fig. 14a) is similar to that in January (Fig. 12j). Nevertheless, images in-between are not clear enough to ascertain whether I96+97 has

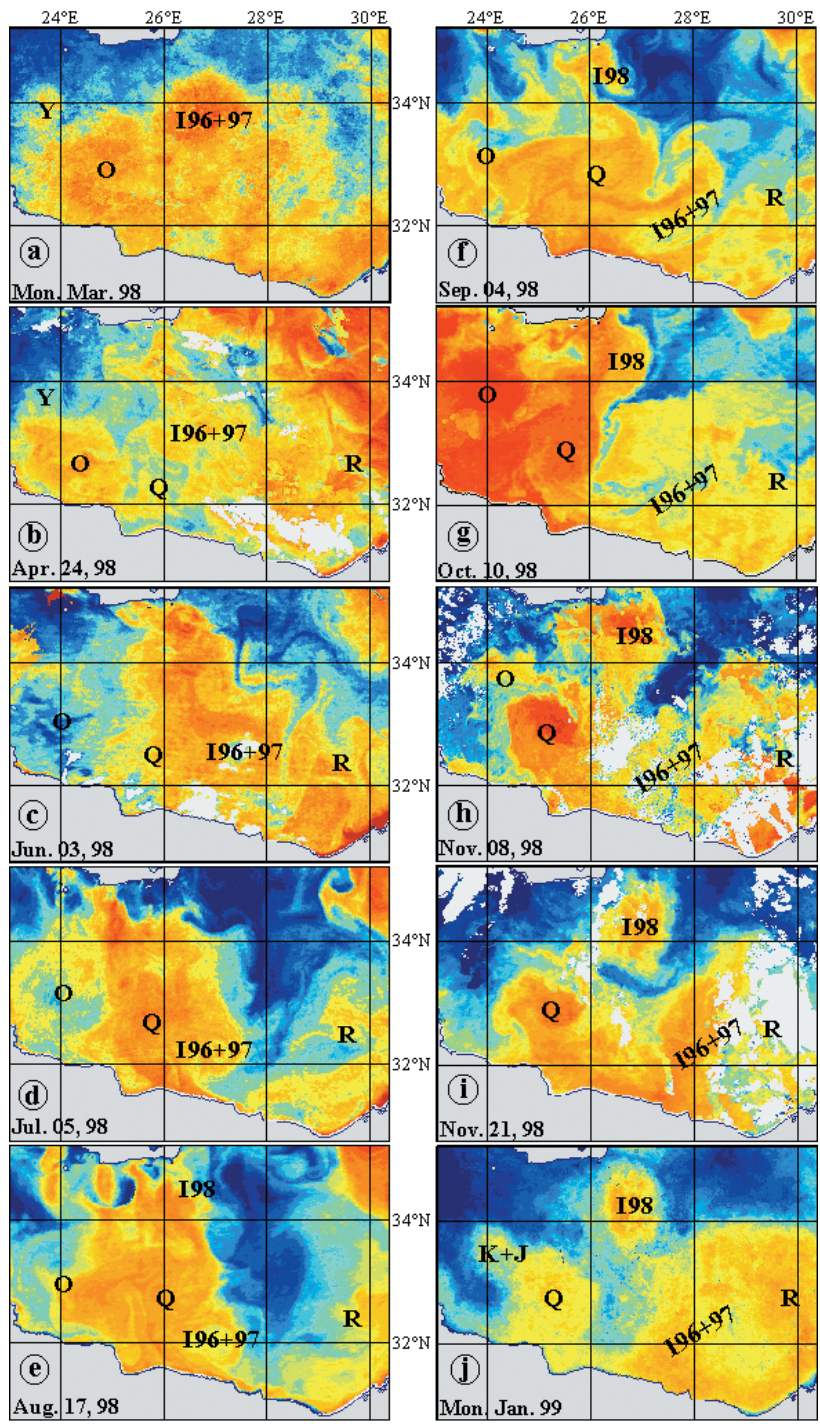


FIG. 12. – The southern Cretan and the western Levantine from March 1998 to January 1999.

persisted. This feature is thus objectively noted I'. While nothing has markedly changed in the southern Cretan, a new feature (S) has grown seawards from I' and R. In April, thermal gradients are weak but images (not shown) allow Q, I98, I', R and S, as well as a new eddy-like feature T to be identified. By mid-May, the situation has changed, except for Q and I98,

since I' extends seawards and interacts with S. The signatures of R and T are difficult to individualise in this image, but their tracking (with images not shown) indicates that R has disappeared, while T maintains its position. In late June I' continues its seawards drift. In late August 1999, I' decays and its remainder appears in-between I98, Q, T and S; U is formed alongslope,

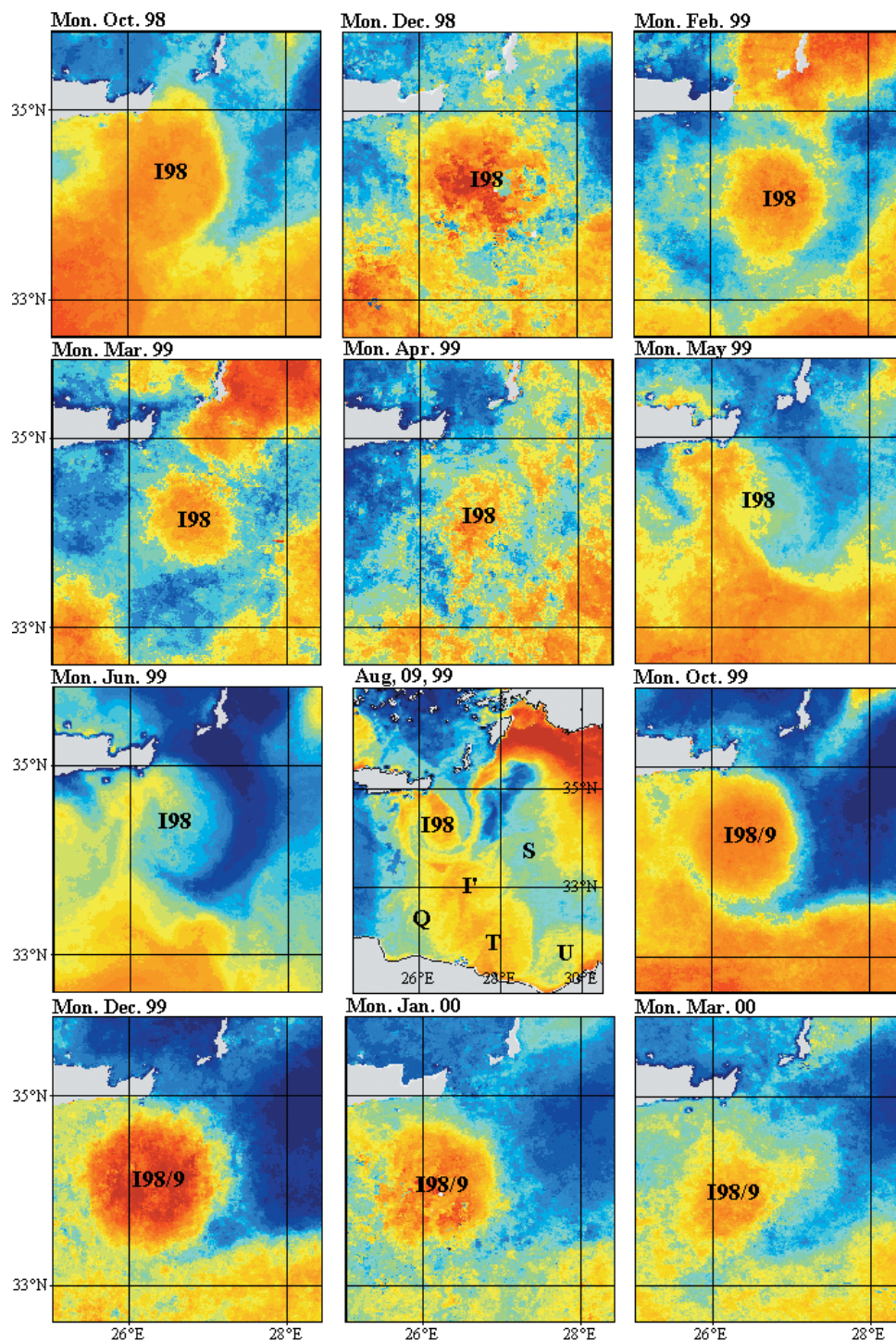


FIG. 13. – Ierapetra from October 1998 to December 2001.

downstream from T. I98 is fed both from the south-east by what remains of I' and from the northeast by the “AMC” continuation (see also Aug. 99 in Fig. 13). By early September T and S interact (warm water initially entrained by T is now entrained by S). Ten days later (Fig. 14g), the warm water is distributed over

both eddies and separating them becomes harder in October (Fig. 14h-j; called MM in the XBT section in Figure 3a of Zervakis *et al.*, 2002). All images available in November and December show that T and S have merged into T+S. Meanwhile, I98 has evolved into I98/9 and has a huge signature (see previous sub-

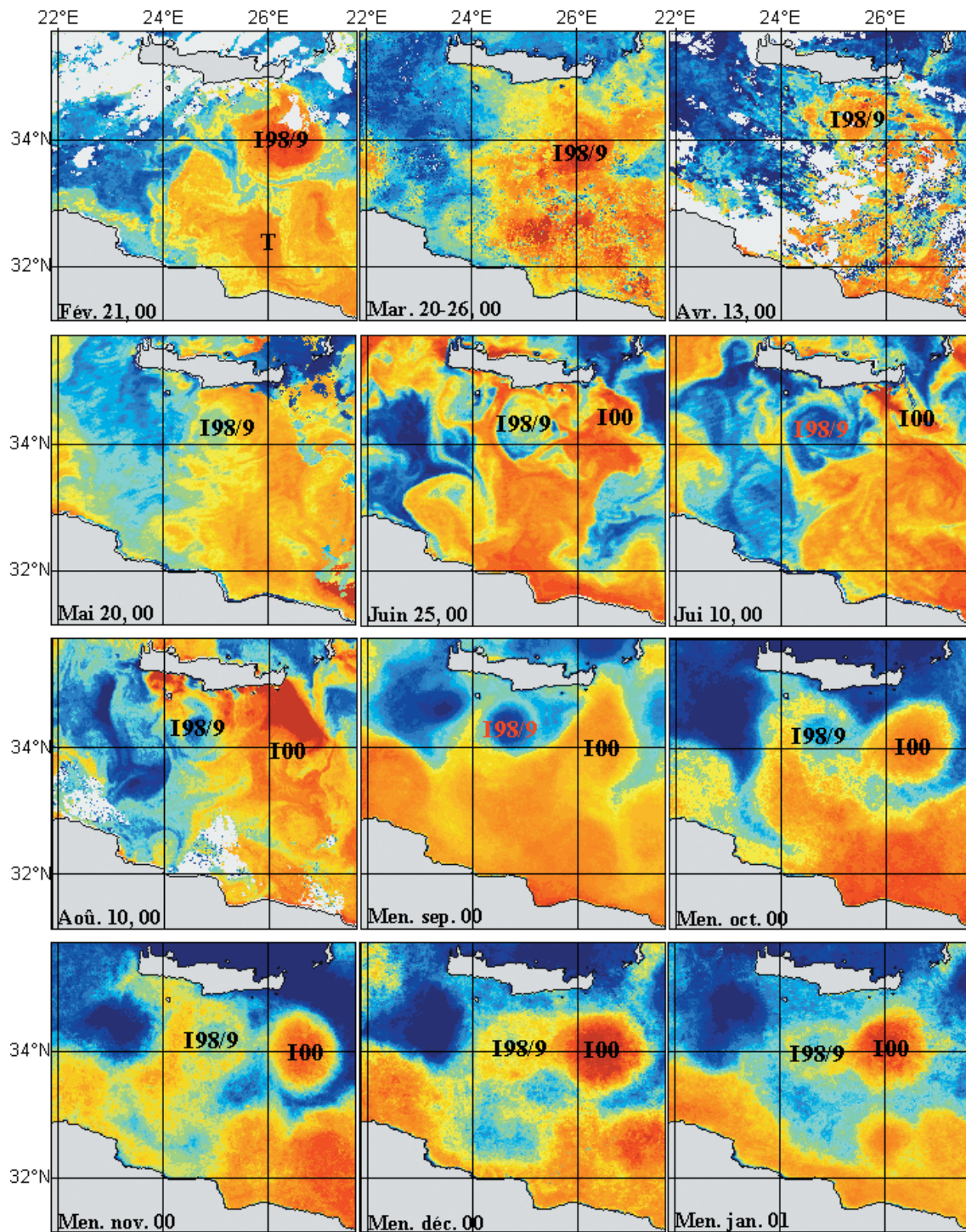


FIG. 13 (Cont.). – Ierapetra from October 1998 to December 2001.

section), Q has decreased, and U or a new coastal eddy grows and propagates downstream. From at least October the images display the continuous signature of the general circulation alongslope. The XBT sections in Figure 3b,c of Zervakis *et al.* (2002) crossed both T+S and I98/9.

The southeastern Levantine in 1996, 1998 and 1999

It is relatively difficult to study the area of anti-cyclonic activity of Shikmona. Firstly because during summertime a warm surface layer develops that

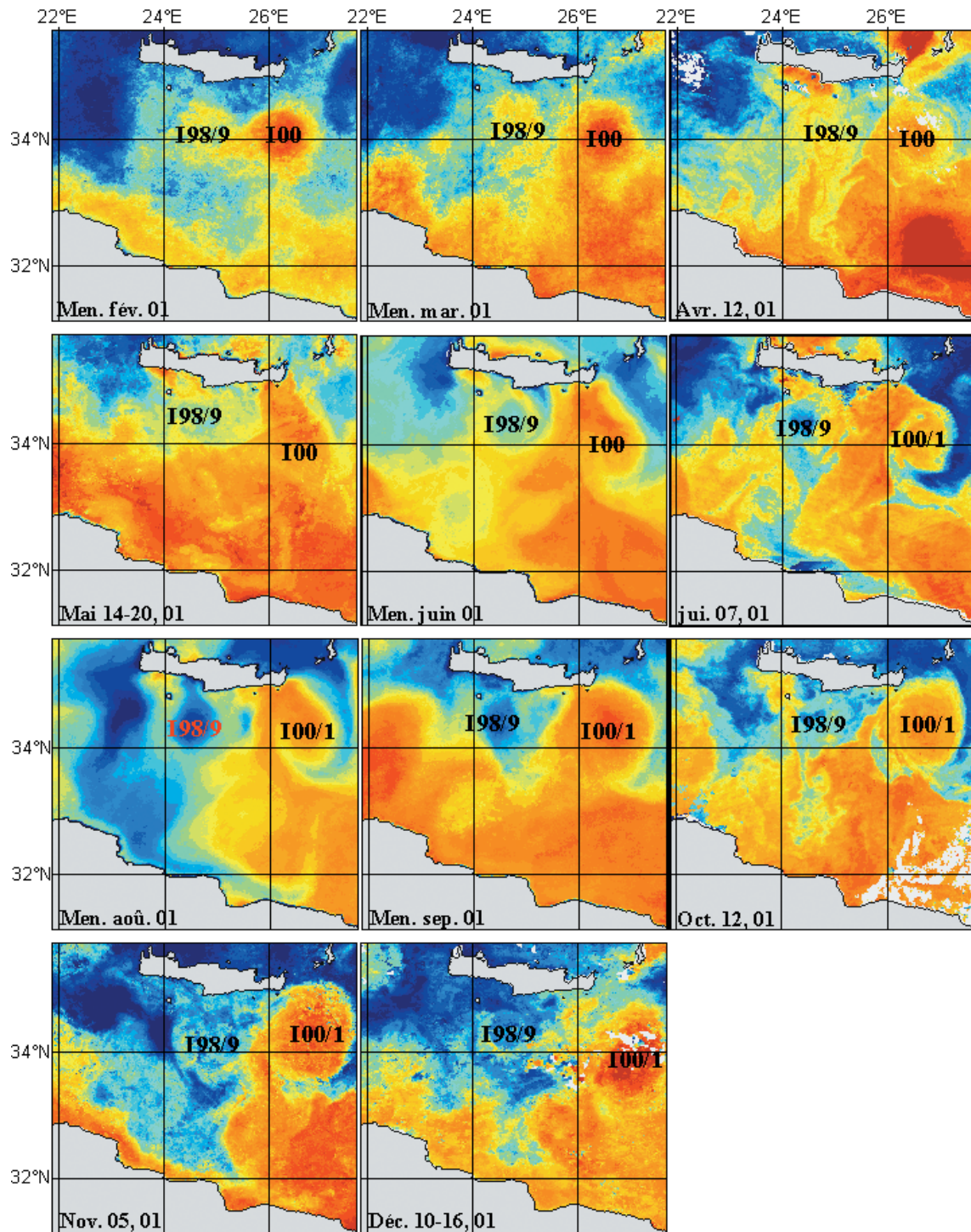


FIG. 13 (Cont.). – Ierapetra from October 1998 to December 2001.

often covers the mesoscale features' thermal signatures. Secondly because mesoscale eddies there have small dimensions and change rapidly in both form and position, and thirdly because many instability processes affect the general alongslope flow and feed the offshore zone. Situations can be

described, nevertheless, and those of summer-autumn 1998, 1996 and 1999 are detailed.

In summer 1998, Figure 15 evidences three eddies named U' (originated from an alongslope flow instability in the southwestern Levantine, Fig. 12c), U'' (suspected to have an origin similar to that

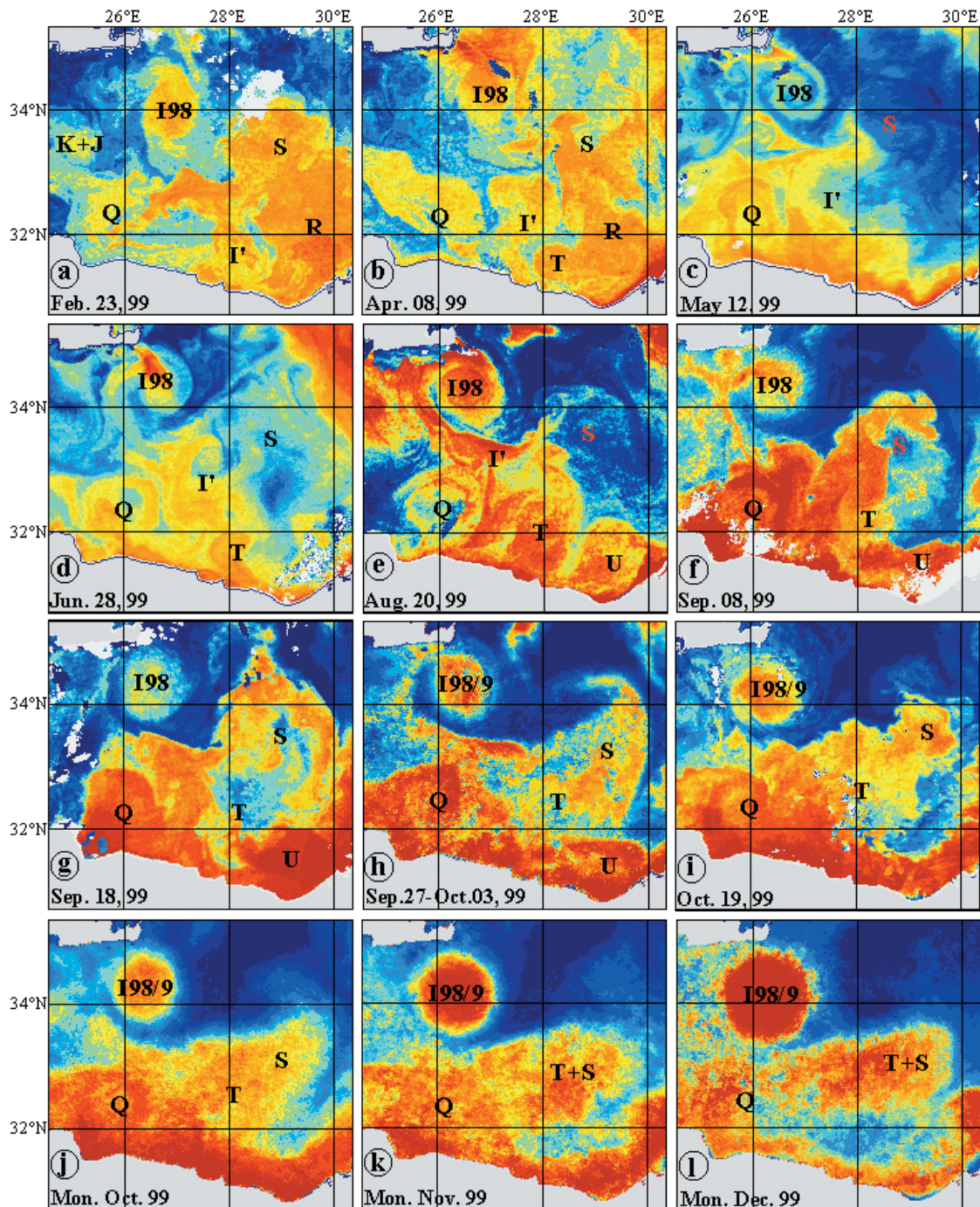


FIG. 14. – The southern Cretan and the southwestern Levantine from late February to December 1999.

of U') and V (that might be of different origin). U' propagates northeastwards and progressively leaves the coast while U'' and V drift more slowly towards north and east-southeast respectively. Several smaller scale features (noted with lower-case letters), that originated from the instability of the alongslope flow, are then entrained by the larger eddies. As a result of these interactions the signatures of the lat-

ter are highly variable: for instance V mainly entrains water from the east in August and November, and from the south in late September. In July U' is clearly embedded in the alongslope flow, it grows and slowly moves northeastwards, so that by November it has pinched off and becomes a part of the Shikmona anticyclonic activity system. In Figure 15l the circulation appears clearly, with a

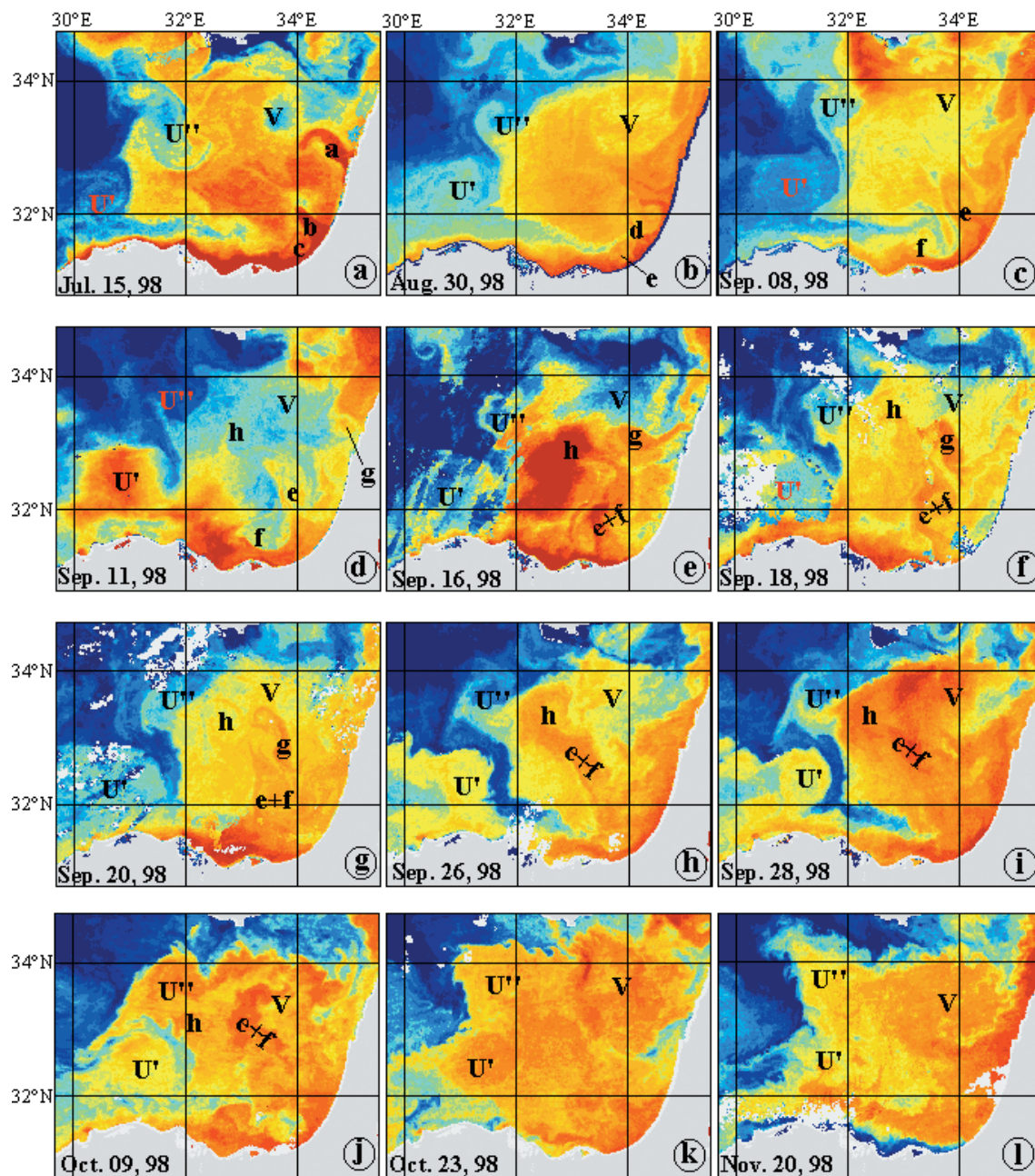


FIG. 15. – The southeastern Levantine from mid-July to mid-November 1998.

flow alongslope in the south that propagates eastward (see the propagation and deformation due to instability of the cooler signature of its outer edge, especially from 15a to 15d, and from 15g to 15j) and its continuation alongslope northwards although locally and temporarily disturbed by V: in Figure 15l the entrainment around 33°N due to V signs a southward (mesoscale) current.

The summer 1996 situation (Fig. 16a-d) differs in that it shows only one large eddy offshore (located slightly north of where V was in Fig. 15), inter-

acting with other anticyclonic eddy-like structures that originated alongslope. By autumn 1996 the general circulation appears to be organised in the same way as it was described in late 1998. The instability of the southern alongslope flow is also well signified by the deformation of the cooler signature of its outer edge (Fig. 16a-d).

Similar features are encountered in summer 1999 (Fig. 16g-l), although if V were a permanent eddy, it would now be located more to the south. The alongslope northward current is evident from the

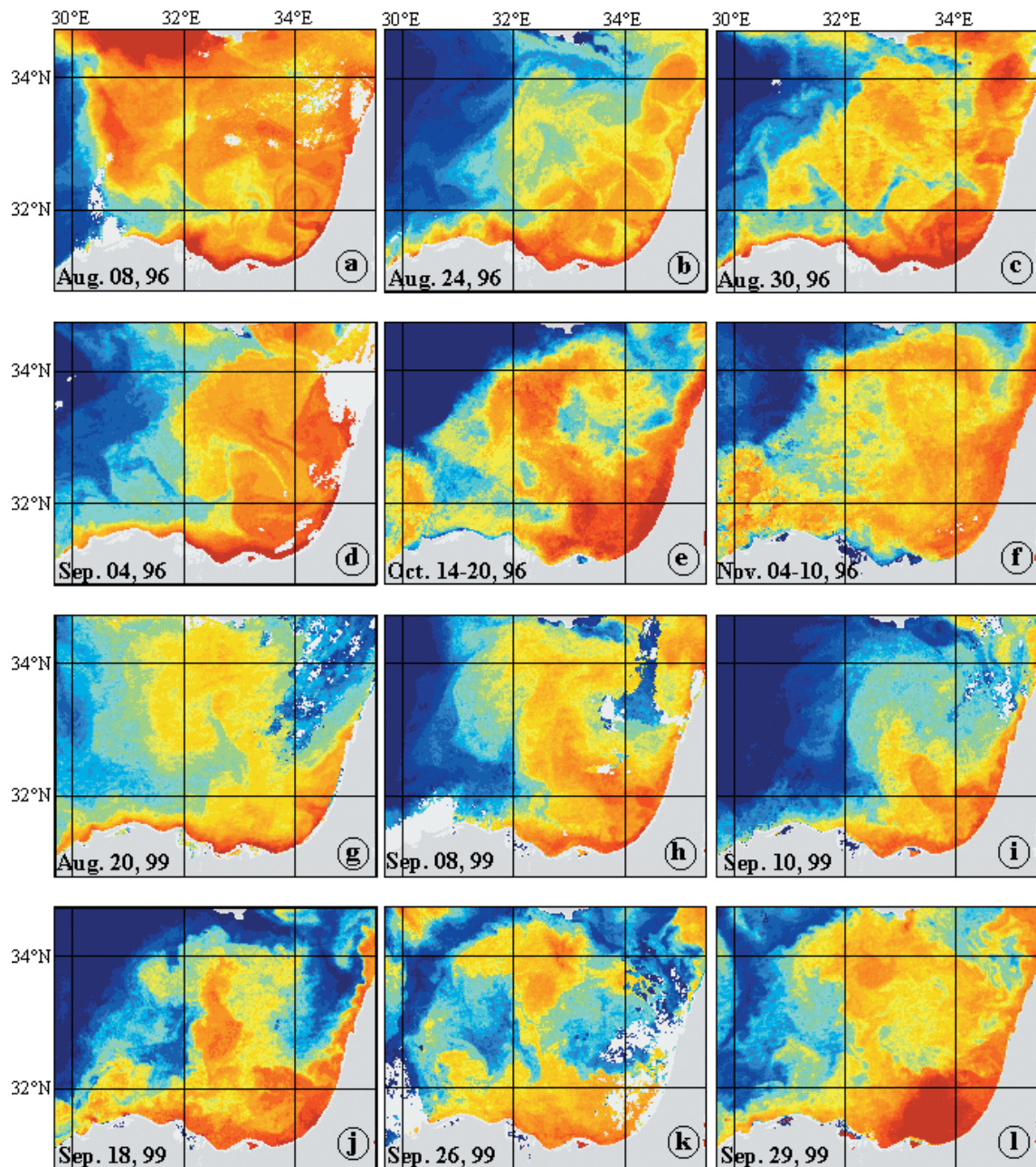


FIG. 16. – The southeastern Levantine from early August to early November 1996 (a-f); from mid-August to late September 1999 (g-l).

propagation of the warm filament-like feature located near 32°N-34°E (Fig. 16g-j).

The northern Levantine from 1996 to 1999

The series in Figure 17 shows, in addition to those in Figures 15 and 16, the continuity of the overall alongslope flow off the Middle East and Turkey. It is rare to observe the AW bypassing Cyprus northwards west of it, and if it does the alongslope circulation co-exists. The small (30-60 km) eddies W1 and W2

propagate downstream at 0-3 km/d off Middle Eastern coasts and rapidly evolve (X1 and X2 are described below). The major aim of this series is to provide a different analysis of the features previously named “Rhodes gyre”, “West Cyprus gyre” and “Latakia eddy” (see Fig. 1d). Indeed, a cyclonic eddy (or gyre) is, from a hydrological point of view, essentially a doming structure that can easily be confused with a zone of dense water, possibly at rest, surrounded by a flow of lighter water. In the case of the “Latakia eddy”, surrounding is partly due to

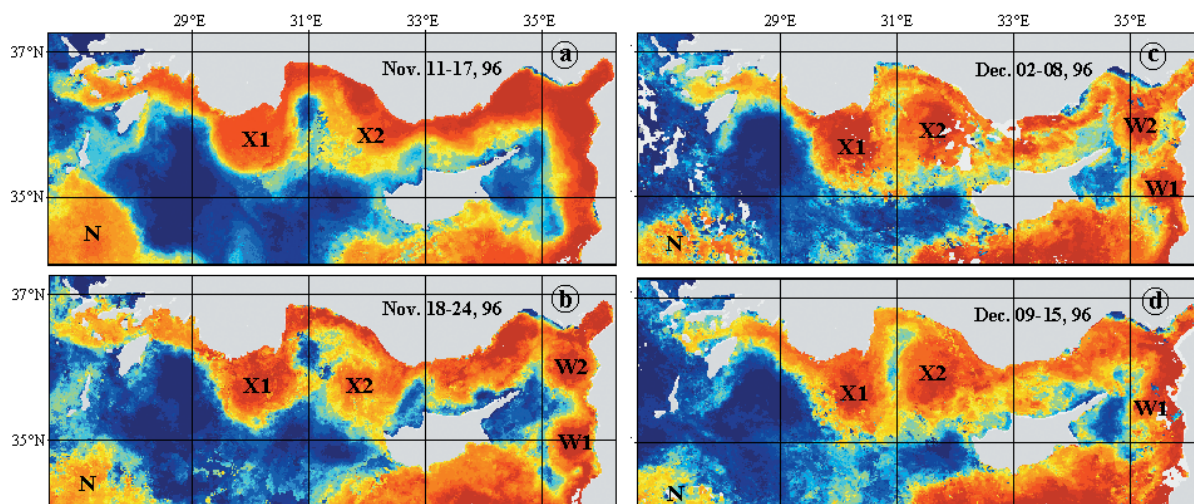


FIG. 17. – The northern Levantine from mid-November 1996 to mid-December 1996.

“Shikmona” and partly due to the angle of the coastline. For the “Rhodes and West Cyprus gyres”, surrounding by the general circulation is always clear in the north but much more variable elsewhere (the origin of N is shown in Fig. 10).

From June to August 1996 (Fig. 18a-c), X1 is stationary off Turkey and seemingly blocks the “AMC”, since part of the latter flows alongslope shoreward from X1 while warm water accumulates upstream at the gulf of Antalya entrance as a huge “AMC” meander. In September-October the “AMC” flows around X1 and the meander continues growing upstream. Finally, the two seaward extensions of the “AMC” join and isolate a patch of cool water in the middle of the gulf that is not a closed cyclonic eddy. From November 1996 to February 1997, X1 has progressed shoreward and is now fully embedded in the “AMC”, while the meander upstream of X1 is now organised as another eddy X2, which looks like X1 (characteristic diameters and propagation speeds are ~ 100 km and 0-3 km/d). However, contrary to X1, which will remain stationary until February 1997 (i.e. at least 8 months total), X2 propagates downstream until February, when it interacts with X1. Then, X1 begins propagating downstream and X2 drifts seaward, and both are seen in March and April. X1 and X2 signatures are lost by May (the signatures are not convincing enough to be tracked).

Figure 19a displays an unusual signature (its eastern (resp. western) side suggests an anticyclonic (resp. cyclonic) motion) at the place where the signature of X2 was lost. This might be due to the monthly composition, although it resembles the sig-

nature encountered from September to November 1996 (partly due to X1 at that time). In addition, an anticyclonic eddy appears downstream close to where X1 was lost. Both new structures are clearly identified as anticyclones in September. They are named X3 and X4, since the continuity with X1 and X2 resp. could not be established. Note that X3 temporarily prevents most of the current flowing between Rhodes and the continent and even entrains water from the Aegean (possibly expelled by the Etesians) into the Levantine (Fig. 19b). From October 1997 to January 1998, X3 propagates downstream south of Rhodes, while X4 develops and seems ready to pinch off. Both eddies are then lost in late winter-spring. In August 1998, a new (possible continuity with X4 could not be established) eddy X5 similar to X1 develops, showing similar interactions with the general flow. However, it soon propagates downstream as far as Rhodes where it is lost in January 1999.

The Aegean and northern Cretan

The Aegean

Most of the variability is seasonal, and the overall SST distribution is mainly governed by the Etesians (well known). We thus analyse monthly composites for a year (1998, Fig. 20).

No overall circulation features appear in May, while the upwelling induced eastward by the Etesians and the associated accumulation of warmer water off Greece appear clearly in June. From July to November, the east-west SST gradient decreases

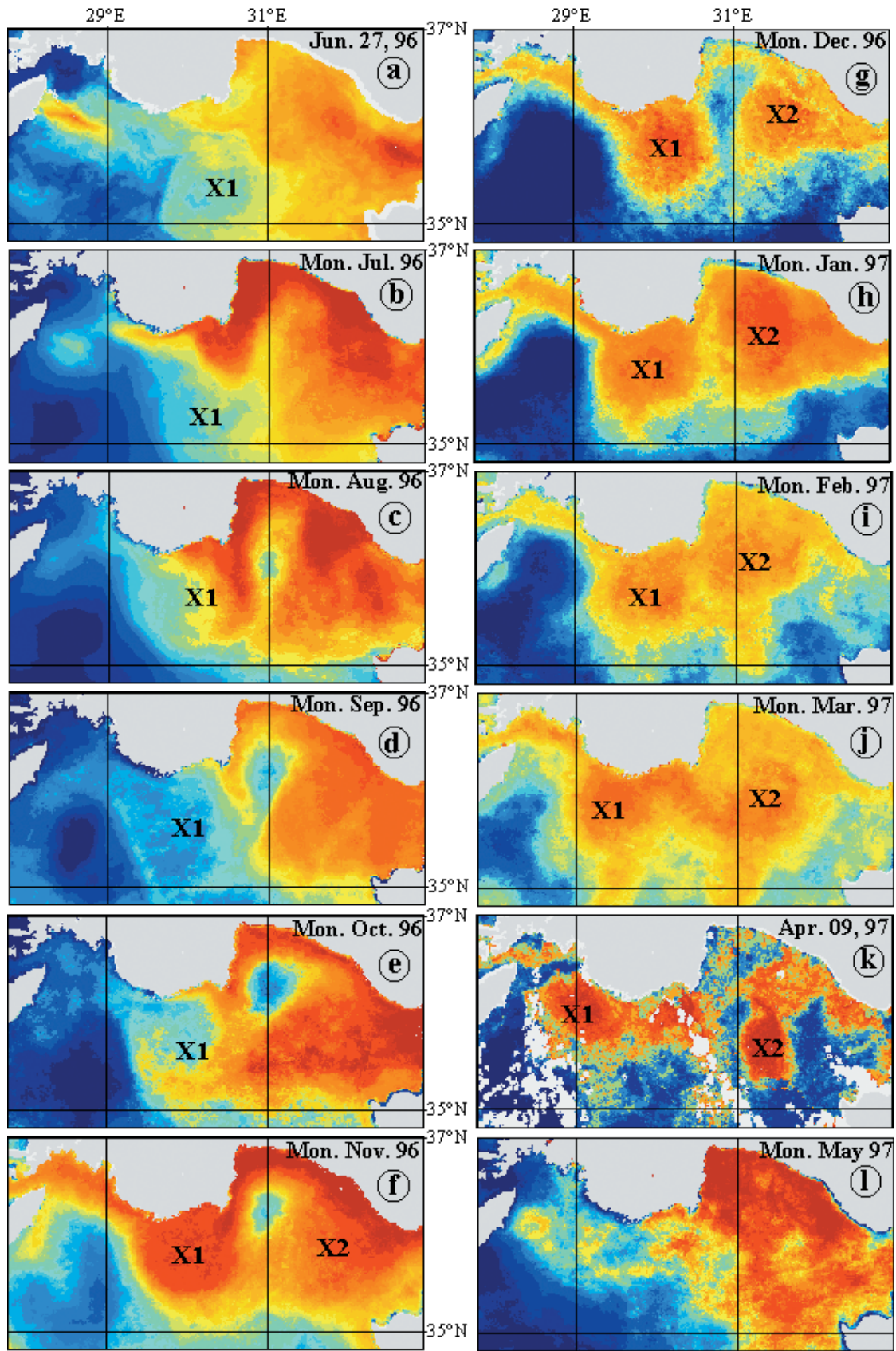


FIG. 18. – The northern Levantine from late June 1996 to May 1997.

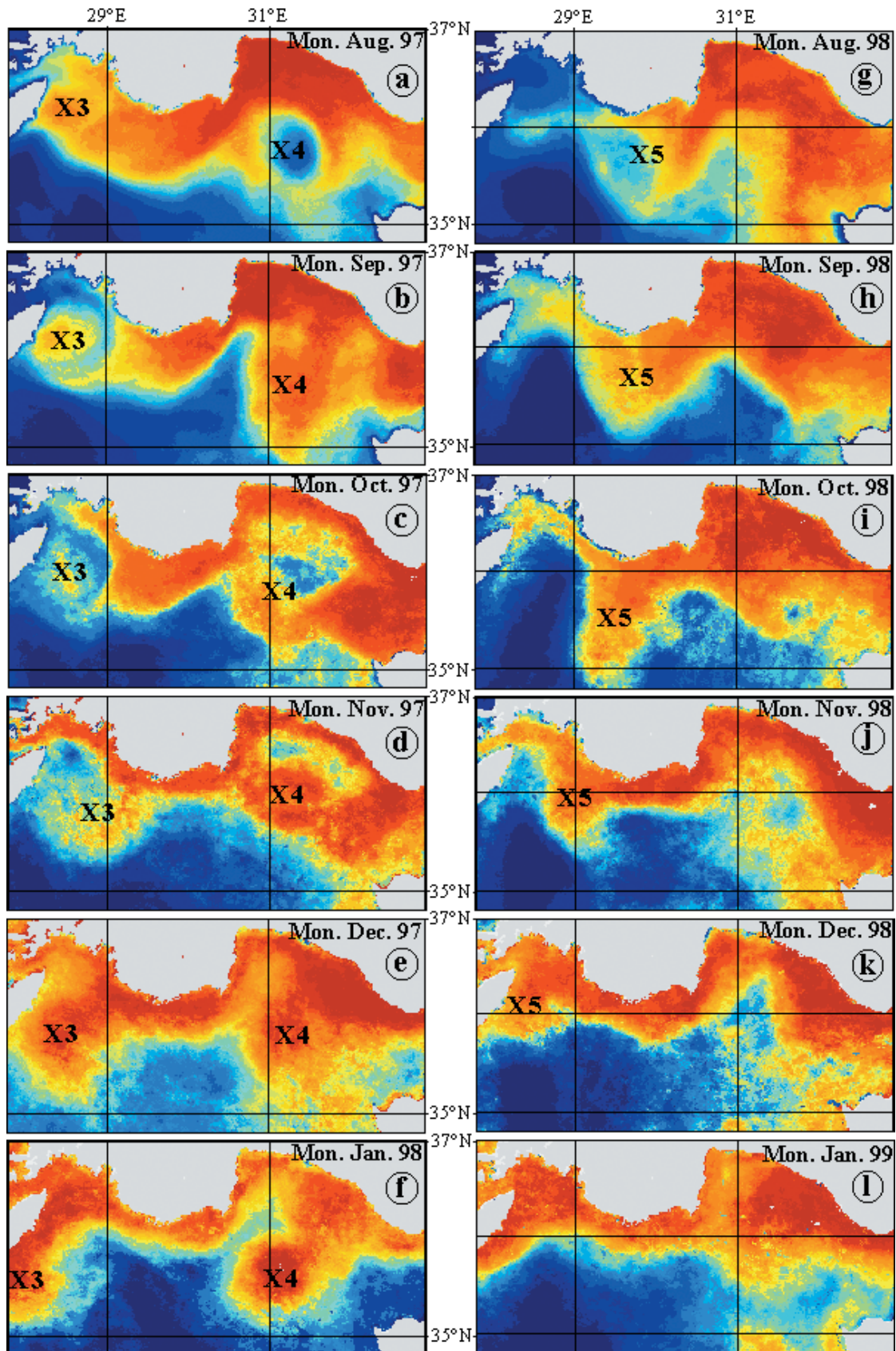


FIG. 19. – The northern Levantine from August 1997 to January 1999.

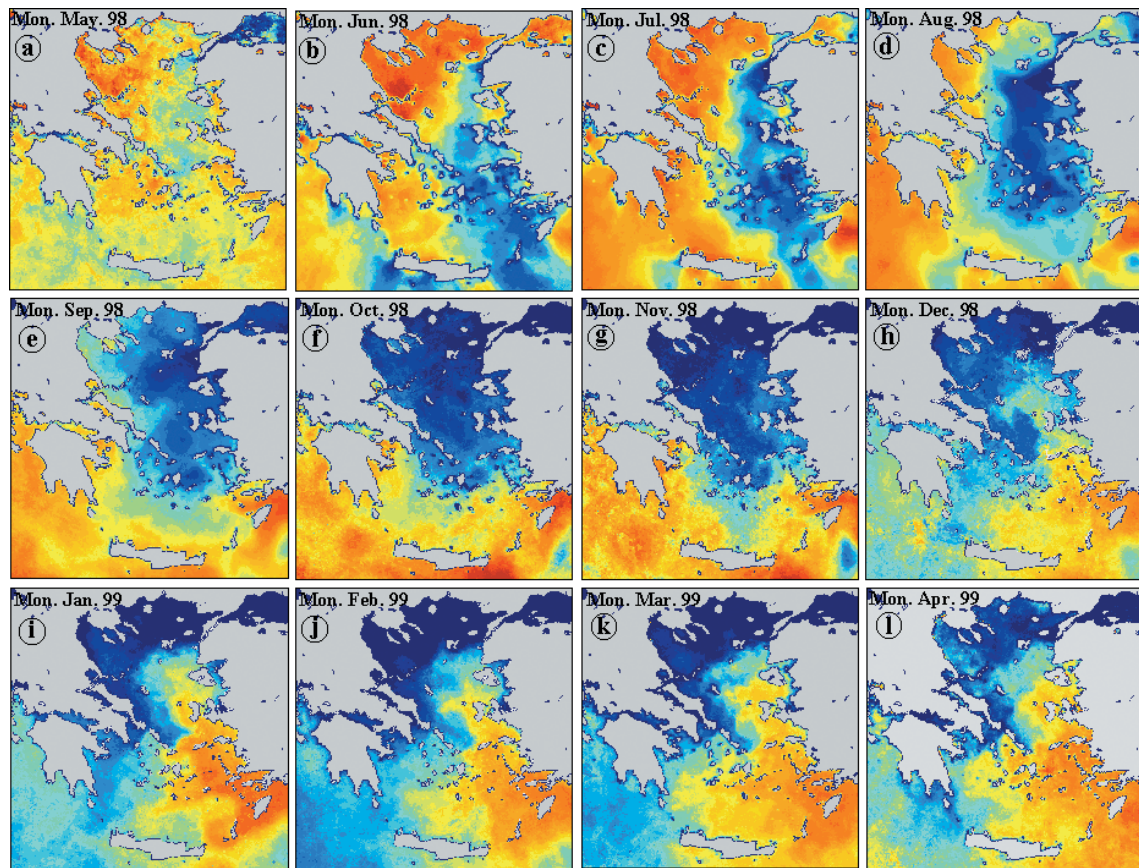


FIG. 20. – The Aegean from May 1998 to April 1999.

since most of the warmer water is progressively entrained partly out of the Aegean and partly along Crete, and also since in early summer the intensification of the Etesians extends mixing. Since wind mixing and drift are reduced by the orography, the coolest waters are observed in the Aegean central part in-between the islands. Warmer waters off Turkey could reveal some northward spreading of the “AMC”, but most of it is confined in the northern Levantine and the northern Cretan. From December to April, the “AMC” penetrates into the Aegean off Turkey and in the northern Cretan while cool waters propagate southwards off Greece.

The northern Cretan

The general situation in the August 1999 composite (Fig. 21a) is similar to that in the July-August 1998 ones (Fig. 20). Figure 21a evidences a 100-km anticyclonic eddy Z1 that propagates eastwards at ~ 1 km/d. In late November another eddy Z2 is created, and both Z1 and Z2 propagate eastwards until February. The signature of Z1 is lost in March after

8 months but, from May to September and maybe November, it or another eddy (noted Z3) is detected where Z1 was lost. In December 2000 Z3 can no longer be tracked, but Z2 is still there, roughly at the place it occupied in February 2000 and even in December 1999, i.e. one year before. Cyclonic eddies of smaller scales and much shorter lifetimes (a few weeks) can be encountered episodically along the eastern Cretan slope.

DISCUSSION

The circulation features we have inferred from the analysis of satellite imagery differ less from the historical schemata than from the recent (POEM-type) ones. The major question is: does AW meander across the central parts of the basin, or does it flow counterclockwise at basin scale, and more precisely alongslope? The POEM in situ data sets did not cover the southernmost part of the basin (see Fig. 2); nevertheless the derived schemata discarded the possibility of an eastward

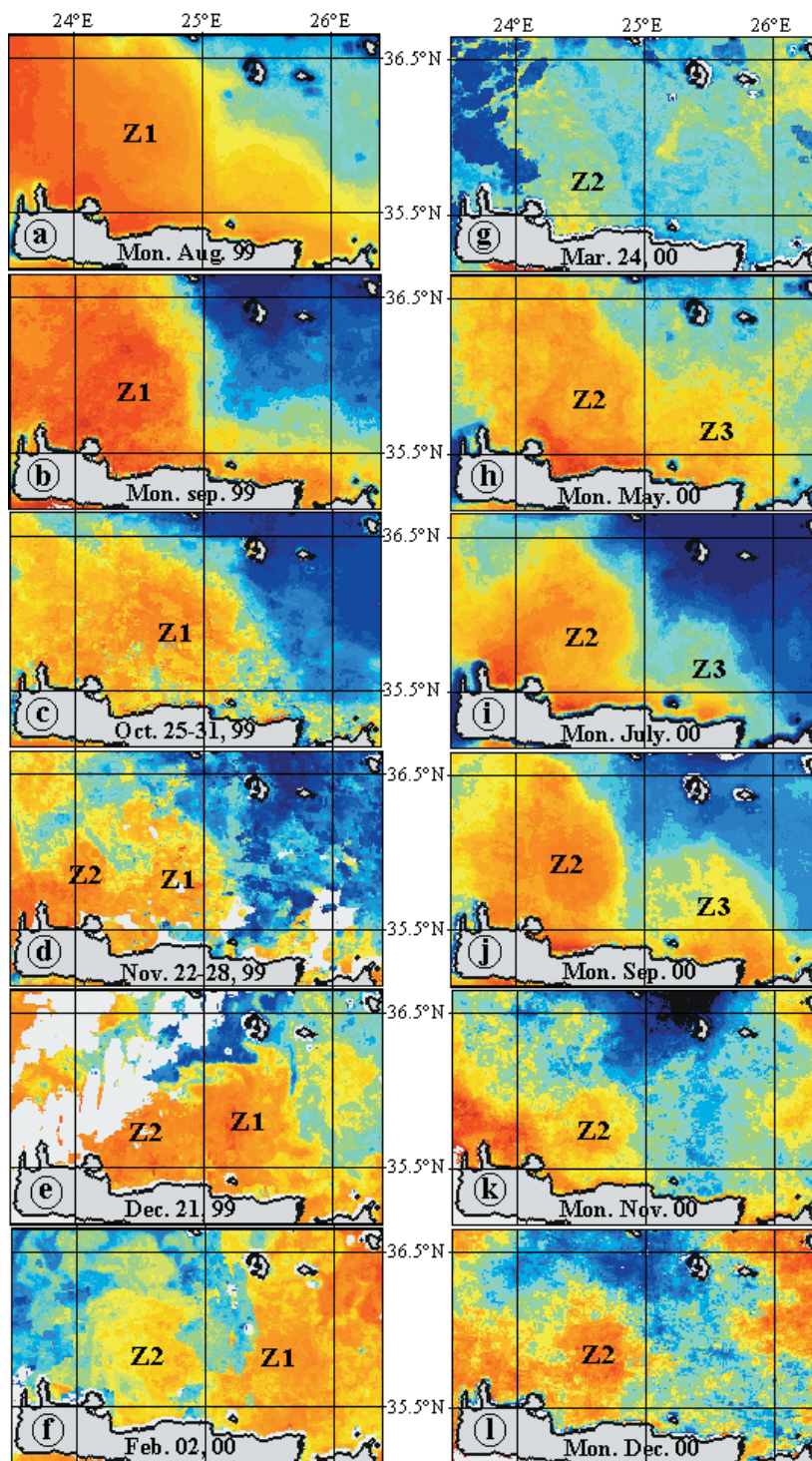


FIG. 21. – The northern Cretan from August 1999 to December 2000.

AW flow off Africa. However, Millot (1992) fostered Nielsen's basic considerations about the effect of the earth's rotation, and also promoted a counterclockwise circulation at basin-scale in the eastern basin. The AW flow at basin scale is discussed in the next subsection.

Currently, interpretations of the same POEM data sets differ: they hold the features named "Mersa-Matruh" and "Shikmona" either as permanent, recurrent and/or transient, when our analysis (also coherent with the POEM observations, see Fig. 2) always shows the presence of different eddies in

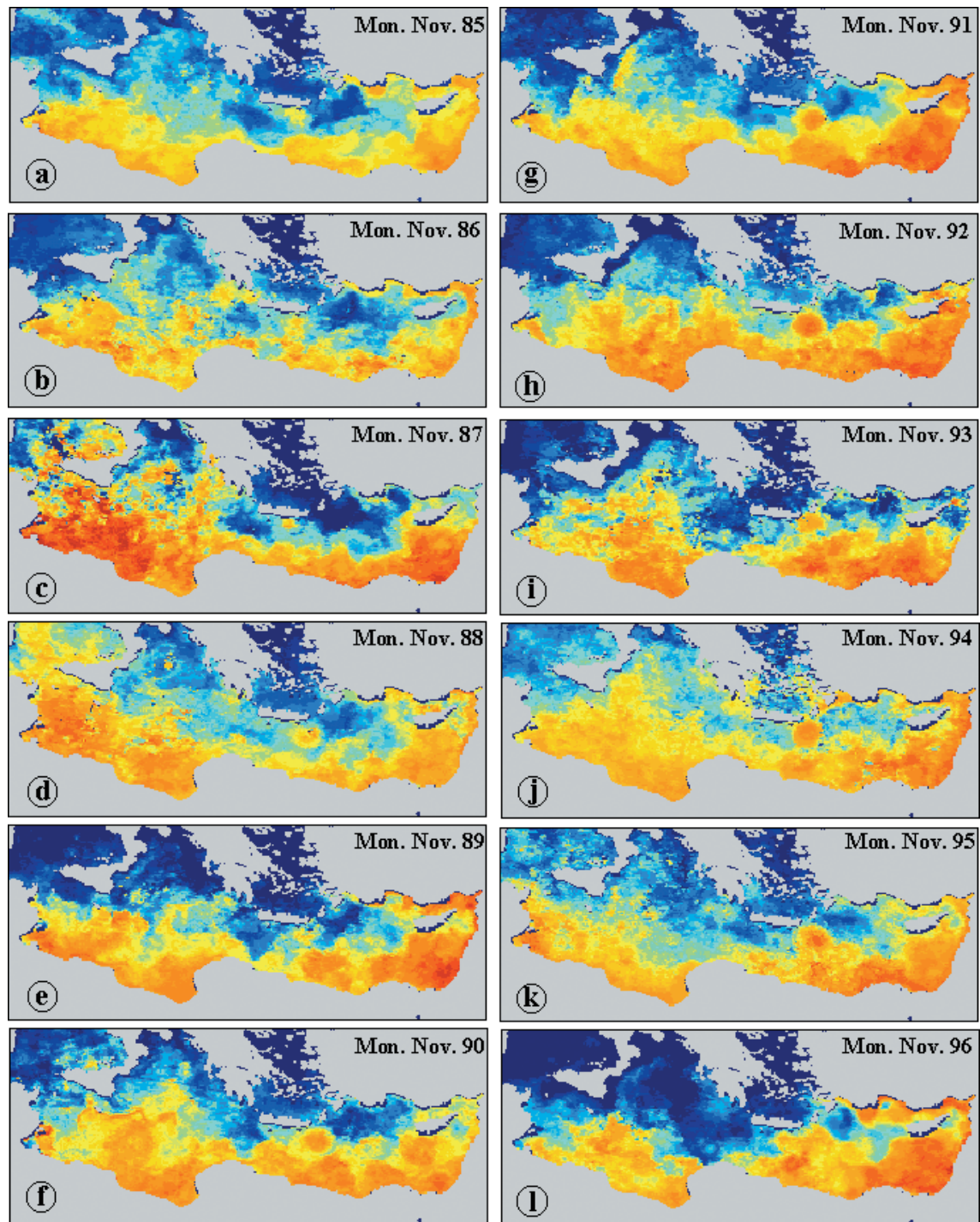


FIG. 22. – The eastern basin of the Mediterranean Sea in December from 1985 to 1996.

these areas. Then the underlying question is: how well have the mesoscale processes and variability been described and understood? The preliminary analysis of IR images by Le Vourch *et al.* (1992) showed that the AW flow is markedly unstable. Millot (1992) emphasised similarities with the western basin, with mesoscale meanders characterising

the flow in the north and large meanders evolving into eddies characterising the flow in the south. The POEM in situ data were collected every \sim half degree, and such a large sampling interval prevents mesoscale features being described correctly. In the same way one survey per year does not yield relevant information about the temporal evolution of the

mesoscale features. We compare our results with the other available analyses region by region in the rest of subsections.

The whole basin

Figure 22 shows the monthly composites for November available from 1985 to 1996 (to cover, in particular, all POEM experiments). Note that all other months display similar overall features except, obviously, those linked to seasonal variability. Although the interannual variability cannot be neglected, the overall features we have inferred in the results section can be evidenced. One is the intensity of the mesoscale activity (eddies) in the southern part, and the activity, to a lesser extent (meanders), in the north. But most importantly, the warmest (lightest) AW is seen alongslope, and it clearly flows counterclockwise around the basin. There is no evidence of any cross-basin flow or jet, all the more since the warmer AW signature is continuous from Libya to at least the entrance of the Aegean. Therefore, it is Nielsen's schema that, up to now, best represents the large-scale features of the AW circulation.

The channel of Sicily

The AW flow splitting at the entrance of the channel of Sicily is better represented by the schema of Nielsen than by the schemata of Ovchinnikov and of Lacombe and Tchernia, since most of the inflow seems to be constrained along the Tunisian slope rather than spreading across the whole channel. At least concerning the splitting, our analysis is consistent with the numerical results of Molcard *et al.* (2002) and shows that it mainly occurs north of Tunisia, just at the channel entrance.

Within the channel, the intense upwelling off Sicily prevents checking the most recent circulation diagram of Robinson *et al.* (1999) there, which indicates a major inflow meandering off Sicily and describes a series of "semi-permanent features" such as vortices and crests. This diagram differs from the ones by Robinson and Golnaraghi (1993, Fig. 1e) and by Malanotte-Rizzoli *et al.* (1997, Fig. 3a) since AW, although still meandering, is represented flowing close to Sicily and north of Malta. In 1994 and 1995, Robinson *et al.* (1999) launched drifters south of Sicily that were entrained northwards alongslope in the Ionian by the branch previously discussed (thus further supporting the consistency between our

image analysis and in situ observations). However, although one drifter launched in the central part of the channel joined the drifters discussed above, several others drifted southwards off Tunisia. Their trajectories further east are unfortunately not shown, probably since this was not the focus of the paper. In any case, care must be taken when attempting to link fluxes to drifter trajectory statistics, since it would require deploying the drifters homogeneously across the flow. In other words, the southward flow would probably have been investigated too if more drifters had been launched closer to Tunisia.

In any case, the images suggest that AW is confined mainly along Tunisia within the channel itself while, just south of the channel, most of the flow progresses in its central part. This could seem inconsistent with basic considerations about the Coriolis effect that should constrain any flow along the continental slope. However, it has been demonstrated that where the shelf is wide (e.g. the Gulf of Lions in the western basin), the general circulation follows the slope (depths >100-200 m) more than the coastline (Millot, 1999), because it has a significant thickness. The alongslope circulation around the Tunisian continental shelf is well evidenced in the numerical results of Pierini and Rubino (2001). It is thus clear that, although one (upper) part of AW continues flowing along the coastline over the Tunisian shelf, the slope guides another part. Both "branches" are due to the Coriolis effect at different depths but, from a kinematic point of view, it might be that the branch on the shelf rapidly slackens due to the bottom stress while the branch along the slope is still intense (as in the Gulf of Lions). For more details see Béranger *et al.* (2004). Far south from the channel, where the Tunisian shelf rapidly reduces (near 12-13°E), the main branch hits the coastline near the Tunisia-Libya border and partly veers to its right before penetrating westwards over the shelf. There, the circulation is quite well represented by the schema of Lacombe and Tchernia (the clockwise gyre in Ovchinnikov's schema is probably too large and not linked with the bathymetry). However, neither the southward flow along the Tunisian coastline nor the variability of the circulation over the Tunisian shelf have been schematised.

The Ionian

This subbasin is one of the most complicated to study with in situ as well as remotely sensed data.

Firstly because the AW flow is markedly disturbed by its passage through the channel of Sicily where bathymetric and meteorological / climatic conditions have a large spatial and temporal variability. Secondly, upon exiting this relatively wide channel mainly in its central part, AW flows into a much wider domain and is thus not very well channelled, so that various complex features can be generated. Finally, the overall counterclockwise circuit closes there (as conceived by Nielsen, Fig. 1a). We focus first on the overall circulation and then on the mesoscale phenomena.

The overall circulation

The first point concerns the “AIS” meandering in the northern part of the Ionian that is said by Malanotte-Rizzoli and Bergamasco (1989, 1991) and Robinson and Golnaraghi (1993) to be a summertime feature and to finally form the “MMJ”. The series of images in Figures 5 and 22 shows that a northward flow off Sicily is an actual feature, although it does not look like a meander. This flow was documented not only by the POEM 1987, 1991 and 1995 hydrological data, but also by drifters’ trajectories between 1994 and 1997 (Poulain, 1998; Robinson *et al.*, 1999). According to Pinardi *et al.* (1997), this meander was established in 1987 by an anomalous wind stress curl that reversed the circulation from clockwise to counterclockwise. Satellite images (e.g. Fig. 5) show that this feature is not seasonal but interannual, was there in the late eighties, and decayed in January-February 1998. Hydrological data indicate that it persisted until August 1998 and confirm that it is an interannual feature, and Manca *et al.* (2003) suggest that it was forced for about one decade by the mean wind stress curl. In 1999 and 2002, recent AW was only found in the southern Ionian (Manca *et al.*, 2002). In addition, the imagery shows that more than a meander that would continue eastwards, this feature must be thought of as a branch spreading northwards and more or less decaying there, without any continuity (after G, Fig. 5, 7) with the circulation in the east. From at least spring 1997 to spring 1998 (Fig. 7), F and G in the branch did not move, which may indicate that the branch was decaying. Moreover, from spring 1998 (Fig. 8), F began drifting southward, i.e. against the direction of the former branch. This analysis is consistent with the drifters’ trajectories of Poulain (1998). The salinity, temperature and

dynamic height distributions in Figure 18 of Malanotte-Rizzoli *et al.* (1997) could also be interpreted as a dead-end branch, rather than the inferred meander schematised in Figure 3a.

The imagery also shows the permanence of the main AW flow along the Libyan slope with roughly constant characteristics, and its dominance when the branch spreading northward decayed (see Fig. 22). It also shows the seasonal variability of the alongslope flow from the Ionian into the Adriatic, which is actually highest in winter (Artegiani *et al.*, 1997), and its eventual splitting before the channel of Otranto that closes the overall counterclockwise circulation, even when a branch spreads northwards from Sicily.

The mesoscale phenomena

All images in the Ionian illustrate the variability of the thermal signature of mesoscale eddies in a very complex environment. This signature (which is also the in situ one!) demonstrates how difficult the inference of a circulation diagram can be without any help from satellite imagery. For instance, sampling only the edges of a series of anticyclonic eddies can lead to misinterpret them as a permanent stream meandering across a subbasin, even if no net transport is associated with such an eddy-field.

We confirm that Pelops is generated by the Etesians in summer south of the Peloponnese before drifting roughly westwards (as indicated by e.g. Matteoda and Glenn, 1996). In addition, we show that it could be generated over some earlier eddies, we have tracked it (P97) for more than one year and we have thus shown that two generations of Pelops (e.g. P97 and P98) could co-exist a few 100 km apart. The Pelops’ counterpart (the “Western Cretan gyre”), although basically different and stationary (as previously described), displays the same seasonal variability.

We have illustrated, for the first time, the generation, propagation (0-3 km/d) and pinching-off of mesoscale (50-250 km) eddies off the western Libyan slope. Interactions with their parent current have also been documented.

Finally, we have tracked for about two years an anticyclonic eddy (F) that crossed most of the sub-basin from north to south (while others were tracked crossing it from northwest to southeast). Initially found just east of Sicily and issuing from the AW branch discussed above, it first remained stationary for ~1 year. Then, it propagated southwards and

reached the Libyan shelf ~1 year later, strongly interacting there with a Libyan anticyclonic eddy in a dramatic, although probably rare, way. Indeed, the interaction generated a small cyclonic eddy that rapidly became relatively large and which then strongly interacted with the alongslope flow itself. The Maltese filament can be entrained around anticyclonic eddies across the whole southern subbasin.

The Adriatic

The schema of Artegiani *et al.* (1997) reproduces most of the features evidenced by the imagery but disagrees with our analysis, since the southern gyre is seen to strengthen in winter. Indeed, the images show a close link between the inflow and the zone of dense water formation that is not schematised, although this is consistent with what is expected in this zone and is clearly supported by drifters' trajectories (Poulain, 2001). The available schemata can thus be improved in the Adriatic.

The southern Cretan and the southwestern Levantine

Although we did not focus on the "Western Cretan gyre", due to the lack of interesting results, we parallel (see previous subsections) the cyclonic-anticyclonic paired eddies found east of the strait of Bonifacio (eddies not named yet) and south of the west-Cretan straits (Pelops and the "Western Cretan gyre"). The main reasons could be a strong orographic effect, relatively narrow straits and the absence of marked alongslope circulation in both places. We differentiate this from what occurs south of the east-Cretan straits, although the dynamics of Ierapetra is similar to that of Pelops. Indeed, the Turkish orography is less marked than the Cretan one, this set of straits is relatively wide and the general circulation is intense there (see subsection on the northern Levantine).

In the western Cretan and northern Bonifacio zones, the wind stress curl entrains (on its left) surface water into a counterclockwise rotation and Ekman pumping creates a doming structure. When the wind stops, geostrophic adjustment tends to generate a cyclonic rim current all around the doming that can persist up to one year (Crépon *et al.*, 1989). However, although one drifter started a cyclonic loop before being lost southwest of Crete (Matteoda and Glenn, 1996), the Cretan cyclone

seems (at least from space) neither intense nor long-lived. Although this cyclone was rarely sampled (at mesoscale at least), it is probably less intense than the Bonifacio cyclone clearly evidenced with drifters (Artale *et al.*, 1994) and seen from space nearly all year long. When warm waters cover such a doming structure after a period of calm or non-adequate winds, their signature is lost from space although it can still be detected with in situ data. This seems to occur (from the imagery analysis) more frequently for the Cretan cyclone than for the Bonifacio one. It is hypothesised that the difference of intensity is not due to winds that are stronger and more frequent in the Bonifacio area, but that the Bonifacio cyclone, cornered between Corsica and the Italian peninsula, is intensified where the overall counterclockwise circulation along the peninsula joins. The Cretan cyclone, as it is far away from the overall alongslope circulation along Africa, does not interact with it.

Ierapetra is generated by the Etesians every summer-autumn off southeastern Crete. It is clearly fed sporadically by water coming from the overall alongslope counterclockwise circulation, according to several processes. Classically, the wind stress curl that generates Ierapetra itself and the western Cretan cyclone induces in-between them a northward flow towards Crete that feeds both eddies. According to the images that show the shadowing effect of Crete on the Etesians up to Africa, it must be considered that, whatever the wind stress curl is, waters pushed against Africa mainly on both sides of Crete flow back to the north more easily leeward of it. In addition, feeding occurs from the south through a paddle-wheel effect via the Libyan anticyclonic eddies. Finally, feeding also occurs from the northeast through the "AMC". Ierapetra can drift (as I96), interact with Ierapetra formed one year later (I97), merge with it (I96+97), drift close to the African slope before, upon decaying (I'), feeding the newly formed Ierapetra (I98). It can also remain stationary. Then, if it survives in spring (as I98 and I00), due to being fed by other eddies or even since it is sustained by any northerly wind, it will give rise to an unusually large Ierapetra one year later (as I98/9 and I00/1). Finally, since a huge Ierapetra (I98/9) drifted westwards and remained there in a relatively quiet area (leeward of Crete and away from the more turbulent area in the south) while another Ierapetra (I00/1) was growing, two generations of Ierapetras can be found close together for a while.

Large (100-250 km) eddies in the African coastal zone result from instability processes affecting the alongslope circulation off Libya and off western Egypt. They have similar characteristics so that we name them Libyo-Egyptian eddies. They propagate at most at 3 km/d, and can be tracked for years (up to ~2 at least). They have been observed deflecting seaward eddies approaching from upstream, feeding Ierapetra, and modifying the whole alongslope flow.

Whatever their origin (i.e. the Ierapetra area or the Libyo-Egyptian slope), mesoscale eddies can merge, making “Mersa-Matruh” an area continuously occupied by slowly propagating and constantly interacting anticyclonic eddies. It is worth noting that T or T+S in late October - November 1999 (Fig. 14i-k) was recognised as “Mersa-Matruh” by Zervakis *et al.* (2002), who sampled it with XBTs (thus validating again our interpretation of its signature) and inferred a transport of more than 4 Sv (reference level at 460 m). Large eddies seem to accumulate in the Mersa-Matruh area. We thus suppose that, similarly to the Algerian eddies, they undergo the planetary β effect and non-linearities (see Taupier-Letage and Millot, 1988) and we hypothesise that their deep extent somehow traps them in the Herodotus trough (~3,000 m, see Fig. 1a). Therefore we suggest naming the associated eddy field SL_w (for area of eddy accumulation in the western Levantine). Instead of a permanent or recurrent “Mersa-Matruh” eddy or gyre we have shown that there were several eddies permanently in this area, which explains the numerous discrepancies in the “Mersa-Matruh” status found in the literature.

Finally, none of the images support the occurrence of a “MMJ” as the warmer signature of AW is quasi-continuous alongslope, and rather patchy (eddy-scale) offshore. Indeed, as stated by Özsoy *et al.* (1993, p. 1082), “*the persistence and continuity of a cross-basin current could not be well defined and the current system cannot be separated from the eddy field that partly defines it*”. As an example, when mesoscale eddies are fully resolved and crossed, there is no structure corresponding to a “MMJ” on hydrological transects (e.g. Figs. 7 and 9 of Marullo *et al.*, 2003). Moreover, while none of the XBT transects performed during the MFSPP experiment evidenced a “MMJ”, all of them evidenced an alongslope eastward circulation off Egypt (Zervakis *et al.*, 2002) that is still called “MMJ” by Fusco *et al.* (2003). It is worth noting that the associated transport of ~1 Sv is relatively low with

respect to those in the larger mesoscale eddies (several Sv), but it is consistent with both the inflow at Sicily and the amount of AW transformed by dense water formation processes in the whole basin.

The southeastern Levantine

The mesoscale phenomena in the Shikmona area can hardly be detailed due to their relatively small scale (mostly 10s of km, up to 100 km) and rapid evolution in shape and position (propagation speeds of 0 to 10 km/d). It might be that the eddy found in the northeast (named V) is the Cyprus anticyclonic eddy previously described, although images do not support the 3-year lifetime indicated by Brenner (1993). However, complex anticyclonic activity (as mentioned by Özsoy *et al.*, 1993) is observed year-round making “Shikmona” an area permanently fed from the south and the east by the alongslope (counterclockwise) flow (note that we did not find any evidence of the “MMJ” feeding “Shikmona” from the northwest, as suggested by the POEM-type schemata). Therefore, we suggest naming the associated eddy field SL_E (for area of eddy accumulation in the eastern Levantine). As in the case of “Mersa-Matruh”, this explanation allows the controversies about the status of “Shikmona” to be settled: since eddies permanently accumulate, those observed there logically have different positions and sizes in time. However, a major difference with SL_w is that there may be only one large eddy.

The northern Levantine

Although a large anticyclone in SL_E can sometimes extend far to the north, so that some water can sporadically flow northwards west of Cyprus, the overall general circulation is clearly alongslope off the Middle East and Turkey. Contrary to what was indicated by Robinson *et al.* (1991), the whole “AMC” does not originate locally from the “CC” but from further upstream (i.e. up to Libya). Sometimes a meander increases at the place where W1 was observed (Fig. 16b-c), which is interpreted as the “Latakia eddy”. However, we have not seen any eddy detach there, and the northward propagation of the features is most common. Therefore, we do not identify a specific “Latakia eddy”. In a similar way, the combination of the alongslope flow, and the presence of a large anticyclone in SL_E and off Cyprus may lead to interpreting a “West Cyprus

gyre” where there is in fact mainly cool water roughly at rest surrounded by the warmer general circulation. However, the Etesians, which blow through the east-Cretan straits and interact with the orography, can generate a cyclone there that is more or less similar to the “Western Cretan gyre”, although less intense since the Turkish orography is smoother than the Cretan one. This might be the reason why some water from the alongslope circulation can be entrained seawards in a cyclonic way (see Fig. 17 south from X1), maybe up to SL_E . This entrainment depends on the wind and seems to be superficial and limited, and there is no evidence of any closed permanent gyre there. Such a tenuous border between the “West Cyprus gyre” and the “Rhodes gyre” has also been described in the western basin between the Ligurian and Provençal sub-basins (Wald, 1985).

The “West Cyprus gyre” and Ierapetra could be considered as the paired cyclonic-anticyclonic eddies associated with the east-Cretan strait, as we did for the “Western Cretan gyre” and Pelops (and for the eddies east of Bonifacio). However, the east-Cretan strait is, when considering northerly winds (i.e. not only the Etesians but also those advecting cold and dry continental air masses in winter), much larger than the other straits are. Therefore, between the zones characterised by large wind stress curl values and occupied by the paired eddies, there is a central zone characterised by much lower curl values and possibly larger speed values. Surface water in this central zone is more mixed than on either side, SST values there are always relatively low. When surface water has been swept away and/or mixed with deeper water in winter, part of the water column is homogenised, and thus can no longer be entrained by the wind, so large amounts of dense water (especially LIW) are formed.

Geostrophic adjustment clearly gives rise to a rim current (e.g. Crépon *et al.*, 1989) around a zone of dense water formation in the open ocean. However, mechanisms are certainly not so simple when the zone is close to the coast because of winds blowing from land. Consistently, no image and no in situ data account for any rim current surrounding these zones that could correspond to the alleged “Rhodes gyre” and “Lion gyre” (e.g. Roussenov *et al.*, 1995). Winter images evidence the “AMC” flowing both into the Aegean off Turkey and along the southern slope of the islands from Turkey to Crete. They also evidence the fact that this “AMC” is disconnected

from the warm waters found in the south that are linked to the numerous mesoscale eddies (e.g. N) described there. Therefore, even if there must be an eastern basin Northern Current linked to the dense water formation in the northern Levantine, we do not conceive a “Rhodes gyre” *stricto sensu*.

The Aegean and northern Cretan

From late autumn to early spring, the northward penetration of the “AMC” over cooler waters is clear because the Etesians have pushed surface waters away from the Turkish coasts. At the same time, waters cooled in the north by air - sea interactions and by mixing with fresh water outflows propagate southwards off Greece, so that there is a clear counterclockwise circulation in most of the Aegean in winter. This circulation does not close in the northern Cretan since part of the warm waters penetrating through the east-Cretan strait tend to follow the slope associated with the islands in the central Aegean and thus flow (always counterclockwise and alongslope) directly towards the west-Cretan strait.

In summer, the Etesians push the warm waters towards Greece and southwards so that the surface circulation is still alongslope and counterclockwise in the western Aegean. It is worth noting that while most of the warm water outflows from the west-Cretan strait, a significant part flows along the northern coast of Crete, generating mesoscale anticyclonic eddies there. Once created, the eddies propagate eastwards and can be tracked for ~1 year (e.g. Z2 in Fig. 21). Surface water can be pushed in this way by northerly winds and create similar eddies during other seasons as well. In summer, the circulation off Turkey is not so clear, and probably less intense, so that the counterclockwise circuit might not be closed.

The schema in Figure 3b-c correctly represents the penetration of the “AMC” into the Aegean, except for its northward extent, while only the schema in Figure 3d gives a consistent idea of the circulation off Greece. None of the characteristics of the mesoscale activity in the northern Cretan (mainly anticyclones ~100 km in diameter stationary or propagating eastwards at ~1 km/day along Crete) are correctly schematised. The overall circulation in the whole area is mainly westwards in the north in winter and eastwards in the south in summer. This year-round alongslope and counterclockwise circulation has not been well schematised up to now.

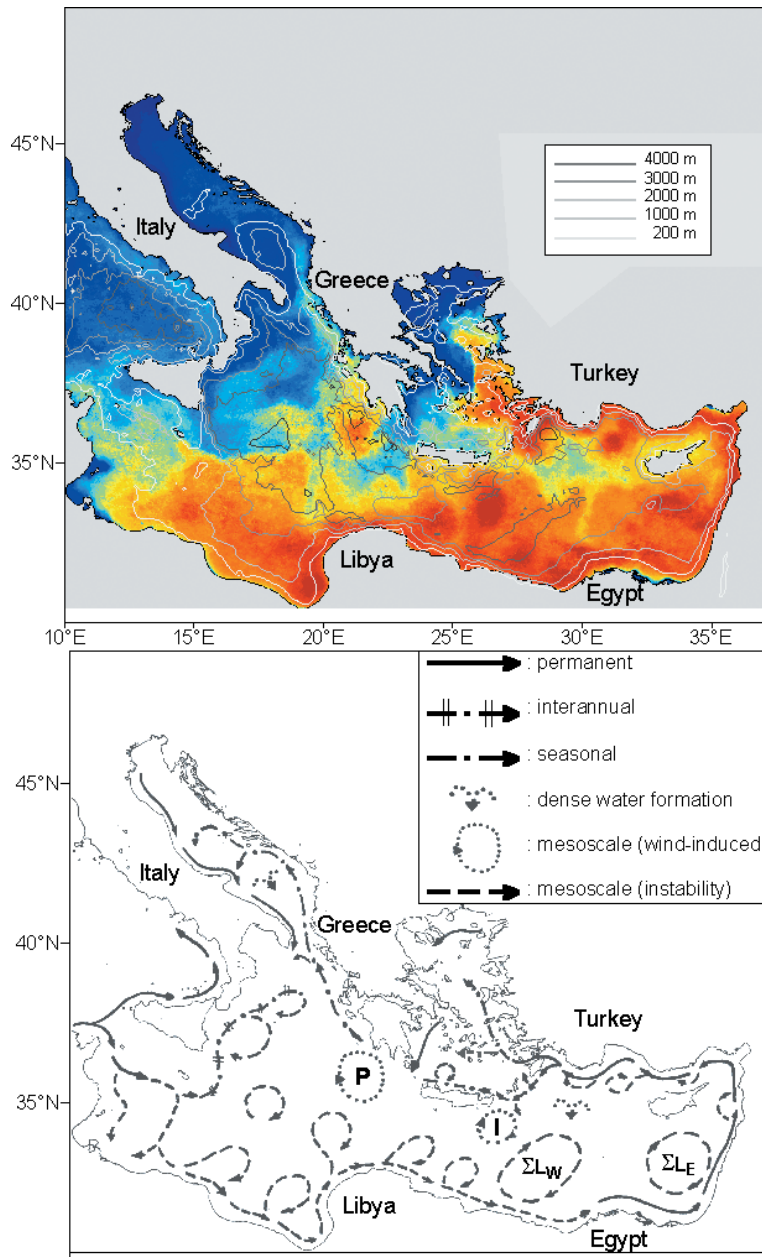


FIG. 23. – The eastern basin of the Mediterranean Sea in January 1998 (a), and the schema of the surface circulation (b).

CONCLUSION

The circulation of the Atlantic Water (AW) in the eastern basin of the Mediterranean Sea has been inferred from the visual analysis of IR satellite images (all monthly composites available from 1985 and weekly and daily composites (~1000) during the period 1996 to 2000). Our approach results from the fact that analysing individual images visually provides more information for understanding processes than performing unsupervised statistical analyses. The present analysis is the follow-up of the analysis

of images spanning the eighties from numerous studies that link remotely sensed and in situ observations in the western basin, and of detailed comparisons between the western and eastern basins. The information we infer is not consistent with any of the basin-scale schemata that have been widely referred to during the last decade, nor with most of the schemata available at subbasin scale. Despite the fact that Nielsen's schema (Fig. 1a) does not evidence any mesoscale feature, which is easily understood, it is the one that we find the most compatible with our analysis, since it emphasises the major

effect of the earth's rotation on the overall circulation. This can be deduced from all images shown above, as well as from the monthly composite of January 1998 we present in Figure 23a. The latter illustrates all the conclusions detailed hereafter, and will help in understanding the circulation schema we propose in Figure 23b.

Our analysis shows that a continuous flow of AW progresses mainly counterclockwise as an alongslope flow around most of the subbasins, hence forming a basin-wide gyre. AW first splits off northern Tunisia and enters the channel of Sicily mainly along Tunisia. Then, most of it spreads in the middle of the channel due to the widening of the Tunisian shelf. A small part of the flow penetrates towards the central Ionian as complex mesoscale eddies that propagate roughly southeastwards and / or as a northward branch probably induced by the wind at an interannual time scale (i.e. not at a seasonal one, and without re-joining the remainder of the flow). Although the relative importance of the branches has yet to be established, it seems that most of the AW flow continues southwards around the Tunisian continental shelf, thus hitting the western Libyan slope and partly turning clockwise over the Tunisian shelf. Finally, most of the AW flow concentrates in the southern Ionian along the eastern Libyan slope. The whole flow clearly continues alongslope in both the southern Cretan and the whole Levantine. In winter especially, and thanks to the decay of the Etesians, the AW flow then penetrates into the Aegean and the northern Cretan where it circulates counterclockwise before progressing around Greece up to inside the Adriatic and along southern Italy. An increasing number of numerical results (e.g. Pinardi and Masetti, 2000; Alhammoud *et al.*, 2003, 2005) and data analyses (Fusco *et al.*, 2003) support such an alongslope counterclockwise general circulation (basin-wide gyre).

The AW flow is unstable all along its circuit and generates mesoscale eddies. In addition, other mesoscale eddies are generated by the interaction of the Etesians with the orography. Original features have been specified at subbasin scale:

- In the Ionian, eddies generated in the central part, either directly from the AW inflow or from the wind-induced branch, can propagate south-southeastwards across the whole basin and finally disturb the circulation along the Libyan slope. Other eddies generated by the instability of the alongslope flow off western Libya can pinch off, follow the deeper

isobath, re-interact with the parent flow around Cyrenaica and then either drift seawards along the deepest isobaths or continue propagating alongslope downstream. Pelops is formed every year by the Etesians south / southwest of the Peloponnese. If it does not decay rapidly, it can then drift westwards for more than 1 year, so that two successive Pelops can be found a few 100 km apart. All these eddies can reach diameters of ~100 to 250 km, have lifetimes of 1 to 2 years, and propagate and/or drift at a few km/d.

- In the southern Cretan, the eddies generated by the instability of the alongslope flow can reach diameters of 200 to 250 km. Some of them seem to pinch off near the place where the deep isobaths divert seaward (~20°E). Most of them propagate downstream at up to ~3 km/d until the southwestern Levantine (we call them Libyo-Egyptian eddies), but they can also remain quasi-stationary and then deflect seaward eddies approaching from upstream.

- Ierapetra is an anticyclonic eddy generated during all summer-autumn periods by the Etesians southeast of Crete, possibly reaching a diameter of ~200 km. Ierapetra is fed by waters entrained by the wind stress curl, associated with the eastern-Crete orography, and by the whole-Crete shadowing effect. Indeed, this effect extends as far as Africa and allows waters pushed there to flow back northwards in the lee of the island. Ierapetra can also be fed from the northeast by the overall AW flow. Ierapetra can have lifetimes of a few years, drift towards the Libyan slope, interact with the Libyo-Egyptian eddies, interact and merge with the Ierapetra of the former generation, or remain stationary, thus being sustained by all northerly wind events, and finally by the Etesians the year after to give rise to an especially intense Ierapetra.

- In the southwestern Levantine, the Libyo-Egyptian eddies formed by instability of the alongslope flow upstream can propagate downstream, remain stationary, occasionally move upstream, interact and / or merge with other eddies and / or decay. New eddies can be generated there and rapidly grow before eventually merging and drifting seawards along the deepest isobaths. The SST signature of eddies there is markedly dependent on the Etesians, although most (if not all) of them are not wind-induced. In any case, the largest eddies (transport of several Sv, Zervakis *et al.*, 2002) do not propagate further east, probably due to their deep extent and to the sloping up of the isobaths, and / or

the planetary β effect and the non-linearities. The 3000 m Herodotus through off Mersa-Matruh seems to trap the eddies (most probably because of their vertical extent), so that eddies are permanently found there. Thus we name this accumulation of (anticyclonic) eddies in the western Levantine SL_w . Then, contrary to what has been accepted hitherto, the area known as “Mersa-Matruh” is not occupied by a recurrent / permanent eddy/gyre, but by slowly propagating and merging anticyclonic eddies that originated elsewhere.

- We suppose that the succession of the northern edges of these mesoscale eddies must have been mistaken for a central meandering eastward “Mid-Mediterranean Jet”.

- In the southeastern Levantine, only medium-sized (100-150 km) anticyclonic eddies can (probably due to topography) propagate downstream alongslope off Egypt at a few km/d before being entrained seawards by the deepest isobaths and contributing to the anticyclonic structure known as “Shikmona”. Smaller-scale features (10s km) issue from the alongslope flow off the Middle East and propagate downstream at up to ~ 10 km/d before generally evolving as plumes, pinching off and then also feeding “Shikmona”. We name this area where (anticyclonic) eddies accumulate, fed either from the east or south by smaller eddies and plumes originated from the alongslope flow, SL_E .

- In the northern Levantine, the instability of the alongslope circulation generates another kind of mesoscale feature: well defined anticyclonic eddies up to ~ 50 km off the easternmost part of Turkey and ~ 100 km in the Antalya-Rhodes area, which are either stationary or propagating downstream at up to 3 km/d for months. These eddies can markedly modify the circulation in the east-Cretan straits.

- In the northern Cretan, the anticyclonic eddies probably originate from the instability of the part of the flow entrained southwards by the Etesians, and which cannot pass through the west-Cretan strait. These eddies have diameters of 50 to 100 km, propagate eastward off Crete at 0 to 2 km/d, and can be tracked for months.

- From Greece to southern Italy, the instability of the gyre does not seem to generate significant mesoscale eddies.

The original description of the surface circulation we came up with leads us to extend the hypothesis about the effect of the bathymetry that was first put forwards by Nielsen (1912) and to propose a

new understanding of the processes. Essentially, the analysis of the IR imagery and our expertise in the western basin lead us to assume that any stable current will be constrained alongslope by the effect of the earth’s rotation. As the surface flow is generally a few 100 metres thick, it roughly follows the 100-200 m isobaths. Now, as soon as an instability develops and an anticyclonic eddy grows, a coupling is created between the surface layer and the deeper one, the larger the eddy the deeper (*a priori*) its vertical extent. Assuming that eddies often extend down to the bottom leads us to assume that they are actually guided by the deeper isobaths. This therefore explains why eddies pinch off preferentially where deeper isobaths spread seaward, and why large eddies with long lifetimes are preferentially found where the bathymetry is deep enough. This might also explain why large eddies propagating downstream skip the southeastern corners of the Ionian and the Levantine. Obviously, this hypothesis, which is consistent with all data sets in the western basin, must be tested with adequate models and theoretical analyses, and be supported by adequate data sets (which is the goal of EGYPT, see www.ifremer.fr/lobtln). In addition, we think that only the wind-induced anticyclonic eddies Pelops and Ierapetra, characterised by their year of formation, should be given a name preserving their geographical reference.

The topography in the eastern basin is relatively complex and the meteorological-climatic conditions there lead to several zones of dense water formation; therefore, several segments of the counterclockwise alongslope circulation could be identified (as before in the western basin). However, we think that this basin-wide gyre has basically two major components. One would be the Libyo-Egyptian Current which generates the relatively large Libyo-Egyptian eddies that will interact, merge and accumulate in the area SL_w , hence directly spreading AW up to the zone where LIW is formed (this current is the exact counterpart of the Algerian Current). The other would be an eastern-basin Northern Current that could be considered as an entity (even though more complex than in the western basin), extending more or less continuously from the Middle East to southern Italy. Note that the similarities and differences that we see between the eastern and western basins, which were first partially emphasised by Millot (1992), have now been specified by Millot and Taupier-Letage (2005b).

To conclude, our understanding of the processes is very different from what has been interpreted up to now. Our analysis is consistent with all available in situ and remote data sets and is supported by the most recent numerical simulations. Instead of considering that there is a continuous meandering jet/stream crossing the whole basin in its central part as in the POEM-schemata, and also considering what is occurring in the south, we believe that i) the AW circulation forms an alongslope and counter-clockwise gyre at basin scale, ii) the mesoscale eddies, either generated by the instability of the gyre in the south (the Libyo-Egyptian Current) or by the winds (the Etesians), play a fundamental role (the eddy-transport is much larger than the gyre-transport), iii) the gyre in the north (the Northern Current) does not form a rim current around the zones of dense water formation.

ACKNOWLEDGEMENTS

Najwa Hamad received support for her PhD from the High Institute of Marine Research, University of Tishreen, Syria. A. Abbas, J.-L. Fuda and G. Rougier are warmly acknowledged for their help. We have used data sets from the archiving and distributing centres of the DFD/DLR (ISIS/EOWEB, AVHRR), NASA (AVHRR Pathfinder), JRC/Ispira (SeaWIFS), CLS-MFSPP (sea level anomalies), and SISMER (hydrological data). We also benefited from the AVHRR images processed by the SATMOS/CMS (Météo-France/INSU agreement), from a catalogue of images kindly provided by A. Lascaratos, and from the XBT data collected during MFSPP.

REFERENCES

- Alhammoud, B., K. Béranger, L. Mortier and M. Crépon. – 2003. A comparison study between a high resolution numerical model results and observations in eastern Mediterranean Sea. In: *Proceedings of the 2nd Int. Conf. on Oceanography of the Eastern Mediterranean and Black Sea*, pp. 344-352. Ankara.
- Alhammoud, B., K. Béranger, L. Mortier, M. Crépon and I. Dekeyser. – 2005. Surface circulation of the Levantine Basin: comparison of model results with observations. *Prog. Oceanogr.*, 66: 299-320.
- Arnone R. and P. La Violette. – 1986. Satellite definition of bio-optical and thermal variation of coastal eddies associated with the African Current. *J. Geophys. Res.*, 91: 2351-2364.
- Artale, V., M. Astraldi, G. Buffoni and G.P. Gasparini. – 1994. Seasonal variability of gyre scale circulation in the northern Tyrrhenian Sea. *J. Geophys. Res.*, 99: 14127-14137.
- Artegiani, A., D. Bregant, E. Paschini, N. Pinardi, F. Raicich and A. Russo. – 1997. The Adriatic Sea General Circulation. Part II: Baroclinic Circulation Structure. *J. Phys. Oceanogr.*, 27: 1515-1532.
- Ayoub, N. – 1997. *Variabilité du niveau de la mer et de la circulation en Méditerranée à partir des données altimétriques et de champs de vent. Comparaison avec des simulations numériques*. Ph.D. thesis, Univ. Paul Sabatier, Toulouse.
- Ayoub, N., P.Y. Le Traon and P. De Mey. – 1998. A description of the Mediterranean surface variable circulation from combined ERS-1 and TOPEX/POSEIDON altimetric data. *J. Mar. Syst.*, 18: 3-40.
- Béranger K., L. Mortier, G.-P. Gasparini, L. Gervasio, M. Astraldi and M. Crépon. – 2004. The dynamics of the Sicily Strait: a comprehensive study from observations and models, *Deep-Sea Res. II*, 51(4-5): 411-440.
- Brankart, J.M. and P. Brasseur. – 1998. The general circulation in the Mediterranean Sea: a climatological approach. *J. Mar. Syst.*, 18: 41-70.
- Brenner, S. – 1989. Structure and evolution of warm core eddies in the eastern Mediterranean Levantine basin. *J. Geophys. Res.*, 94 (C9): 12593-12602.
- Brenner, S. – 1993. Long-term evolution and dynamics of a persistent warm core eddy in the Eastern Mediterranean Sea. *Deep-Sea Res.*, 40(6): 1193-1206.
- Burman, I. and O.H. Oren. – 1970. Water outflow close to bottom from the Aegean. *Cah. Oceanogr.*, 22: 775-780.
- Burnett, W.H., J.A. Price and P.E. La Violette. – 1991. The surface circulation around Crete inferred from drifter buoy trajectories and satellite imagery. *Mar. Technol. Soc. Conf.*: 869-875.
- Cardin, V. and N. Hamad. – 2003. Cretan Sea circulation from ADCP and SST data during 2000-2001. In: *Proceedings of the 2nd Int. Conf. on Oceanography of the Eastern Mediterranean and Black Sea*, pp. 47-53. Ankara.
- Champagne-Philippe, M., D. Guevel and R. Frouin. – 1982. Etude du Front de Malte à partir de données de télédétection et de mesures in situ. *Ann. Hydro.*, 757: 65-98.
- Crépon, M., L. Wald and J.M. Monget. – 1982. Low-frequency waves in the Ligurian Sea during December 1977. *J. Phys. Oceanogr.*, 87: 595-600.
- Crépon, M., M. Boukthir, M. Barnier and F. Aikman III. – 1989. Horizontal ocean circulation forced by deep water formation. Part I: An analytical study. *J. Phys. Oceanogr.*, 19: 1781-1792.
- Feliks, Y. and S. Itzikowitz. – 1987. Movement and geographical distribution of anticyclonic eddies in the Eastern Levantine Basin. *Deep-Sea Res.*, 34 (9): 1499-1508.
- Font J., J. Isern-Fontanet and J. Salas. – 2004. Tracking a big anticyclonic eddy in the western Mediterranean Sea. *Sci. Mar.*, 68(3): 331-342.
- Fuda, J.L., C. Millot, I. Taupier-Letage, U. Send and J.M. Bocognano. – 2000. XBT monitoring of a meridian section across the Western Mediterranean Sea. *Deep-Sea Res. I*, 47: 2191-2218.
- Fuda, J.L., G. Etiope, C. Millot, P. Favali, M. Calcara, G. Smriglio and E. Boschi. – 2002. Warming, salting and origin of the Tyrrhenian Deep Water. *Geophys. Res. Lett.*, 29(19):1898, doi:10.1029/2001GL014072.
- Fusco, G., G.M.R. Manzella, A. Cruzado, M. Gacic, G.P. Gasparini, V. Kovacevic, C. Millot, C. Tziavos, Z. Velásquez, A. Walne, V. Zervakis and G. Zodiatis. – 2003. Variability of mesoscale features in the Mediterranean Sea from XBT data analysis. *Ann. Geophys.*, 21: 21-32.
- Golnaraghi, M. – 1993. Dynamical studies of the Mersa Matruh gyre: Intense meander and ring formation events. *Deep-Sea Res.*, 40 (6): 1247-1267.
- Golnaraghi, M. and A.R. Robinson. – 1994. Dynamical studies of the Eastern Mediterranean circulation. In: P. Malanotte-Rizzoli and A.R. Robinson (eds.) *Ocean processes in Climate Dynamics: Global and Mediterranean Examples*, NATO ASI Series, 419, pp. 395-406. Kluwer Academic Publ., Dordrecht.
- Hamad, N. – 2003. *La circulation de surface dans le bassin oriental de la Méditerranée d'après les observations satellitaires infrarouges*. Ph.D. thesis, Univ. Méditerranée.
- Hamad, N., C. Millot and I. Taupier-Letage. – 2004. The surface circulation in the eastern basin of the Mediterranean Sea: new elements. In: *Proceedings of the 2nd Int. Conf. on Oceanography of the Eastern Mediterranean and Black Sea*, pp. 2-9. Ankara.
- Hamad N., C. Millot and I. Taupier-Letage. – 2005. A new hypoth-

- esis about the surface circulation in the eastern basin of the Mediterranean Sea. *Prog. Oceanogr.* 66: 287-298.
- Hecht, A., N. Pinardi and A.R. Robinson. – 1988. Currents, water masses, eddies and jets in the Mediterranean Levantine Basin. *J. Phys. Oceanogr.*, 18: 1320-1353.
- Hecht, A. and I. Gertman. – 2001. Physical features of the Eastern Mediterranean resulting from the integration of POEM data with Russian Mediterranean Cruises. *Deep-Sea Res.*, 48: 1847-1876.
- Horton, C., J. Kerling, G. Athey, J. Schmitz and M. Clifford. – 1994. Airborne expendable bathythermograph surveys of the Eastern Mediterranean. *J. Geophys. Res.*, 99(C5): 9891-9905.
- Kotsovinos, N.E. – 1997. The Ierapetra and Rhodes Gyres: an assumption for their generation. *Proc. Hell. Symp. Oceanogr. Fish*, 1: 161-164.
- Lacombe, H., P. Tchernia and G. Benoist. – 1958. Contribution à l'étude hydrologique de la mer Egée en période d'été. *Bull. Inf. Coec.*, 8: 454-468.
- Lacombe, H. and P. Tchernia. – 1972. Caractères hydrologiques et circulation des eaux en Méditerranée. In: D. Stanley (ed.), *The Mediterranean Sea: a natural sedimentation laboratory*, pp. 25-36. Dowden, Hutchinson and Ross Inc., Stroudsburg.
- Larnicol, G., P.Y. Le Traon, N. Ayoub and P. De Mey. – 1995. Mean sea level and surface circulation variability of Mediterranean Sea from 2 years of TOPEX/POSEIDON altimetry. *J. Geophys. Res.*, 100: 25163-25177.
- Larnicol, G., N. Ayoub and P.Y. Le Traon. – 2002. Major changes in Mediterranean Sea level variability from 7 years of TOPEX/POSEIDON and ERS-1/2 data. *J. Mar. Syst.*, 33-34: 63-89.
- Lascaratos, A. and S. Tsantilas. – 1997. Study of the seasonal circle of the Ierapetra gyra, using satellite imager. *Proc. Hell. Symp. Oceanogr. Fish*, 1: 165-168.
- Le Vouché, J., C. Millot, N. Castagné, P. Le Borgne and J.P. Olry. – 1992. Atlas of thermal fronts of the Mediterranean Sea derived from satellite imagery. *Mém. Inst. Océanogr. Monaco*, 16.
- Malanotte-Rizzoli, P. and A. Bergamasco. – 1989. The circulation of the Eastern Mediterranean, part I: The barotropic, wind-driven circulation. *Oceanol. Acta*, 12 (4): 335-351.
- Malanotte-Rizzoli, P. and A. Bergamasco. – 1991. The wind and thermally driven circulation of the eastern Mediterranean Sea. Part II: the baroclinic case. *Dyn. Atm. Oceans*, 15 (3-5): 355-419.
- Malanotte-Rizzoli, P. – 1994. Modeling the general circulation of the Mediterranean. In: P. Malanotte-Rizzoli and A.R. Robinson (eds.) *Ocean processes in Climate Dynamics: Global and Mediterranean Examples*, NATO ASI Series, 419, pp. 307-321. Kluwer Academic Publ., Dordrecht.
- Malanotte-Rizzoli, P., B.B. Manca, M. Ribera d'Alcala, A. Theocharis, A. Bergamasco, D. Bregant, G. Budillon, G. Civitarese, D. Georgopoulos, A. Michelato, E. Sansone, P. Scarazzato and E. Souvermezoglou. – 1997. A synthesis of the Ionian Sea hydrography, circulation and water mass pathways during POEM-Phase I. *Prog. Oceanogr.*, 39: 153-204.
- Malanotte-Rizzoli, P., B.B. Manca, M. Ribera d'Alcala, A. Theocharis, S. Brenner, G. Budillon and E. Özsoy. – 1999. The Eastern Mediterranean in the 80s and in the 90s: the big transition in the intermediate and deep circulations. *Dyn. Atm. Oceans*, 29: 365-395.
- Manca, B.B., Ursella, L. and P. Scarazzato. – 2002. New development of the Eastern Mediterranean circulation based on hydrological observations and current measurements. In: F. Boero *et al.* (eds.) *2nd National Conference of Conisma, Mar. Ecol., PSZN*, 23 (1): 237-257.
- Manca, B.B., A. Crise, and L. Ursella. – 2003. Recent advances in observing the upper thermocline circulation in the Ionian Sea in response to changes in wind stress curl. In: *Proceedings of the 2nd Int. Conf. on Oceanography of the Eastern Mediterranean and Black Sea*, pp. 10-17. Ankara.
- Manzella, G. M. R., V. Cardin, A. Cruzado, G. Fusco, G. Gacic, C. Galli, C., G. – P. Gasparini, T. Gervais, V. Kovacevic, C. Millot, L. Petit De la Villeon, G. Spaggiari, M. Tonani, C. Tziavos, Z. Velásquez, A. Walne, V. Zervakis and G. Zodiatis. – 2001. EU-sponsored effort improves monitoring of circulation variability in the Mediterranean. *EOS Trans. AGU*, 82 (43): 497-504.
- Marullo, S., R. Santoleri, P. Malanotte-Rizzoli and A. Bergamasco. – 1999a. The sea surface temperature field in the Eastern Mediterranean from the advanced very high resolution radiometer (AVHRR) data - Part I. Seasonal variability. *J. Mar. Syst.*, 20: 63-81.
- Marullo, S., R. Santoleri, P. Malanotte-Rizzoli and A. Bergamasco. – 1999b. The sea surface temperature field in the Eastern Mediterranean from the advanced very high resolution radiometer (AVHRR) data - Part II. Interannual variability. *J. Mar. Syst.*, 20: 83-112.
- Marullo S., E. Napolitano, R. Santoleri, B. B. Manca and R. Evans. – 2003. The variability of Rhodes and Ierapetra gyres studied by remote sensing observation, hydrographic data and model simulations during LIWEX (october 1994-april 1995). *J. Geophys. Res.*, 108(C9): 8119, DOI: 10.1029/2002JC001393.
- Matteoda, A.M. and S.M.Glenn. -1996. Observations of recurrent mesoscale eddies in the Eastern Mediterranean. *J. Geophys. Res.*, 101(C9): 20687-20709.
- Millot, C. – 1985. Some features of the Algerian Current. *J. Geophys. Res.*, 90(C4): 7169-7176.
- Millot, C. – 1987. Circulation in the Western Mediterranean Sea. *Oceanol. Acta*, 10: 143-149.
- Millot, C. – 1991. Mesoscale and seasonal variabilities of the circulation in the Western Mediterranean. *Dyn. Atm. Oceans*, 15: 179-214.
- Millot, C. – 1992. Are there major differences between the largest Mediterranean Seas? A preliminary investigation. *Bull. Inst. Oceanogr. Monaco*, 11: 3-25.
- Millot, C. – 1999. Circulation in the Western Mediterranean Sea. *J. Mar. Syst.*, 20: 423-442.
- Millot C. – 2005. Circulation in the Mediterranean Sea: evidences, debates and unanswered questions. In: C. Marrasé and P. Abelló (eds.) *Promoting marine science: Contributions to celebrate the 50th anniversary of Scientia Marina, Sci. Mar.*, 69 (Suppl. 1): 5-21.
- Millot, C., I. Taupier-Letage and M. Benzohra. – 1990. The Algerian eddies. *Earth-Sci. Rev.*, 27, 203-219.
- Millot, C., M. Benzohra and I. Taupier-Letage. – 1997. Circulation off Algeria inferred from the medipro-5 current meters. *Deep-Sea Res.*, 44 (9): 1467-1495.
- Millot C. and I. Taupier-Letage. – 2005a. Additional evidence of LIW entrainment across the Algerian Basin by mesoscale eddies and not by a permanent westward-flowing vein. *Prog. Oceanogr.*, 66: 231-250.
- Millot C. and I. Taupier-Letage. – 2005b. Circulation in the Mediterranean Sea. In: A. Salot (ed.) *The Handbook of Environmental Chemistry*, 5 (K), pp. 29-66. Springer-Verlag, Heidelberg.
- Molcard, A., L. Gervasio, A. Griffa, G.-P. Gasparini, L. Mortier and T. Özgökmen. – 2002. Numerical investigation of the Sicily Channel dynamics: density current and water mass advection. *J. Mar. Syst.*, 36 (3-4): 219-238.
- Napolitano, E., T. Oguz, P. Malanotte-Rizzoli, A. Yilmaz and E. Sansone. – 2000. Simulations of biological production in the Rhodes and Ionian basins of the Eastern Mediterranean. *J. Mar. Syst.*, 24: 277-298.
- Nielsen, J.N. – 1912. Hydrography of the Mediterranean and adjacent waters. *Rep. Dan. Oceanogr. Exp. Medit.*, 1: 77-192.
- Obaton, D., C. Millot, G. Chabert D'Hières and I. Taupier-Letage. – 2000. The Algerian Current: comparisons between in situ and laboratory measurements. *Deep-Sea Res. I*, 47: 2159-2190.
- Ovchinnikov, I.M. – 1966. Circulation in the surface and Intermediate Layers of the Mediterranean. *Oceanology*, 6: 48-59.
- Özsoy, E., A. Hecht and Ü. Ünlüata. – 1989. Circulation and hydrography of the Levantine Basin. Results of POEM coordinated experiments 1985-1986. *Prog. Oceanogr.*, 22: 125-170.
- Özsoy, E., A. Hecht, Ü. Ünlüata, S. Brenner, T. Oguz, J. Bishop, M.A. Latif and Z. Rozentraub. – 1991. A review of the Levantine Basin circulation and its variability during 1985-1988. *Dyn. Atm. Oceans*, 15: 421-456.
- Özsoy, E., A. Hecht, Ü. Ünlüata, S. Brenner, H.I. Sur, J. Bishop, M.A. Latif, Z. Rozentraub and T. Oguz. – 1993. A synthesis of the Levantine Basin circulation and hydrography 1985-1990. *Deep-Sea Res.*, 40: 1075-1119.
- Pierini, S. and A. Rubino. – 2001. Modeling the oceanic circulation in the area of the strait of Sicily: the remotely forced dynamics. *J. Phys. Oceanogr.*, 31(6): 1397-1412.
- Pinardi, N., G. Korres, A. Lascaratos, V. Roussenov and E. Stanev. – 1997. Numerical simulation of the interannual variability of

- the Mediterranean Sea upper circulation. *Geophys. Res. Lett.*, 24(4): 425-428.
- Pinardi, N. and E. Masetti. – 2000. Variability of the large scale general circulation of the Mediterranean Sea from observations and modelling: a review. *Palaeogeogr., Palaeoclimatol., Palaeoecol.*, 158: 153-173.
- POEM Group. – 1992. General circulation of the Eastern Mediterranean. *Earth Sci. Rev.*, 32: 285-309.
- Poulain, P.M. – 1998. Lagrangian measurements of surface circulation in the Adriatic and Ionian seas between November 1994 and March 1997. *Rapp. Comm. int. Mer Médit.*, 35: 190-191.
- Poulain, P.M. – 2001. Adriatic Sea surface circulation as derived from drifter data between 1990 and 1999. *J. Mar. Syst.*, 29: 3-32.
- Puillat, I., I. Taupier-Letage. and C. Millot. – 2002. Algerian Eddies lifetime can near 3 years. *J. Mar. Syst.*, 31: 245-259.
- Robinson, A.R., M. Golnaraghi, W.G. Leslie, A. Artegiani, A. Hecht, E. Lazzoni, A. Michelato, E. Sansone, A. Theocharis and Ü. Ünlüata - 1991. The Eastern Mediterranean general circulation : features, structure and variability. *Dyn. Atm. Oceans*, 15: 215-240.
- Robinson, A.R. and M. Golnaraghi. – 1993. Circulation and dynamics of the Eastern Mediterranean Sea; Quasi-Synoptic data-driven simulations. *Deep-Sea Res.*, 40(6): 1207-1246.
- Robinson, A.R., J. Sellschopp, A. Warn-Varnas, W.G. Leslie, C.J. Lozano, P.J. Haley Jr, L.A. Anderson and P.F.J. Lermusiaux. – 1999. The Atlantic Ionian Stream. *J. Mar. Syst.*, 20: 129-156.
- Roussenov, V., E. Stanev, V. Artale and N. Pinardi. – 1995. A seasonal model of the Mediterranean Sea general circulation. *J. Geophys. Res.*, 100 (C7): 13515 -13538.
- Ruiz, S., J. Font, M. Emelianov, J. Isern-Fontanet, C. Millot and I. Taupier-Letage. – 2002. Deep structure of an open sea eddy in the Algerian Basin. *J. Mar. Syst.*, 33-34: 179-195.
- Said, M.A. – 1984. *Water circulation in the central and Eastern basins of the Mediterranean Sea and the formation of the intermediate water masses*. Ph. D. thesis, Univ. Odessa (in Russian).
- Salas, J., C. Millot, J. Font and E. García-Ladona, 2002. Analysis of mesoscale phenomena in the Algerian Basin observed with drifting buoys and infrared images. *Deep-Sea Res.*, 49(2): 245-266.
- Sammari, C., C. Millot and L. Prieur. – 1995. The circulation in the Ligurian Sea inferred from the Prolog-2 experiment. *Deep-Sea Res.*, 42(6): 893-917
- Spall, M. (2004). Boundary currents and watermass transformation in marginal seas. *J. Phys. Oceanogr.*, 34: 1197-1213.
- Taupier-Letage, I. and C. Millot. – 1988. Surface circulation in the Algerian basin during 1984. *Oceanol. Acta*, sp. issue 9: 79-85.
- Taupier-Letage, I. and C. Millot. – 2003. Why biological time series require physical ones?. In: *Mediterranean biological time series, CIESM Workshop Monograph*, 22: 93-100.
- Taupier-Letage, I., C. Millot, S. Dech, R. Meisner, J-L. Fuda, I. Puillat, C. Bégué, B. Rey and C. Albérola. – 1998. Suivi des structures dynamiques de moyenne échelle dans le bassin algérien pendant l'opération ELISA (1997-1998) par l'imagerie satellitale thermique NOAA/AVHRR: les obstacles potentiels à une reconnaissance automatique. *Oceanis*, 24(3): 153-174.
- Taupier-Letage, I., I. Puillat, P. Raimbault and C. Millot. – 2003. Biological response to mesoscale eddies in the Algerian Basin. *J. Geophys. Res.*, 108(C8): 3245-3267.
- Theocharis, A., D. Georgopoulos, A. Lascaratos and K. Nittis. – 1993. Water masses and circulation in the central region of the Eastern Mediterranean : Eastern Ionian, South Aegean and Northwest Levantine, 1986-1987. *Deep-Sea Res.*, 40 (6): 1121-1142.
- Theocharis, A., E. Balopoulos, S. Kioroglou, H. Kontoyiannis and A. Iona. – 1999. A synthesis of the circulation and hydrography of the South Aegean Sea and the straits of the Cretan Arc (March 1994-January 1995). *Prog. Oceanogr.*, 44: 469 -509.
- Theodorou, A., A. Theocharis and E. Balopoulos. – 1997. Circulation in the Cretan Sea and adjacent regions in late winter 1994. *Oceanol. Acta*, 20 (4): 585 -596.
- Tziperman, E. and P. Malanotte-Rizzoli. – 1991. The climatological seasonal circulation of the Mediterranean Sea. *J. Mar. Res.*, 49: 411 - 434.
- Wald, L. – 1985. *Apport de la télédétection spatiale en infrarouge proche et moyen à la connaissance du milieu marin*. Ph. D. thesis, Univ. Toulon et du Var.
- Zavatarelli, M. and G.L. Mellor. – 1995. A numerical study of the Mediterranean Sea circulation. *J. Phys. Oceanogr.*, 25(6): 1384-1414.
- Zervakis, V., G. Papadoniou, C. Tziavos and A. Lascaratos. – 2002. Seasonal variability and geostrophic circulation in the Eastern Mediterranean as revealed through a repeated XBT transect. *Ann. Geophys.*, 20: 1-15.
- Zodiatis, G. – 1992. On the seasonal variability of the water masses circulation in the NW Levantine Basin-Cretan Sea and flows through the eastern Cretan Arc straits. *Ann. Geophys.*, 10: 12-24.
- Zodiatis, G. – 1993. Circulation of the Cretan Sea water masses (Eastern Mediterranean Sea). *Oceanol. Acta*, 16(2): 107-114.
- Zodiatis, G., A. Theodorou and A. Demetropoulos. – 1998. Hydrography and circulation south of Cyprus in late summer 1995 and in spring 1996. *Oceanol. Acta*, 21: 447-458.

Scient. ed.: J. Font

Received March 17, 2005. Accepted March 20, 2006.

Published online July 14, 2006.

